

**The Anti-tumor Activities of Steroid Saponin HK18
on Human Hepatocellular Carcinoma Cell Line
HepG2 and Multidrug Resistant Human
Hepatocellular Carcinoma Cell Line R-HepG2 and
Its Action Mechanisms**

by

Cheung Yuen-Nei

B. Sc. (Hon.)

The Chinese University of Hong Kong

A Thesis Submitted as Partial Fulfillment of the Requirements
for the Degree of Master of Philosophy in the
Department of Biochemistry
The Chinese University of Hong Kong

September, 2002

The Chinese University of Hong Kong holds the copyright of this thesis. Any person(s) intending to use a part or whole of the materials in the thesis in a proposed publication must seek copyright release from the Dean of the Graduate School.



Acknowledgement

I would like to express my deepest gratitude to my supervisor Prof. K. P. Fung, for his valuable advice and infinite guidance in various aspects throughout the course of my project.

I would like to thank Prof. Yu Biao of the Shanghai Institute of Organic Chemistry, Chinese Academy of Sciences for providing HK18 throughout the research. Also I would like to thank the financial support given by the Shanghai Hong Kong Anson Research Foundation.

Special thanks are given to the examiners of this project, for spending a lot of valuable time in reading the thesis that has led to further improvement.

I would like to express my gratefulness to the members of Prof. Fung's laboratory for providing me a comfortable, cooperative and friendly working environment.

Finally I would like to thank my family as well as my good friends Ms Eunice Chan and Ms Chris Leung for their endless cares, warmth and supports.

Abstract

Saponins are high molecular weight glycosides that composed of a sugar moiety (glycone) and a steroid or triterpenoid moiety (aglycone). Polyphyllin D is a steroid saponin, which can be found in the Traditional Chinese Medicine (TCM) *Paris Polyphylla*. It was organic synthesized and was nomenclatured as Hong Kong compound 18 (HK18). In this project, we have studied the anti-tumor activities and the action mechanisms of HK18 on human hepatocellular carcinoma cell line HepG2 and multidrug resistant cell line R-HepG2.

By MTT and tryphan blue exclusion assays, we have found that HK18 was cytotoxic to both HepG2 and R-HepG2 cells in a dose and time dependent manner. It was less toxic to normal tissues as demonstrated by incubating with macrophages and *in vivo* study. And low concentrations of HK18 only induced a very small percentage of hemolysis.

HK18 could induce apoptosis as illustrated by DNA fragmentation and phosphatidylserine externalization on both cancer cell lines. It could induce mitochondrial membrane potential (Ψ_m) depolarization in a dose dependent manner. Addition of the inhibitor of mitochondrial permeability transition (MPT), Bongkreik acid could lower the cytotoxic effect of HK18. By using flow cytometry, it has been found that intracellular hydrogen peroxide and calcium levels were enhanced in HK18-treated HepG2 and R-HepG2 cells which are the mediators of MPT.

Besides, caspase 3 was activated in HK18-treated HepG2 and R-HepG2 cells as indicated by Western blot with decreased pro-caspase 3 level and increased PARP cleavage in a dose and time dependent manner in both cancer cell lines. It was further confirmed by enzymatic assays. Both of caspase 3 and caspase 9 enzymatic activities were enhanced while caspase 8 activity remained unchanged.

Apart from this, the release of apoptogenic proteins from mitochondria of HK18 treated HepG2 cells was examined. Cytochrome c and apoptosis inducing factor (AIF) have been found to be released upon treatment.

Furthermore, the effects of HK18 on the Bcl-2 family were analyzed. It has been found that the anti-apoptotic protein Bcl-2 level decreased in a dose dependent manner as assessed by Western blot analysis on the two cancer cell lines. Besides,

RT-PCR was employed to study at the mRNA level. It has been found that HK18 could lower the anti-apoptotic bcl-2 and bcl-X_L levels but no effect on the pro-apoptotic gene bak of HepG2 cells.

The effect of HK18 on the expression of P-glycoprotein (P-gp) in R-HepG2 cells was investigated. It has been found that treating R-HepG2 cells with HK18 would down-regulate the expression of P-gp gradually. In combining with the neutral property of HK18, we proposed that HK18 was not a substrate of P-gp.

In sum, HK18 can induce both HepG2 cells and R-HepG2 cells to undergo apoptotic cell death. The possible action mechanism involves the mitochondrial-dependent apoptotic pathway.

摘要

皂甙 (又名皂素或黃酮甘)是高分子量的配糖,它由糖及固醇配糖基或三醇配糖基所組成。從七葉一枝花中可提煉出一種名為甾體皂甙(polyphyllin D) 的固醇類皂甙；透過有機合成方法我們合成了這種甾體皂甙並稱之為 Hong Kong 18 (HK18)。在這項研究計劃中，我們研究了 HK18 對細胞系 HepG2 和 R-HepG2 的抗癌療用，以及對它的抗癌機制。

透過細胞增生或存活分析及 tryphan blue 排斥分析，我們發現 HK18 對細胞系 HepG2 和 R-Hep2 皆有劑量及時間依賴性的毒殺細胞作用。從使用巨噬細胞及在活的有機體內實驗中我們發現它對正常組織的影響較低。此外我們發現低濃度的 HK18 只引致很小的溶血現象。

我們發現 HK18 能將這兩癌細胞系的脫氧核糖核酸(Deoxyribonucleic Acid, DNA)切成片斷，並能導致磷脂醯絲氨酸 (Phosphatidylserine)外露，因此 HK18 能導致細胞凋亡。研究結果顯示 HK18 會引致線粒體膜電位(Mitochondrial Membrane Potential, Ψ_m) 隨劑量而下降。我們發現線粒體滲透轉移的抑壓劑 Bongkreic acid 能降低 HK18 的毒性，另外 HK18 能提升細胞內的線粒體滲透轉移中介物過氧化氫及鈣離子的濃度。

而透過西方轉漬法 (Western Blot)，我們發現 HK18 會刺激 HepG2 及 R-HepG2 細胞內的三號卡斯帕西斯 (casapse 3) 的活動，這由 procaspase 3 的蛋白質分量下降而其受質(substrate) 聚二磷酸腺甘聚合酵素(PARP)的分解則增多反影出來。另外透過酵素活動的實驗我們證實了細胞的三號及九號卡斯帕西斯的活動受到 HK18 的刺激而八號卡斯帕西斯則不受影響。

我們亦發現 HK18 會引致 HepG2 細胞的線粒體釋放細胞凋亡蛋白 (apoptogenic protein)：細胞色素 c (Cytochrome c) 及 apoptotic inducing factor (AIF)。

我們還發現 HepG2 和 R-HepG2 細胞的 Bcl-2 蛋白水平會隨著 HK18 的劑量而下降；而透過反轉錄聚合每鏈鎖反應 (RT-PCR)則反影出 HepG2 細胞內

的 *bcl-2* 及 *bcl-X_L* 的 mRNA 水平會因 HK18 而下降，但 *bak* 則不受其影響。

我們更對 R-HepG2 細胞內的 P 醣蛋白水平作出研究，結果顯示 HK18 會導致 P 醣蛋白的水平隨著作用時間而減少；加上 HK18 是中性的複合物，故此我們推斷 HK18 不是 P 醣蛋白的受質(substrate)。

總括來說，HK18 會導致 HepG2 和 R-HepG2 細胞進行凋亡，而經線粒體導致的凋亡是其中可能出現的機制。

Contents

Acknowledgement	i
Abstract	ii
摘要	iv
Contents	vi
List of Figures	xii
List of Tables	xv
Abbreviations	xvi
Chapter 1 Introduction	1
1 Introduction	2
1.1 Characteristic of Saponins	3
1.1.1 Occurrence of Saponins	3
1.1.2 General Properties of Saponins	3
1.1.2.1 Emulsifying Agents	3
1.1.2.2 Forming Complex with Cholesterol	4
1.1.2.3 Hemolytic Property	4
1.1.3 Structure of Saponins	5
1.1.3.1 Categories of Saponins	5
1.1.3.1.1 Triterpene Saponins	5
1.1.3.1.2 Steroid Saponins	5
1.1.3.2 Monodesmosidic and Bidesmosidic Saponins	7
1.1.4 Biological and Pharmacological Properties of Saponins	9
1.1.4.1 Anti-microbial Activity	9
1.1.4.1.1 Anti-fungal Activities	9
1.1.4.1.2 Anti-bacterial Activities	10
1.1.4.1.3 Anti-viral Activities	10
1.1.4.2 Insecticidal Activity	10
1.1.4.3 Molluscicidal Activity	10
1.1.4.4 Hypocholesterolemic Activity	11
1.1.4.5 Anti-ulcer Activity	11

1.1.4.6	Contraceptive Activity	12
1.1.4.7	Immunomodulatory Activities	12
1.1.4.7.1	Direct Immunostimulation	12
1.1.4.7.2	Acting as Immuno-adjuvants	13
1.1.4.8	Anti-tumor Activity	14
1.1.4.8.1	Anti-carcinogenesis	15
1.1.4.8.2	Suppression of Tumor Growth	16
1.1.5	Anti-tumor Activity of Steroid Saponins	18
1.1.5.1	Diosgenin Steroid Saponin	18
1.1.5.2	Hong Kong Compounds	18
1.1.5.3	Hong Kong 18	21
1.2	Human Hepatocellular Carcinoma (HCC)	24
1.2.1	The Incidence of Liver Cancer	24
1.2.2	Classification of Liver Cancer	24
1.2.3	Human Hepatocellular Carcinoma Cell Lines	25
1.2.3.1	Human Hepatocellular Carcinoma Cell Line HepG2	25
1.2.3.2	Multidrug Resistant Human Hepatocellular Carcinoma Cell Line R-HepG2	27
1.2.3.2.1	Mechanisms of Multidrug Resistance	28
1.2.3.2.2	Structure and Characteristics of P-glycoprotein	29
1.2.3.2.3	Methods in Dealing with P-glycoprotein Over-expressed MDR Cells	31
1.3	Objectives of the Project	32
1.3.1	Study of the Anti-tumor Activities of Hong Kong 18 on Human Hepatocellular Carcinoma Cell Line HepG2 and Unravel the Underlying Mechanisms	32
1.3.2	Study of the Anti-tumor Activities of Hong Kong 18 on Multidrug Resistant Human Hepatocellular Carcinoma Cell Line R-HepG2 and Unravel the Underlying Mechanisms	32
 Chapter 2 Materials and Methods		 33
2.1	Materials	34
2.1.1	Cell Culture	34
2.1.1.1	Cell Lines	34
2.1.1.2	Culture Media	35

	2.1.2 Reagents and Buffers	36
	2.1.2.1 Phosphate Buffered Saline (PBS)	36
	2.1.2.2 Reagents and Buffers for DNA Fragmentation	36
	2.1.2.3 Reagents and Buffers for Western Analysis	37
	2.1.2.4 Reagents and Buffer for Caspases Activities	39
	2.1.2.5 Fluorescent Dyes used for Flow Cytometry	39
	2.1.3 Chemicals	39
2.2	Methods	46
	2.2.1 MTT Assay	46
	2.2.2 Determination of Cell Viability	46
	2.2.3 Purification of Macrophages from balb/c Mice	47
	2.2.4 Hemolysis Assay	47
	2.2.5 <i>In vivo</i> Studies of the Toxicity of HK18	48
	2.2.6 DNA Fragmentation Assay	50
	2.2.7 Detection of Apoptotic and Necrotic / Late Apoptotic Cells Death by Flow Cytometry with Annexin V-FITC / PI	51
	2.2.8 Detection of Mitochondrial Membrane Potential by JC-1 Fluorescent Dye	52
	2.2.9 Detection of Intracellular Ca ²⁺ Level by Flow Cytometry with Fluo-3 Fluorescent Dye	52
	2.2.10 Detection of Intracellular Hydrogen Peroxide Level by Flow Cytometry with DCF Fluorescence Dye	53
	2.2.11 Simultaneous Detection of Mitochondrial Membrane Potential and Intracellular Ca ²⁺ or Mitochondrial Membrane Potential and Intracellular Hydrogen Peroxide	54
	2.2.12 Western Analysis	55
	2.2.12.1 Total Protein Extraction	55
	2.2.12.2 Extraction of Cytosolic Proteins	59
	2.2.13 Determination of Caspases Enzymatic Activity	63
	2.2.14 Reverse Transcriptase Polymerase Chain Reaction (RT-PCR)	67
	2.2.14.1 RNA Extraction by TRIzol Reagent	67
	2.2.14.2 Reverse Transcription	68
	2.2.14.3 Polymerase Chain Reaction	68
2.3	Statistic Analysis	71

Chapter 3 Cytotoxicity of HK18	72
3.1 Cytotoxicity of HK18 on HepG2 Cells	73
3.1.1 Study of the Cytotoxic Activity of HK18 on HepG2 Cells by MTT Assay	73
3.1.2 Study of the Cytotoxic Activity of HK18 on HepG2 Cells by Tryphan Blue Exclusion Assay	76
3.2 Cytotoxicity of HK18 on R-HepG2 Cells	78
3.2.1 Study of the Cytotoxic Activity of HK18 on R-HepG2 Cells by MTT Assay	78
3.2.2 Study of the Cytotoxic Activity of HK18 on R-HepG2 Cells by Tryphan Blue Exclusion Assay	81
3.3 Cytotoxicity of HK18 on Macrophages	83
3.4 Hemolytic Activity of HK18	85
3.5 <i>In vivo</i> Study of the Toxicity of HK18	87
Chapter 4 Mechanistic Study of HK18 on HepG2 Cells	90
4.1 Hallmarks of Apoptosis Induced by HK18 on HepG2 Cells	91
4.1.1 Induction of Phosphatidylserine Externalization by HK18 on HepG2 Cells	91
4.1.2 Induction of DNA Fragmentation by HK18 of HepG2 Cells	97
4.2 Study of the Underlying Mechanisms of HK18 Induced Apoptosis in HepG2 Cells	99
4.2.1 The Role of Mitochondria in HK18 Induced Apoptosis of HepG2 Cells	99
4.2.1.1 HK18 Induced Mitochondrial Membrane Depolarization in HepG2 Cells	101
4.2.1.2 Addition of Bongkreikic Acid Reduced HK18 Cytotoxicity on HepG2 Cells	105
4.2.1.3 Elevation of Intracellular Hydrogen Peroxide Level in HK18 Treated HepG2 Cells	108
4.2.1.4 Elevation of Intracellular Ca ²⁺ Level in HK18 Treated HepG2 Cells	114
4.2.1.5 HK18 Induced Cytochrome c and AIF Released from Mitochondria of HepG2 Cells	120
4.3 Downstream Biochemical Changes Induced by HK18 on HepG2 Cells	123

4.3.1	Activation of Caspase 3 of HepG2 Cells by HK18 as Demonstrated by Western Blot	123
4.3.2	Induction of Caspases Activities of HepG2 Cells by HK18 as Demonstrated by Enzymatic Activity Assays	125
4.4	Down-regulation of Anti-apoptotic Bcl-2 Family Members of HepG2 Cells by HK18	129
 Chapter 5 Mechanistic Study of HK18 on R-HepG2 Cells		133
5.1	Hallmarks of Apoptosis Induced by HK18 on R-HepG2 Cells	134
5.1.1	Induction of Phosphatidylserine Externalization by HK18 on R-HepG2 Cells	134
5.1.2	Induction of DNA Fragmentation by HK18 of R-HepG2 Cells	137
5.2	Study of the Underlying Mechanisms of HK18 Induced Apoptosis in R-HepG2 Cells	139
5.2.1	The Role of Mitochondria in HK18 Induced Apoptosis of R-HepG2 Cells	139
5.2.1.1	HK18 Induced Mitochondrial Membrane Depolarization in R-HepG2 Cells	139
5.2.1.2	Addition of Bongkreikic Acid Reduced HK18 Cytotoxicity on R-HepG2 Cells	142
5.2.1.3	Elevation of Intracellular Hydrogen Peroxide Level in HK18 Treated R-HepG2 Cells	144
5.2.1.4	Elevation of Intracellular Ca ²⁺ Level in HK18 Treated R-HepG2 Cells	146
5.3	Downstream Biochemical Changes Induced by HK18 on R-HepG2 Cells	148
5.3.1	Activation of Caspase 3 of R-HepG2 Cells by HK18 as Demonstrated by Western Blot	148
5.3.2	Induction of Caspases Activation of R-HepG2 Cells by HK18 as Demonstrated by Enzymatic Activity Assays	150
5.4	Down-regulation of the Anti-apoptotic Bcl-2 Protein of R-HepG2 Cells by HK18	154
5.5	HK18 was Not a Substrate of P-glycoprotein	156

Chapter 6 Discussion	158
6.1 Cytotoxicity of HK18	159
6.1.1 HK18 was Cytotoxic to the Human Hepatocellular Carcinoma Cell Line HepG2 and Multidrug Resistant Human Hepatocellular Carcinoma Cell Line R-HepG2	159
6.1.2 Study of the Toxicity of HK18	160
6.2 Mechanistic Studies of the Cytotoxic Effects of HK18 on HepG2 Cells	161
6.2.1 Apoptotic Cell Death Induction of HK18 on HepG2 Cells	161
6.2.2 Studies of the Underlying Mechanisms of HK18 Induced Apoptosis of HepG2 Cells	162
6.3 Mechanistic Studies of the Cytotoxic Effects of HK18 on R-HepG2 Cells	181
6.3.1 Apoptotic Cell Death Induction of HK18 on R-HepG2 Cells	181
6.3.2 Studies of the Underlying Mechanisms of HK18 Induced Apoptosis of HepG2 Cells	181
Chapter 7 Future Perspectives	190
Chapter 8 References	193

List of Figures

Fig 1.1	Basic structures of saponins	6
Fig 1.2	Basic structures of monodesmosidic and bidesmosidic saponins	8
Fig 1.3	Structures of Hong Kong compounds	20
Fig 1.4	Photographs of <i>Paris Polyphylla</i>	22
Fig 1.5	Structure of Hong Kong 18 (polyphyllin D)	23
Fig 1.6	Photograph showing the electron microscope of human hepatocellular carcinoma cell line HepG2	26
Fig 1.7	Schematic diagram of P-glycoprotein	30
Fig 2.1	BSA protein standard curve used for protein concentration determination	56
Fig 2.2	Determination of digitonin concentration	62
Fig 2.3	Standard curves of AMC and AFC for determination of caspases enzymatic activities	66
Fig 3.1	Study of cytotoxicity of HK18 and DOX on HepG2 cells for 24 and 48 hours by MTT assay	74
Fig 3.2	Study of the cytotoxicity of HK18 on HepG2 cells by tryphan blue exclusion assay	77
Fig 3.3	Study of cytotoxicity of HK18 and DOX on R-HepG2 for 24 and 48 hours by MTT assay	79
Fig 3.4	Study of the cytotoxicity of HK18 on R-HepG2 cells by Tryphan blue exclusion assay	82
Fig 3.5	Comparison of the cytotoxicity of HK18 on macrophages, HepG2 and R-HepG2 cells	84
Fig 3.6	Study of the hemolytic activity of HK18	86
Fig 3.7	<i>In vivo</i> studies of the toxicity of HK18 by measuring the heart tissue specific enzymes CK and LDH	88
Fig 3.8	<i>In vivo</i> studies of the toxicity of HK18 by measuring the liver tissue specific enzymes AST and ALT	89
Fig 4.1	Quantification of apoptosis by Annexin V-FITC conjugate and PI by flow cytometry	94
Fig 4.2	Phosphatidylserine externalization induced by HK18 on HepG2 cells	96

List of Figures

Fig 4.3	Induction of DNA fragmentation in HK18 treated HepG2 cells	98
Fig 4.4	Proposed schematic diagram of MPT pore complex	100
Fig 4.5	Induction of mitochondrial membrane potential depolarization in HK18 treated Hep2 cells	104
Fig 4.6	Addition of BA would reduce the cytotoxicity of HK18 toward HepG2 cells	107
Fig 4.7	Intracellular H ₂ O ₂ level of HepG2 cells was enhanced by HK18	111
Fig 4.8	Study of the intracellular H ₂ O ₂ level and Ψ m simultaneously of HK18 treated HepG2 cells	113
Fig 4.9	Intracellular Ca ²⁺ level of HepG2 cells was enhanced by HK18	117
Fig 4.10	Study of the intracellular Ca ²⁺ level and Ψ m simultaneously of HK18 treated HepG2 cells	119
Fig 4.11	HK18 induce mitochondrial cytochrome c and AIF release of HepG2 cells	122
Fig 4.12	Activation of caspase 3 and induction of PARP cleavage by HK18 on HepG2 cells	124
Fig 4.13	Caspase 3 enzymatic activity of HepG2 cells was enhanced by HK18	126
Fig 4.14	Caspase 9 enzymatic activity of HepG2 cells was enhanced by HK18 but not caspase 8	128
Fig 4.15	Down-regulation of Bcl-2 expression of HepG2 cells by HK18	130
Fig 4.16	Down-regulation of bcl-2 and bcl-X _L genes transcription of HepG2 cells by HK18	132
Fig 5.1	Induction of phosphatidylserine externalization by HK18 on R-HepG2 cells	136
Fig 5.2	Induction of DNA fragmentation in HK18 treated R-HepG2 cells	138
Fig 5.3	Induction of mitochondrial membrane potential depolarization in HK18 treated R-Hep2 cells	141
Fig 5.4	Addition of Bongkreikic acid (BA) reduced HK18 cytotoxicity on R-HepG2 cells	143
Fig 5.5	Intracellular H ₂ O ₂ level of R-HepG2 cells was enhanced by HK18	145

Fig 5.6	Intracellular Ca ²⁺ level of R-HepG2 cells was enhanced by HK18	147
Fig 5.7	Activation of caspase 3 and induction of PARP cleavage by HK18 on R-HepG2 cells	149
Fig 5.8	Caspase 3 enzymatic activity of R-HepG2 cells was enhanced by HK18	151
Fig 5.9	Caspase 9 enzymatic activity of R-HepG2 cells was enhanced by HK18 but not caspase 8	153
Fug 5.10	Down-regulation of Bcl-2 expression of R-HepG2 by HK18	155
Fig 5.11	HK18 was not a substrate of P-glycoprotein	157
Fig 6.1	Summary of the possible action mechanisms of HK18 exerted of HepG2 cells	180
Fig 6.2	Structures of three substrates of P-gp	186
Fig 6.3	Summary of the possible action mechanisms of HK18 exerted of R-HepG2 cells	189

List of Tables

Table 1.1	Families of anti-tumor drugs and their action mechanisms	27
Table 2.1	List of the chemicals being used in this research project	43
Table 2.2	The compositions of various percentage of SDS gel	57
Table 2.3	List of the anti-bodies used in this project with the corresponding target protein molecular weight, dilution ratio and purchasing companies	59
Table 2.4	List of the sequences of primers used in this project and their corresponding PCR conditions and size of PCR products	70
Table 3.1	Summary of the IC ₅₀ of HK18 and DOX on HepG2 cells treating for 24 and 48 hours by MTT assay	75
Table 3.2	Summary of the IC ₅₀ of HK18 and DOX on R-HepG2 cells treating for 24 and 48 hours by MTT assay	80

Abbreviation

%	Percentage
Ψ_m	Mitochondrial membrane potential
ABC	ATP-binding cassette
Ac-DEVD-AMC	Acetyl-Asp-Glu-Val-Asp-7-amido-4-methylcoumarin
Ac-IETD-AMC	N-Acetyl-Ile2-Glu-Thr-Asp-7-amido-4-methylcoumarin
Ac-LEHD-AFC	N-Acetyl-Leu-Glu-His-Asp-7-amido-4-trifluoromethylcoumarin
ADP	Adenosine diphosphate
AFC	7-amido-4-trifluoromethylcoumarin
AIF	Apoptosis inducing factor
ALT	Alanine transaminase
AMC	7-amido-4-methylcoumarin
ANT	Adenine nucleotide translocator
Apaf-1	Apoptotic protease activating factors –1
APS	Ammonium persulphate
AST	Aspartate transaminase
ATP	Adenosine triphosphate
B[a]P	benzo[<i>a</i>]pyrene
BA	Bongkrelic acid
Bad	Bcl-x _L /Bcl-2 Associated Death Promoter
Bak	Bcl-2 Antagonist/Killer
Bax	Bcl-2 Associated x protein
BCA	Bicinchoninic acid solution

Abbreviation

Bcl-2	B-Cell Leukemia/Lymphoma-2
Bid	BH-3 Interacting Domain Death Agonist
bp	Base pairs
BSA	Bovine serum albumin
<i>C. elegans</i>	<i>Caenorhabditis elegans</i>
Ca ²⁺	Calcium ions
CAD	Caspase-activated Dnase
Caspase	Cysteiny Aspartic Acid-Protease
cDNA	Complimentary Deoxyribonucleic Acid
CK	Creatine kinase
cm ²	Centimeter Square
CO ₂	Carbon dioxide
CsA	Cyclosporin A
Cyp-D	Cyclophilin D
DCF	5-(and 6-)-carboxy-2',7-dichlorodihydrofluorescein diacetate
DED	Death effector domain
DIABLO	Direct IAP binding protein with low pI
DMSO	Dimethylsulfoxide
DNA	Deoxyribonucleic acid
dNTP	Deoxynucleic Triphosphate
DOX	Doxorubicin
E-blot buffer	Electroblotting buffer
ECL	Enhanced chemiluminescence reagents
EDTA	Ethylenediaminetetraacetic acid

Abbreviation

ER	endoplasmic reticulum
FADD	Fas-associated death domain
FBS	Fetal Bovine Serum
Fluo-3	Fluo-3/AM
FSC	Forward scatter
H ₂ O ₂	Hydrogen peroxide
HK	Hexokinase
HK18	Hong Kong compound 18
HPR	Horseradish peroxidase
IAPs	Inhibitor of apoptosis proteins
IC ₅₀	50 % Inhibitory concentration
JC-1	5,5',6,6'-tetrachloro-1,1',3,3'-tetraethylbenzimidazolylcarbocyanine
	Iodide
LDH	Lactate dehydrogenase
MDR	Multidrug resistance
MDR	Multidrug resistant gene
Mn-SOD	Mitochondrial superoxide dismutase
MPT	Mitochondrial permeability transition
MTT	3-(4,5-dimethylthiazol-2-yl)-2,5-diphenyltetrazoliumbromide
MΦ	Macrophages
NaCl	Sodium chloride
NAPH	Nicotinamide adenine dinucleotide
NFκB	Nuclear Factor Kappa B
nm	Nanometer

Abbreviation

nM	Nanomolar
°C	Degree Celsius
OD	Optical density
p	P Value
PARP	Poly(ADP-ribose) polymerase
PBR	Peripheral benzodiazepin receptor
PBS	Phosphate buffered saline
P-gp	P-glycoprotein
PI	Propidium iodide
PMSF	Phenylmethyl-sulphonyl fluoride
PS	Phosphatidylserine
PVDF	polyvinylidene fluoride
RBC	Red blood cell
RNA	Ribonucleic acid
RNase A	Ribonuclease A
ROS	Reactive oxygen species
RPMI	Roswell Park Memorial Institute tissue culture medium
RT-PCR	Reverse transcriptase polymerase chain reaction
SDS	Sodium didecyl sulphate
Smac	Second mitochondria-derived activator of caspase
SOD	Superoxide dismutase
SSC	Side scatter
TBS-T	Tris-buffered saline-Tween-20
TCM	Traditional Chinese Medicine

Abbreviation

TMRE	Tetramethylrhodamine, ethyl ester, perchlorate
TPA	12- <i>O</i> -tetradecanoylphorbol-13-acetate
v/v	Volume by Volume
VDAC	Voltage-dependent anion channel
Vin	Vincristine
w/v	Weight by Volume
z-DEVD-fmk	z-Asp(Ome)-Glu(Ome)-Val-Asp(Ome)-CH ₂ F
z-IETD-fmk	z-Ile-Glu(Ome)-Thr-Asp(Ome)-CH ₂ F
z-LEHD-fmk	z-Leu-Glu(Ome)-His-Asp(Ome)-fmk
μg	Micogram
μl	Microliter
μM	Micromolar



Chapter 1

Introduction

1. INTRODUCTION

In these few decades, the medicinal and pharmacological effects of natural products aroused a great interest for scientists. It is because they possess diverse pharmacological effects such as hypolipidemic, anti-platelet, anti-tumor and immunomodulatory activities with relatively low side effects. These biological activities are useful in reducing the risk of cardiovascular disease and cancer development, which are the leading causes of death worldwide (Craig, 1999; Gerber *et al.*, 2002; Wargovich, 1999; Kucuk, 2002). From these natural products, a wide variety of phytochemicals have been identified. For example, flavonoids of many edible plants such as green tea and citrus have been proven to exhibit anti-tumor activities, anti-inflammation and cardiovascular protective activities (Kris-Etherton and Keen, 2002; Manthey *et al.*, 2001; Riemersma *et al.*, 2001). Polyphenolics such as resveratrol from grapes and red wine have been found to possess anti-tumor activities and can inhibit oxidation of low density lipoprotein and hence reduce the risk of atherosclerosis and coronary heart diseases (Frankel *et al.*, 1993; Surh *et al.*, 1999; Jang *et al.*, 1997). Apart from these, other active components from natural products such as lignans, plant sterols, curcumins, coumarins and saponins also have significant health promoting activities (Craig, 1999). Among these phytochemicals, saponin is one of the focuses. It is because saponins exhibit diverse biological activities and can be found in many plants that we consume.

1.1 Characteristic of Saponins

Saponins are high molecular weight glycosides, which comprise of two main parts: a saccharide moiety linked with a steroid or triterpene group. They can be found in many plants and some marine animals. Some of them are surface active and hence used as detergent for centuries. The common feature of forming soapy lather when shaken with water was used as a primary method in determining the presence of saponins (although some saponins do not form lather with water). Actually the name “saponin” is derived from the Latin word “sapo” which means soap (Hostettmann and Marston, 1995a)

1.1.1 Occurrence of Saponins

Saponins are widely distributed in the plant kingdom. They can be found in many plants, which are consumed by human beings. For examples, soybeans, peanuts, broad beans, kidney beans, garlic, potatoes, tomatoes, onions, tea (Oleszek, 2000) and some Traditional Chinese Medicine (TCM) such as *Panax ginseng*. Besides, they are found in different parts of a plant including roots, shoots, flowers and seeds. Some marine animals particularly the echinoderms such as sea cucumbers and starfishes also contain saponins (Hostettmann and Marston, 1995b).

1.1.2 General Properties of Saponins

1.1.2.1 Emulsifying Agents

Saponins are amphiphilic in nature. The steroid or triterpene group is responsible for the hydrophobic property while the saccharide moiety contributes to the hydrophilic character. Therefore, saponins are surface active and form micelles in

the same way as detergents (Hostettmann and Marston, 1995d).

1.1.2.2 Forming Complex with Cholesterol

Saponins can form complex with cholesterol, lecithin, ergosterol, phenols and thiophene (Hostettmann and Marston, 1995d). Systematic studies on the ability of saponins to complex with cholesterol have been carried out. This saponin-cholesterol complex formation property is making use of vaccination, which will be discussed later.

1.1.2.3 Hemolytic Property

Some of the saponins are hemolytic. The emulsifying nature of saponins reduces the surface tension of the aqueous and lipid phases of red blood cell membrane, which leads to departure of lipids from the membrane. Hence, the red blood cell membrane becomes permeable and allows water and Na^+ influx and K^+ ions to leave. Finally, membrane rupture and hemoglobin leaks out (Hostettmann and Marston, 1995d). Incubating the saponin of interest with red blood cells and then measuring the amount of hemoglobin released can be used to study this property. The higher the hemolytic activity, the larger the amount of hemoglobin released. The hemolytic activity varies considerably with the structure of glycoside. In general, hemolytic activity of saponins decreased with the length and the branching of the sugar chain (Romussi *et al.*, 1980).

1.1.3 Structure of Saponins

Saponins are high molecular weight glycosides, which consist of two main parts. A polycyclic backbone linked with a saccharide moiety via ether or ester linkage. The non-saccharide or aglycone part is called sapogenin. Structural variations of saponins mainly lie in the attachment of different saccharide group to the sapogenin. Actually saponins can be divided into two categories based on the structure of sapogenin. They are triterpene saponins and steroid saponins (Hostettmann and Marston, 1995a).

1.1.3.1 Categories of Saponins

1.1.3.1.1 Triterpene Saponins

In the world, most saponins found belong to this category. They have been found in many families of plants such as Leguminosae and Araliaceae (Hostettmann and Marston, 1995b) (Fig.1.1 A).

1.1.3.1.2 Steroid Saponins

Steroid saponins are relatively less abundant than triterpene saponins. They have been found in the family of Liliaceae, Agavaceae as well as Dioscoreaceae (Hostettmann and Marston, 1995b). And the herb genera commonly used in China that contain steroid saponins as active component include *Dioscorea*, *Paris*, *Polygonatum*, *Ophiopogon* and *Allium* (Yu and Hui, 20021). They are further sub-divided into spirostan saponins and furostan saponins (Oleszek, 2000) (Fig.1.1B, C).

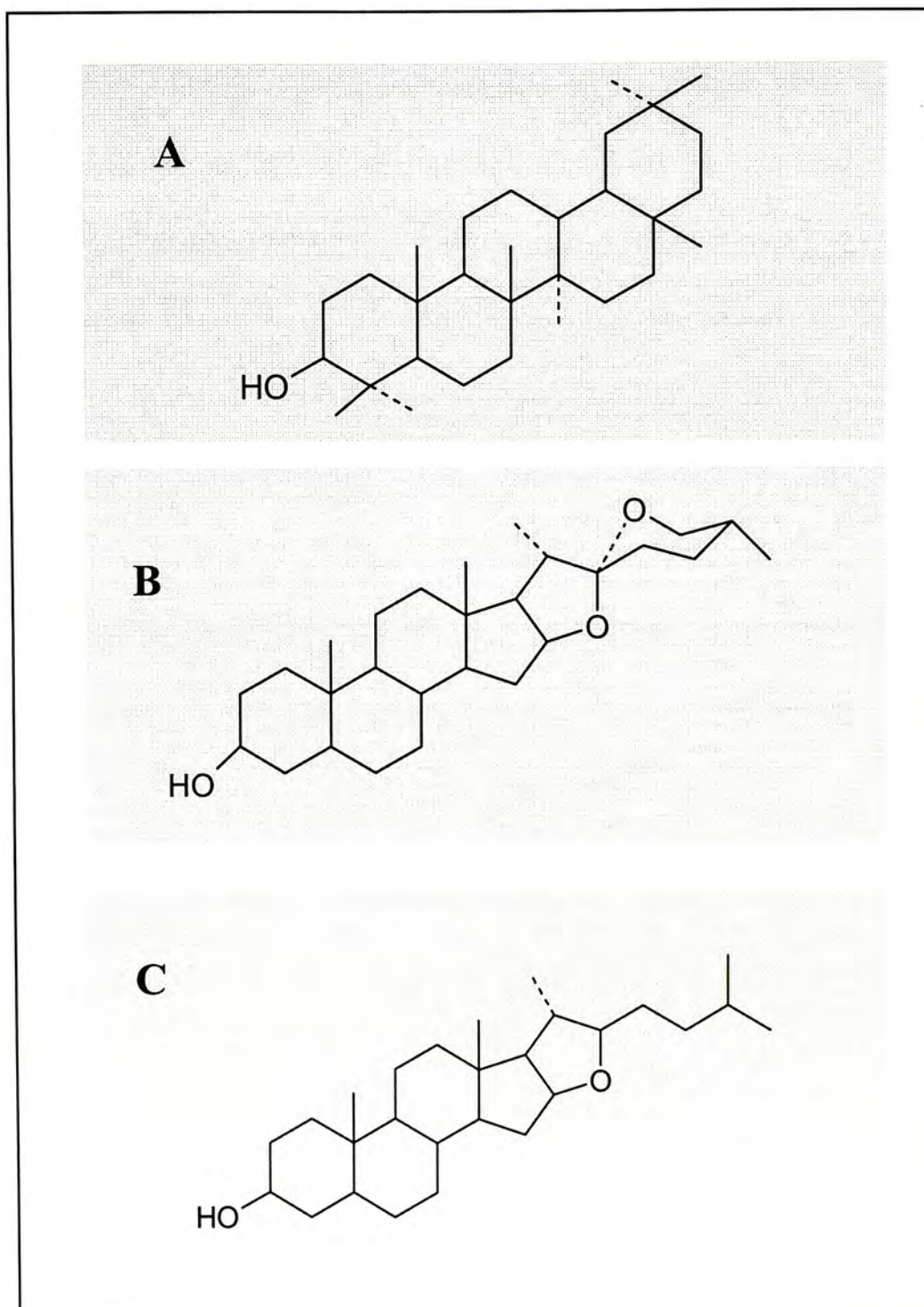


Fig 1.1 Basic structures of saponins. (A) Triterpene saponin. (B) Spirostan steroid saponin and (C) Furostan steroid saponin.

1.1.3.2 Monodesmosidic and Bidesmosidic Saponins

The sapogenin can be linked with one or two saccharide chains, which are called monodesmosidic and bidesmosidic saponins (Greek *desmos* = chain) (Oleszek, 2000). For the one linked with one saccharide at the C-3 position is known as monodesmosidic saponins. While bidesmosidic saponins have two saccharide chains with one normally attached at the C-3 position and another at the C-28 position for triterpene saponins or at the C-26 position for the furostanol steroid saponins (Hostettmann and Marston, 1995a; Oleszek, 2000) (Fig.1.2).

The saccharide moiety can be either linear or branched and the most common saccharides found are D-glucose, D-galactose, D-glucuronic acid, D-galacturonic acid, L-rhaminose, L-arabiose, D-xylose and D-furose (Hostettmann and Marston, 1995a).

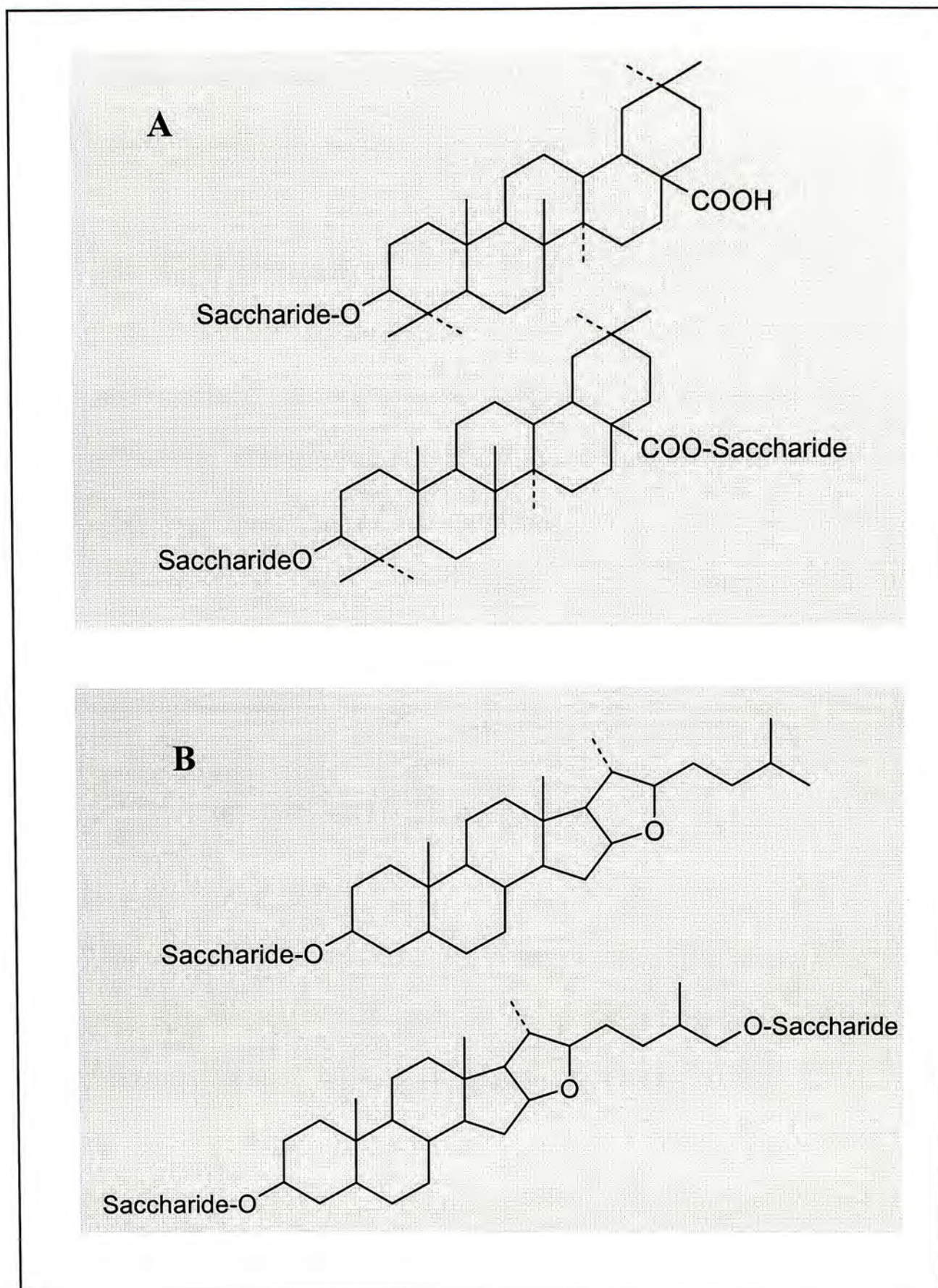


Fig 1.2 Basic structures of monodesmosidic and bidesmosidic saponins.

(A) Tritepene saponins. (B) Steroid Saponins

1.1.4 Biological and Pharmacological Properties of Saponins

Saponins have a variety of biological and pharmacological activities such as anti-microbial, spermdicidal and anti-tumor activity.

1.1.4.1 Anti-microbial Activity

Since saponins are widely distributed in plants, it seems that they play a vital role in their producer. Researches have found that they protect the plant from microbial invasion including fungal, bacterial and viral infections (Hostettmann and Marston, 1995d; Hostettmann and Marston, 1995c). The saponin content of the plant usually increases in the region under attack. It has been proposed that during invasion, the water soluble inactive form of saponin will transports to the infected region where it converts into the active form and acts on the microbial (Hostettmann and Marston, 1995d).

1.1.4.1.1 Anti-fungal Activities

Studies indicated that there are many fungal species respond to the anti-fungal activities of saponins such as *Phytophthora cinnamoni* and *Rhizopus mucco* (Zablotowicz *et al.*, 1996; Timberkova *et al.*, 1996). The mechanism of how saponins kill the fungi has not yet been determined, but it was proposed that saponins interact with the fungal membrane components such as sterols, proteins or phospholipids and hence destroy the cellular semi-permeability and leading to death (Gruiz, 1996; Osbourn *et al.*, 1996). Recently, scientists have been trying to apply these anti-fungal activities on human fungal infectious diseases (Zehavi and Polacheck, 1996).

1.1.4.1.2 Anti-bacterial Activities

Several saponins have anti-bacterial activities. In general, the potency of steroid saponins is higher than tritenepene saponins and gram positive bacteria are more sensitive than gram negative bacteria (Oleszek, 2000; Hostettmann and Marston, 1995d).

1.1.4.1.3 Anti-viral Activities

It has been found that some saponins can reduce viral infection and possibly by acting on one or more steps of the viral replication cycle and inhibit virus-host cell attachment (Hostettmann and Marston, 1995d). Enveloped virus is generally more sensitive than naked virus (Oleszek, 2000). The viruses, which can be inhibited by saponins such as glycyrrhizin (甘草)(Hasegawa *et al.*, 1994), include Herpes simplex virus, poliovirus (Oleszek, 2000) as well as human immunodeficiency virus (HIV) (Oleszek, 2000).

1.1.4.2 Insecticide Activity

Reports have shown that some saponins are insecticidal. For example, some woods are resistant to termite attack due to the presence of saponins (Hostettmann and Marston, 1995d; Tava and Odoardi, 2002).

1.1.4.3 Molluscicidal Activity

Some saponins are toxic to the organisms, which use gills for breathing such as fishes and frogs. Binding of the saponins to the gill membrane will increase its permeability and cause the losses of important physiological electrolytes

(Hostettmann and Marston, 1995d). Besides, some saponins are toxic to mollusk such as snails. This property has been made use of to control the schistosomiasis, a parasite disease that affects millions of people in South America, Africa and Asia. Snail is required as the vector for this parasite (Hostettmann *et al.*, 2002; Thiilborg *et al.*, 2002). By eliminating the vector, the spreading of the parasite can be controlled.

1.1.4.4 Hypocholesterolemic Activity

Studies have found that consumption of saponins can reduce the amount of cholesterol in circulation and tissues (Hostettmann and Marston, 1995d). They form insoluble complex with cholesterol, hence intestinal absorption of both endogenous and exogenous cholesterol is prohibited. Besides they form mixed micelles with the enterohepatic circulating bile acids and thus inhibit their reabsorption from the terminal ileum (Oakenfull, 2001). A study has shown that the saponin fractions of garlic lowered the plasma total cholesterol and LDL-cholesterol levels in a hypercholesterolemic animal model and hence reduced the risk of cardiovascular disease (Matsuura, 2001).

1.1.4.5 Anti-ulcer Activity

Most of the gastric ulcer is emerged when gastric acid or pepsin is over-secreted or the protective mucosal lining barrier is weaken. Some saponins possess anti-ulcer activity by promoting mucus formation or directly activating the gastric membrane protective factors (Hostettmann and Marston, 1995d). For example, the saponins isolated from the rhizome of *Panax japonicus* have been demonstrated to have gastro-protective properties (Borrelli and Izzo, 2000). Actually, a patent

anti-ulcer tablets contains quillaiasaponins (Hostettmann and Marston, 1995d).

1.1.4.6 Contraceptive Activity

Recently, numerous of medicinal plants have been investigated for their anti-fertility activity in order to find out a new source of conceptive agents. It has been found that some of saponins such as those from *Mollugo pentaphylla* and *Acacia auriculiformis* are potential contraceptive agents due to their spermicidal and sperm immobilizing activity (Garg *et al.*, 1994; Rajasekaran *et al.*, 1993; Pakrashi *et al.*, 1991; Dhar *et al.*, 1989).

1.1.4.7 Immunomodulatory Activities

It is well known that the immune system plays an important role in maintaining health of an organism. For example, patients of human immunodeficiency disease (HIV) are far easier to die from complications since their immune systems are defective. Therefore, a substance, which is able to improve the immune system, is a useful agent and many saponins have found to exhibit immunomodulatory activity.

1.1.4.7.1 Direct Immunostimulation

In vitro studies have shown that some saponins are able to induce the proliferation of both B- and T-lymphocytes directly as well as potentiate the mitogenic responses of T cells and B cells toward phytohemagglutinin (PHA), concanavalin (ConA) and lipopolysaccharides (LPS) (Chavali *et al.*, 1987; Calis *et al.*, 1997; Lacaille-Dubois *et al.*, 1993). One of the saponins isolated from *Panax*

ginseng has been found to induce T-helper cells production (Kenarova *et al.*, 1990) and natural killing cell activity (Kenarova *et al.*, 1990; Zhang *et al.*, 1990). Moreover, it has been reported that phagocytosis of macrophage and interleukin-1 production could be enhanced by saponins (Kenarova *et al.*, 1990; Plohmann *et al.*, 1997). For *in vivo* studies, saponins could promote spleen lymphocytes proliferation in mice (Xu *et al.*, 1992) and increase the phagocytotic activities of peritoneal macrophages including spreading activity, phagocytosis, lysosomal enzyme activity and intracellular killing activity (Lacaille-Dubois, 1998).

1.1.4.7.2 Acting as Immuno-adjuvants

Apart from direct immunostimulation, saponins can be used as vaccine adjuvants. Traditionally, vaccines are made of live-attenuated or inactivated whole bacteria or viruses. Although the microorganisms are inactivated, the recipients still have the risk of developing side effects and in some rare cases may cause death. Immunosuppressed patients are more prone to such risks. Thus, the new generations of vaccines are made of antigen subunits either derived from the pathogens or prepared by molecular, biological or chemical techniques. These preparations are much safer but they are less immunogenic. To solve this problem, immuno-adjuvants are used. An immuno-adjuvant is any substance that enhances the immune response to an antigen with which it mixed. Saponins are one of the classes of adjuvants used nowadays.

The most well known and widely used saponin-type adjuvant are derived from the inner bark of the South American soap tree, *Quillaja saponaria*

(Lacaille-Dubois, 1998). For example, in the presence of *Quillaja* saponin, rabies vaccine stimulates significantly higher serum neutralizing antibody responses than orally administered the vaccine alone (Chavali *et al.*, 1988; Chavali and Campbell, 1987). Also, there was increased T-helper and B cell co-operation and hence enhanced antibody production. Moreover, it may act by induction of gamma interferon release (Lacaille-Dubois, 1998; Sasaki *et al.*, 1998).

Besides, saponins are used to synthesize immune stimulating complex (ISCOM) by making use of their cholesterol-binding characteristic (Lacaille-Dubois, 1998). ISCOM is an immuno-adjuvant which is made by mixing cholesterol, phospholipids and *Quillaja* saponins in a ratio of 1 : 1 : 5. The complex forms a cage-like structure with hydrophobic inner space. Thus, the hydrophobic part of an antigen can be inserted into the structure with hydrophilic part stay outside the complex (Lacaille-Dubois, 1998) (Smith *et al.*, 1999).

1.1.4.8 Anti-tumor Activity

Apart from the biological functions mentioned in the above paragraphs, the anti-tumor activities of saponins have arouse a great interest to scientists since cancer is the most leading cause of death in the world. Actually cancer development is a complicated process. It involved three main stages, which are initiation, promotion and progression. The tumor cannot be reversed once it is established. Thus, compounds that can inhibit tumor initiation and promotion are useful anti-tumor agents and are regarded as chemopreventive agents.

1.1.4.8.1 Anti-carcinogenesis

Panax ginseng C. A. Meyer (人參), which belongs to the *Araliaceae* family, is a famous TCM and is believed to prolong, strengthen life and invigorate bodies. Actually it has been reported that ginseng has modulatory effect on central nervous system, cardiovascular system, endocrine system and immune system. Recently, researchers have found that one of the active components is saponin. The triterpene saponins isolated from ginseng exhibit anti-tumor promoting activities as demonstrated by the two-stage mouse hepatic carcinogenesis test by using the initiator N-nitrosodiethylamine and the promoter phenobarbital (Konoshima *et al.*, 1999) as well as in the two-stage mouse skin carcinogenesis test by using peroxyxynitrite as initiator and 12-*O*-tetradecanoylphorbol-13-acetate (TPA) as promoter (Konoshima *et al.*, 1999). In addition, ginseng saponins metabolites were able to inhibit the tumor initiating activity of the well-known tumor initiator benzo[*a*]pyrene (B[*a*]P) (Lee *et al.*, 1998). And apart from ginseng saponins, saponins from other TCM and natural products also exhibit potent anti-carcinogenesis activity. For example, the saponins from leguminous plants inhibit cancer development in the two-stage mouse skin carcinogenesis test with 7,12-dimethylbenz[*a*]anthracene as initiator and TPA as promoter (Hanausek *et al.*, 2001). And other steroid saponins such as *Lilium speciosum* (豔紅鹿子百合) have been found to inhibit the promoting activity of the tumor promoter TPA as well (Nakamura *et al.*, 1994). Moreover, the crude extracts of some TCM which are rich in saponins such as *Paris polyphylla* (七葉一枝花) have found to inhibit the tumor-initiating activity of B[*a*]P and picrolonic acid (Lee and Lin, 1988).

1.1.4.8.2 Suppression of Tumor Growth

Nowadays, there are several approaches in treating cancer. They are surgical removal of the tumor, radiation and administered of chemotherapeutic drugs to kill the cancer cells. Apart from killing the cancer cells, most of the chemotherapeutic drugs also exert toxic effects on normal tissues. Thus researchers keep on finding substitution and much attention was paid on natural products because they usually possess fewer side effects relatively. Many studies have found that some saponins have anti-tumor activities (Rao and Sung, 1995). For example, some of the ginseng saponins and their metabolites were cytotoxic to several cancer cell lines including prostate cancer LNCaP cells, human myeloid leukemia HL-60 cells, pulmonary adenocarcinoma PC-14 cells, gastric adenocarcinoma MKN-45 cells and human hepatocellular carcinoma HepG2 cells (Lee *et al.*, 1999). Moreover, they have been found to induce apoptosis in hepatocellular carcinoma cell line SK-HEP-1 cells (Kim *et al.*, 1999b) as well as brain tumor rat C6 gliomal cells (Kim *et al.*, 1999a). The occurrence of apoptosis in saponins-treated cells was demonstrated as morphological change, DNA fragmentation, appearance of sub-G1 peak in PI staining of flow cytometric analysis (Lee *et al.*, 2000) and the mechanism of apoptosis including caspase 3 activation (Lee *et al.*, 2000; Liu *et al.*, 2000; Park *et al.*, 1997), cytochrome c release (Lee *et al.*, 2000) and over-expression of p53 protein (Kim *et al.*, 1999b). On the other hand, some studies have found that the bcl-2 protein level was down-regulated (Liu *et al.*, 2000) while some studies found that they were bcl-2 independent (Kim *et al.*, 1999a). Apart from these, soybean saponins and steroid saponins from *Lilaceae* plants also have anti-tumor activity on several cancer cell lines including HL-60 cells and human T-lymphocyte leukemia MOLT-4 cells

(Hirano *et al.*, 1996; Qian *et al.*, 1999). Furthermore, two steroid saponins extracted from *Cordyceps sinensis* (冬蟲夏草) inhibited the proliferation of several cancer cell lines including HL-60 cells, erythroleukemia K562 cells, T-lymphoblastic Jukat cells, malignant melanoma WM1341 cells and multiple myeloma RPMI 8226 cells (Bok *et al.*, 1999).

Besides of inducing apoptosis, some saponins can induce cell cycle arrest. The saponins of the bulbs of *Ornithogalum saundersiae*, a *Liliaceae* family plant have been found to induce cell cycle arrest at the G2 / M phase of HL-60 cells (Lee and Lin, 1988). And ginseng saponins have been found to induce cell cycle arrest at the G1 / S phase with down-regulation of cyclins E- and A-dependent kinase activities (Kim *et al.*, 1999b).

In the later phase of cancer, the tumor cells may gain invasive power and leave the primary tumor site and invade other organs or tissues. This process is known as metastasis. Actually metastasis is the major cause of death in cancer patients. Thus agents, which can reduce the occurrence of metastasis, can save many lives. Recent studies found that several saponins could reduce metastasis both *in vitro* and *in vivo* (Mochizuki *et al.*, 1995; Shinkai *et al.*, 1996). And they could inhibit angiogenesis, formation of new blood vessel, a process that is important for the growth of tumor (Shinkai *et al.*, 1996).

1.1.5 Anti-tumor Activity of Steroid Saponins

From these studies, it indicated that some saponins possess anti-tumor activities in various respects. And it seems that steroid saponin is a potential candidate for cancer treatments. Since they are originated from natural products, which are used for medicinal purposes with a long history, most probably have lower toxicity. Therefore we are interested in further study the anti-tumor activities of steroid saponins.

1.1.5.1 Diosgenin Steroid Saponin

Among the various plant families, *Dioscoreaceae* (薯蕷科) and *Liliaceae* (百合科) are the most abundant sources of steroid saponins (Hostettmann and Marston, 1995b). Saponins isolated from these families share the same steroid aglycone called diosgenin, which linked with various saccharide side chains. The rhizomes of *Dioscorea collettii* var. *hypoglauca* (紛背薯蕷) are used in the TCM “Fen Bei Bi Xie” for the treatment of cervical carcinoma, carcinoma of urinary bladder and renal tumor in China (Hu *et al.*, 1999). It was included in the Pharmacopoeia of People’s Republic of China (1990 version). A study has found that the steroid saponins isolated from this medicine were anti-neoplastic (Hu *et al.*, 1999).

1.1.5.2 Hong Kong Compounds

Diao Xin Xue Kang (地奧心血康) is a cardioprotective drug commonly used in China. From this drug, several diosgenin saponins were isolated and were organic synthesized which we named as Hong Kong Compounds (HK) 3, 5 and 9. Under the kind co-operation with Professor Yu Biao (俞飈) of the Shanghai Institute of

Organic Chemistry, Chinese Academy of Science, a series of HK compounds were synthesized based on the structure of the HK compounds found in Dio Xin Xue Kang. There are totally fifteen Hong Kong compounds synthesized. All these HK compounds share the same diosgenin aglycone linked with various structures of saccharide chains (Fig 1.3).

The HK compounds were total organic synthesized (Deng *et al.*, 1999; Li *et al.*, 2001) in the form of powder and were stored at 4°C. They were dissolved in DMSO and then diluted with buffer for studies. The stock solution was kept and used within two weeks. In order to study the potency of the HK compounds, 2 µM of each HK compounds were used to incubate with HepG2 cells and HL-60 cells for 24 hours for screening. Moreover, the HK compounds were incubated with the normal Lung fibroblast cell line WI-38 cells to study their toxicity. After incubation, MTT assay was carried out. We have found previously in our laboratory that all the saponins were non-toxic against WI-38 cells. And among the derivatives, HK18 possessed the most cytotoxic effects on both cancer cell lines (data not shown). Therefore, we chose HK18 for further study.

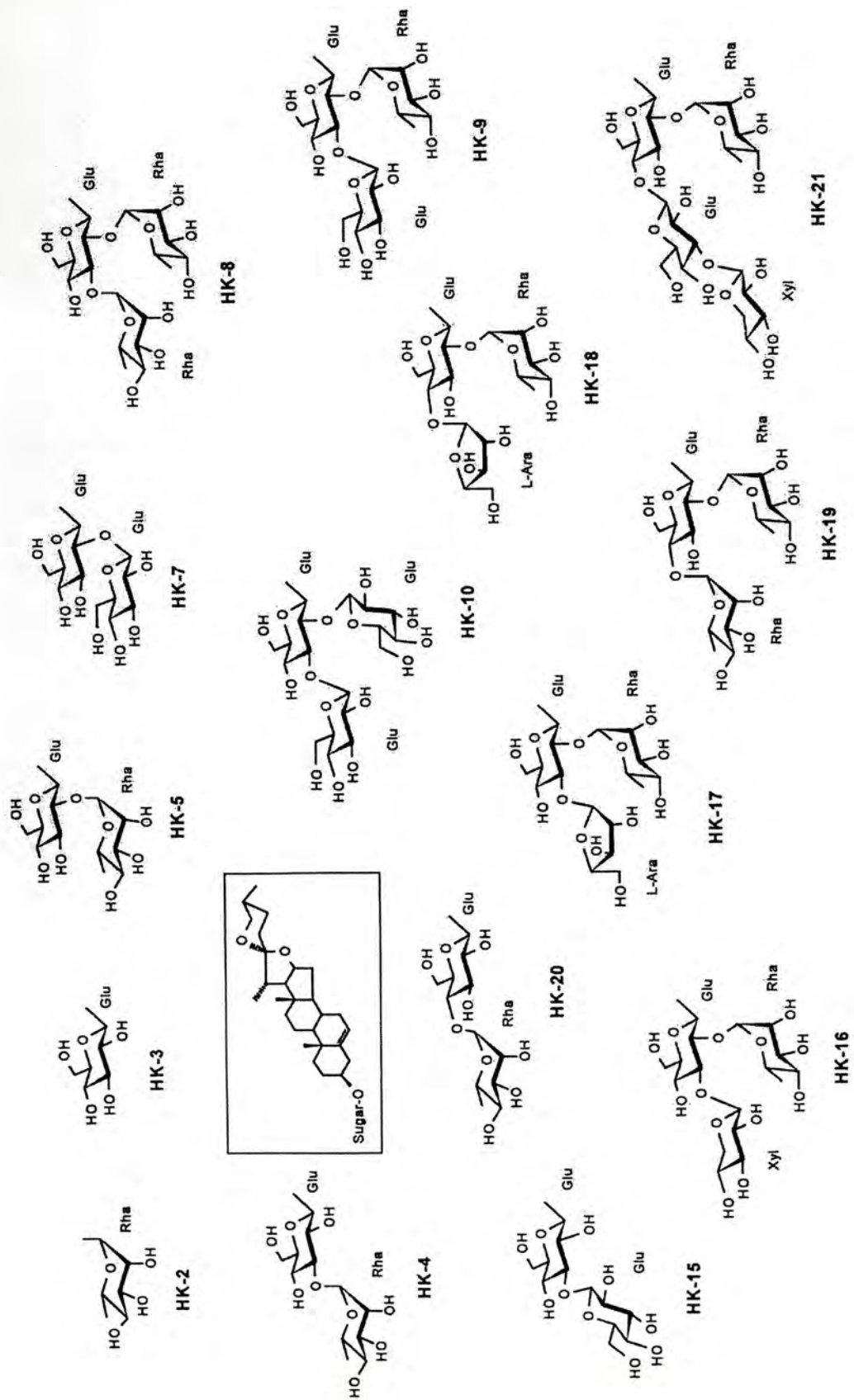


Fig 1.3 Structures of Hong Kong compounds.

1.1.5.3 Hong Kong 18

Actually HK18 (scientific name polyphyllin D) can be found in the Chinese herbal drug *Yunan Bai Yao* (雲南白藥) and the *Liliaceae* family plant *Paris polyphylla* (七葉一枝花) (Deng *et al.*, 1999; Ravikumar *et al.*, 1979) (Fig 1.4). It has been found that polyphyllin D was cytotoxic to leukemia P-388, lymphocytic leukemia L-1210 and human nasopharynx tumor 9KB cell lines (Ravikumar *et al.*, 1979). *Paris polyphylla* was used as folk medicine in China. The rhizome of the plant is known as Chong-lou (重樓) and was prescribed to cure mastitis, sore throat, convulsion and tuberculous meningitis etc. Also, it is used to treat tumors of respiratory system, digestive tract, liver, pancreas, urinary bladder, brain and leukemia (<http://www.healthphone.com>). Scientific researches have found that it exhibited several pharmacological activities including anti-inflammatory, spermicidal, hemostatic, anti-bacterial, sedative, analgesic and anti-tumor activities. In fact, *Paris polyphylla* is commonly used to treat liver cancer as well as nose and throat cancers in China (<http://www.brave-souls.com/resources/cancer13.html>).



Fig 1.4 Photographs of *Paris Polyphylla*.

The systematic name of polyphyllin D (HK18) is diosgenyl α -L-rhamnopyranosyl-(1 \rightarrow 2)-[(α -L-arabinofuranosyl-(1 \rightarrow 4))- β -D-glucopyranoside (Fig 1.5). It was synthesized by Professor Yu Biao by the means of stepwise glucosylation (Deng *et al.*, 1999; Li *et al.*, 2001). Its molecular formula is $C_{44}H_{72}O_{16}$ and molecular weight is 855.02. Since it is an amphiphilic compound, it is not soluble in water but soluble in DMSO and γ -cyclodextrin. We made use of these solvents to prepare HK18 solutions for studying the anti-tumor effect of HK18 on human hepatocellular carcinoma cells.

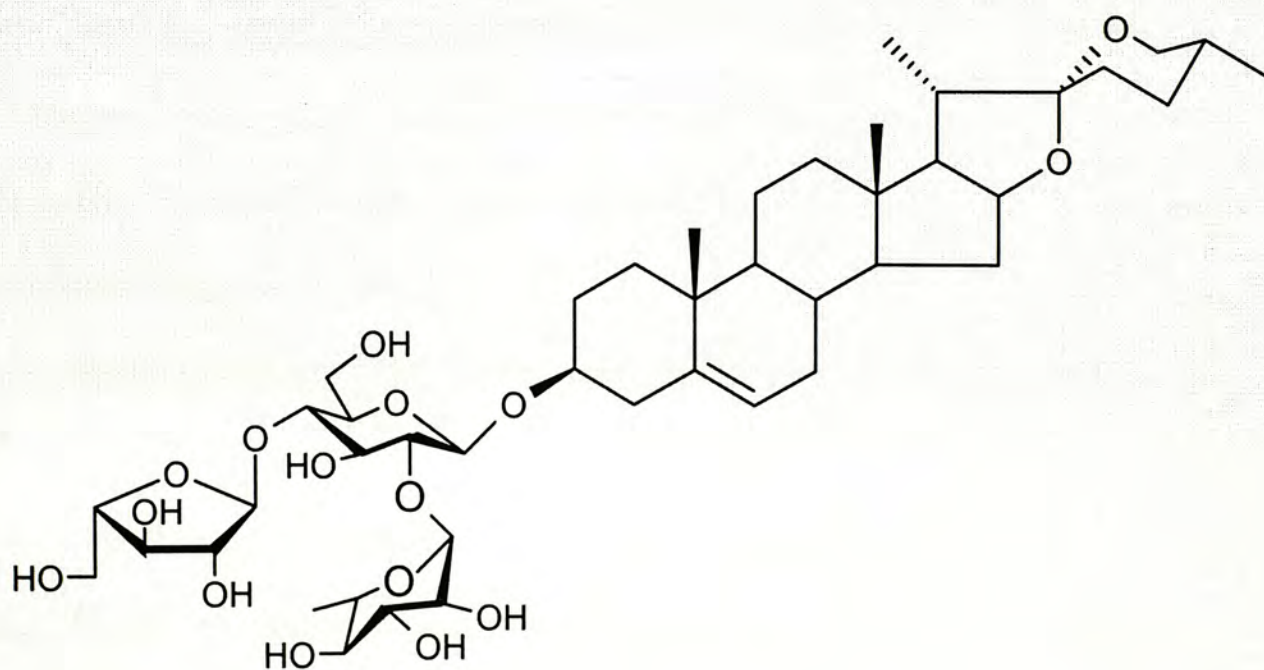


Fig 1.5 Structure of Hong Kong 18 (polyphyllin D).

1.2 Human Hepatocellular Carcinoma (HCC)

1.2.1 The Incidence of Liver Cancer

In Hong Kong, the most leading causes of death are malignant cancer, heart diseases and cerebrovascular diseases. Among these leading causes, malignant cancer is the number one killer, which accounted for around 32 % of mortality. And among the different kinds of cancer, liver cancer is the second commonest (<http://www.ha.org.hk/hesd/nsapi>).

1.2.2 Classification of Liver Cancer

There are two classes of adult primary liver cancer; they are hepatocellular carcinoma (HCC) (肝細胞癌) and cholangioma (膽管瘤) (<http://www.cancerbacup.org.uk/info/liver.htm>). Cholangioma is derived from intrahepatic biliary epithelial cells which accounted for around 13 % of liver cancer. While HCC is originated from liver parenchymal cells (hepatocytes), which accounts for around 75 % of liver cancer (http://health.yahoo.com/health/cancer_center/acs_crc/liver_cancer/index.html).

HCC is often extensively invasive or multicentric, hence it is difficult for surgical removal. And it is positively associated with hepatitis B and C infection, liver cirrhosis and exposure to aflatoxin (the toxin produced by the mould of peanuts). It causes about one million of deaths worldwide per year. And since the incidence rate of hepatitis in Asia is high, the occurrence of HCC in Asia is higher than the Western countries. It is no doubt that HCC causes a great loss to us; thus, it is need to search new remedies for its treatment.

1.2.3 Human Hepatocellular Carcinoma Cell Lines

1.2.3.1 Human Hepatocellular Carcinoma Cell Line HepG2

In my research project, the human hepatocellular carcinoma cell line HepG2 was employed for studies. HepG2 cells are epithelial in shape and resemble liver parenchymal cells morphologically. Fig 1.6 shows the electron microscopy of the cells (Miyazaki and Namba, 1994).

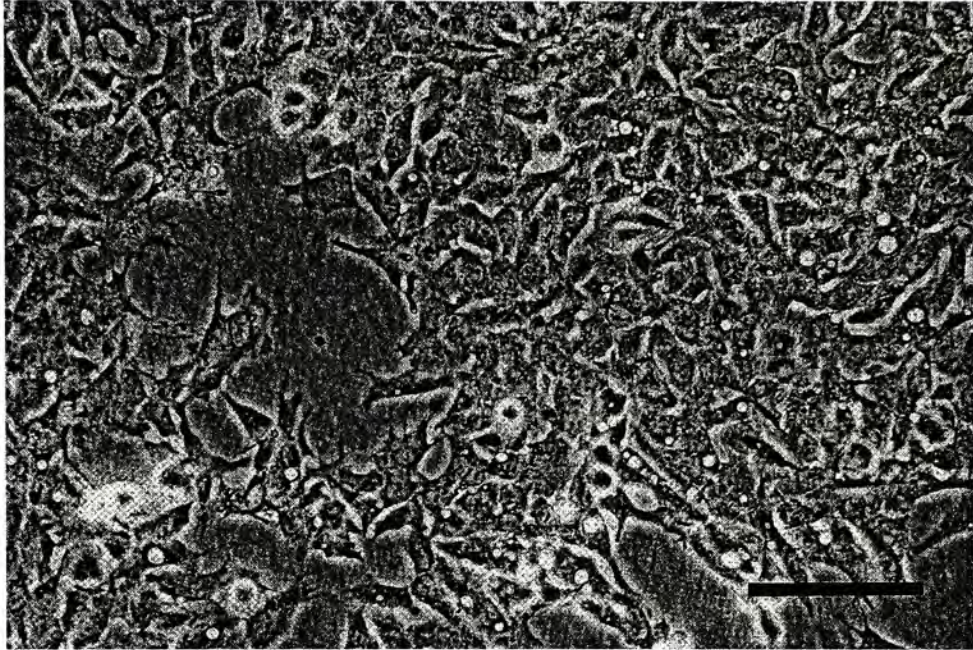


Fig 1.6 Photograph showing the electron microscope of human hepatocellular carcinoma cell line HepG2 (Adapted from Miyazaki and Namba, 1994).

1.2.3.2 Multidrug Resistant Human Hepatocellular Carcinoma Cell Line R-HepG2

Apart from HepG2 cells, multidrug resistant HepG2 cell line (R-HepG2) was also used. This cell line was developed in our laboratory by incubating HepG2 cells with stepwise increasing concentrations of Doxorubicin as will be introduced in the material and method chapter. The established cell population possesses over-expressed p-glycoprotein as demonstrated by Northern Blot and Western Blot analysis (Chan *et al.*, 2000). Besides, this cell line has shown to become multidrug resistant including resistant to the cytotoxic effects of Doxorubicin, Vincristine and Methotrexate (Chan *et al.*, 2000).

Multidrug resistance (MRD) is the avoidance of tumor cells from the actions of a numerous chemotherapeutic drugs differing in chemical structures and action mechanisms. Treatment of cultured cells with a single anti-tumor drug resulted in the establishment of a cell population, which resist to numerous unrelated drugs, i.e. cross-resistance (Stavrovskaya, 2000). Table 1.1 listed the families of anti-tumor drugs that have been found to be resistant by MDR with their action mechanisms.

Families of anti-cancer drugs	Example of drugs	Action mechanisms
Anti-cancer antibiotics	Doxorubicin	Topoisomerase inhibition
Anti-metabolites	Methotrexate	Inhibition of enzymes participating in DNA and RNA synthesis
Drugs derivated from plants	Vinca alkaloids (Vincristine)	Microtubules disassembling

Table 1.1 Families of anti-tumor drugs and their action mechanisms.

1.2.3.2.1 Mechanisms of Multidrug Resistance (MDR)

The emergence of multidrug resistance (MDR) of tumor cells is the major barrier for cancer chemotherapy. Some tumor cells are intrinsic MDR that means the cells are already resistant to anti-cancer drugs before treatment. This type of MDR may happen in some genetically pre-disposed tumor cells or due to the location of the tumor. For example, brain tumors are resistant to chemotherapy due to the blood-brain barrier (Stavrovskaya, 2000).

On the other hand, some tumor cells acquire MDR during anti-cancer treatments. There are several mechanisms that cause the cells to become MDR. First of all, the detoxification enzymes may be activated such as superoxide dismutase and the glutathione detoxification system e.g. glutathione S-transferase. And the genes involved in the control of apoptosis such as p53 and Bcl-2 may alter. Moreover, alternation of drug targets or enhancement of target repair may occur. For example, topoisomerase II inhibitors act on topoisomerase II to prevent DNA replication, however, in MDR cells, the topoisomerase II was mutated and so the inhibitors cannot act on it. Another example is the enhancement of DNA repairment and hence reverses the DNA damaging introduced by anti-cancer drugs (Stavrovskaya, 2000; Arceci, 2000). Apart from these, another mechanism has been under intensive study, is the decrease of drug accumulation in cells by increasing drug efflux. This kind of MDR can be achieved by activation of the transmembrane proteins efflux pump such as P-glycoprotein (P-gp) (Arceci, 2000).

1.2.3.2.2 Structure and Characteristics of P-glycoprotein

P-glycoprotein (P-gp) is a 170 kDa plasma membrane protein encoded by the MDR genes which located at the chromosome 7 in human. Only the P-gp encoded by MDR1 gene accounted for the phenotype of MDR. It is a member of the ABC (ATP-Binding Cassette) transporters that means it possesses an ATP binding domain and ATP is required for its function. It transverses the plasma membrane twelve times and forms a pore across the membrane (Fig 1.7). The pore diameter of hamster P-gp has been found to be 5 nm (Rosenberg *et al.*, 1997). It has a negatively charged hydrophobic cavity. It is proposed that cationic lipophilic substrates (including some anti-cancer drugs) will be pumped out from intracellular space in the expense of ATP. As a result, it reduces the quantity of anti-cancer drugs inside tumor cells and hence reduces their anti-tumor activities (Di Pietro *et al.*, 1999; Mickley and Fojo, 1998).

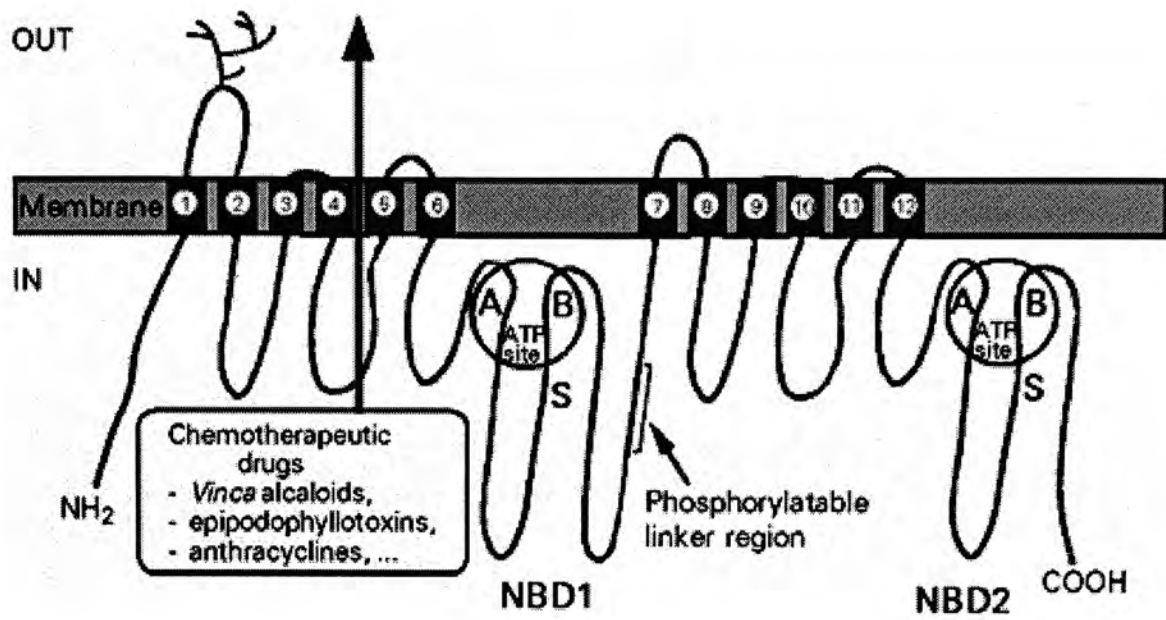


Fig 1.7 Schematic diagram of P-glycoprotein (Adapted from Di Pietro *et al.*, 1999).

1.2.3.2.3 Methods in Dealing with P-glycoprotein Over-expressed MDR Cells

Since some tumor cells may acquire over-expressoion of P-gp during chemotherapeutic treatments and once the MDR developed, the patient will become irresponsive to a numerous anti-tumor drugs, researchers keep on finding agents which can reverse the P-gp-MDR or agents which can by-pass the action of P-gp. The most popular P-gp activity inhibitors include cyclosporin A and calcium blockers such as verapamil. However, these agents more or less exhibit side effects to patients. Thus, the most direct and effective solution is to find out anti-tumor agents that can function in P-gp over-expressing cells.

1.3 Objectives of the Projection

1.3.1 Study of the Anti-tumor Activities of Hong Kong 18 on Human Hepatocellular Carcinoma Cell Line HepG2 and Unravel the Underlying Mechanisms

In this research project, the anti-tumor activities of the steroid saponin Hong Kong 18 (HK18), i.e. polyphyllin D, were studied. As mentioned above, some saponins were able to induce apoptosis in several cancer cell lines including the human hepatocellular carcinoma cell line HepG2, we would like to study the apoptotic inducing activities of HK18 on HepG2. Besides, the underlying mechanisms of HK18 induced apoptosis in HepG2 were our interests.

1.3.2 Study of the Anti-tumor Activities of Hong Kong 18 on Multidrug Resistant Human Hepatocellular Carcinoma Cell line R-HepG2 and Unravel the Underlying Mechanisms

In the view of the problem posed by P-gp-MDR on the treatment of cancer patients, the potential of HK18 on the treatment of multidrug resistant human hepatocellular carcinoma cell line R-HepG2 was studied. The apoptotic inducing activities and the underlying mechanism would be elucidated.



Chapter 2

Materials and Methods

2.1 Materials

2.1.1 Cell Culture

2.1.1.1 Cell Lines

Human Hepatocellular carcinoma cell line HepG2 was purchased from American Type Culture Collection (ATCC number HB-8065), which was derived from a 15 years old Caucassian male. They are adherent cells with epithelial morphology. They were cultured in complete RPMI 1640 medium (GibcoBRL, USA) supplemented with 10% (v/v) fetal calf serum (GibcoBRL, USA) and 1% (v/v) penicillin-streptomycin (Gibco BRL, USA) as complete medium. The cells were maintained at 37°C, 5% carbon dioxide incubator with humidified atmosphere. Cells were cultured in 25, 75 or 150 cm² tissue culture flasks (Corning / IWAKI) and were passed every 3 or 4 days. For each passage, medium was discarded and cells were washed with PBS once. Then cell were collected by trypsinization and were subjected to centrifugation at 450 x g for 3 minutes. The cell pellet was then resuspended in complete medium and cultured in a new tissue culture flask.

Another cell line, multidrug resistant human hepatocellular carcinoma cell line R-HepG2, was developed by our group. To develop R-HepG2 cells, HepG2 cells were incubated with 0.1 µM Doxorubicin (Sigma). Dead non-resistant cells were removed and viable cells were further incubated with stepwise increasing concentrations of Doxorubicin until 100 µM. The property of multidrug resistance was tested by treating the HpeG2 and R-HepG2 cells with chemotherapeutic drugs including Doxorubicin, Vincristine and Methotrexate for 48 hours and MTT assay was carried out to determine the percentage survival of cells. The overexpression of

p-glycoprotein and upregulation of MDR1 gene was confirmed by Western analysis and Northern analysis (Chan *et al.*, 2000). The developed resistant cells were maintained in complete medium with 1.2 μ M Doxorubicin and were kept at 37 °C, 5% carbon dioxide humidified incubator. The method of passage of the resistant cells was the same as its parental cells.

2.1.1.2 Culture Media

RPMI 1640 medium (Roswell Park Memorial Institute tissue culture medium 1640) was used for culturing HepG2 and R-HepG2 cells. Each pack of RPMI 1640 powder with phenol red, L-glutamine and 0.5 mM HEPES was dissolved in 1 L distilled water and two grams of sodium bicarbonate was added and the pH was adjusted to 7.2. The medium was then sterilized by filtration with 0.22 μ m bottle-top filter (Millipore). 3 ml of filtered medium was then incubated at 37 °C, 5 % carbon dioxide humidified incubator for 48 hours to check the sterilization. Sterilized medium was stored at 4 °C. Complete medium was obtained by supplemented with 10 % (v/v) fetal calf serum and 1% (v/v) penicillin/streptomycin (10,000 units/ml) to the sterilized RPMI medium. In some experiments, phenol red free RPMI medium was used. Its was prepared by dissolving one pack of phenol red free RPMI powder with L-glutamine in 1 L distilled water and two grams of sodium bicarbonate was added. The pH was adjusted to 7.2 and was sterilized by filtration as described above.

2.1.2 Reagents and Buffers

2.1.2.1 Phosphate Buffered Saline (PBS)

PBS was prepared by dissolving 136 mM NaCl, 2.7 mM KCl, 1.5 mM KH_2PO_4 and 8 mM Na_2HPO_4 in distilled water with pH 7.4. It was then sterilized by autoclave and was stored at 4°C.

2.1.2.2 Reagents and Buffers for DNA Fragmentation

DNA lysis buffer was prepared by dissolving 200 mM Tris-HCl (pH8.3), 100 mM EDTA and 1 % SDS in distilled water.

Tris-EDTA (TE) buffer was prepared by dissolving 10 mM Tris-Cl (pH 8.0) and 1mM EDTA in distilled water.

Proteinase K (14 units/mg powder) (Sigma) was dissolved in distilled water to prepare a stock concentration of 10mg/ml and was stored at -20°C.

Ribonuclease A (RNase A) (59 Kunitz units/mg powder) (Sigma) was dissolved in TE buffer to prepare a stock concentration of 0.2 mg/ml and was stored at -20°C

Tris-Acetate (TAE) buffer was first prepared as 50X concentrated stock solution. It was composed of 242 g Tris base, 57.1 ml glacial acetic acid and 100 ml 0.5 M EDTA (pH8.0) in 1 L water. It was then diluted into 1X by distilled water before use.

6X DNA loading dye was prepared by mixing 0.25 % (w/v) bromophenol blue, 0.25 % (w/v) xylene cyanol FF and 40% (w/v) sucrose in distilled water.

100 base pair DNA marker was prepared by mixing 2 μ l 100 base pair DNA marker (Amersham Pharmacia Biotech Inc.) with 4 μ l 6X DNA loading dye and 5 μ l distilled water.

2.1.2.3 Reagents and Buffers for Western Analysis

Lysis buffer for total protein extraction was composed of 2 % SDS, 10 % glycerol, 0.0625 M Tris-HCl pH 6.8, β -mercaptoethanol (5 %v/v), 0.002 % bromophenol blue.

Lysis buffer for cytochrome c extraction was prepared by mixing 75 mM NaCl, 1 mM NaH₂PO₄, 8 mM Na₂HPO₄ and 250 mM sucrose. The buffer was stored at 4°C. 21 μ g/ml aprotinin, 5 μ g/ml leupeptin, 1 mM PMSF and various concentration of digitonin were added to the buffer just prior use.

4X lower gel buffer was prepared by dissolving 90.8 g of Tris base and 2 g of SDS in 500ml of distilled water. The pH was adjusted to 8.8.

4X upper gel buffer was prepared by dissolving 30.3 g of Tris base and 2 g of SDS in 500 ml of distilled water. The pH was adjusted to 6.8 with HCl.

10X SDS running buffer was prepared by dissolving 30.3 g of Tris base,

144 g of glycine and 10 g of SDS in 1 L of distilled water. The concentrated stock solution was diluted 10-fold with distilled water to give the 1X working buffer.

10% Ammonium Persulfate (APS) was prepared by dissolving 10 % (w/v) APS (BioRad) in distilled water and was stored at 4 °C.

2X SDS loading dye was prepared by mixing 10 % (v/v) glycerol, 0.4 % (w/v) SDS, 0.05 % (w/v) bromophenol blue, 20 mM EDTA in 0.5 M Tris-Cl with pH 7.5 and 5 % (v/v) 2-mercaptoethanol and was stored at 4 °C.

Electroblotting buffer (E-Blot Buffer) was prepared by mixing 66.7 ml of 10X Tris-glycine (30.3 g of Tris base and 144 g of glycine in 1 L of distilled water) (pH 8.3), 100 ml of methanol and 500 ml of distilled water.

Commassie Blue staining solution for SDS gel staining was prepared by mixing acetic acids, methanol and distilled water in the ratio of 1:3:10 with 0.05 % (w/v) commassie brilliant blue R-250.

De-staining solution was prepared by mixing acetic acid, methanol and distilled water in the ratio of 4:1:5.

Tris-buffered saline-Tween-20 (TBS-T) 10X TBS stock was prepared by dissolving 12.114 g of Tris and 87.66 g of NaCl in 1 L of distilled water. The pH was adjusted to 8. The stock solution was then diluted 10 fold to give the 1X working

concentration. For 1 L of 1X TBS, 1ml of Tween-20 was added.

2.1.2.4 Reagent and Buffers for Caspases Activities

Cell lysis buffer was prepared by dissolving 1 % Igepal-CA 630, 150 mM NaCl, 50 mM Tris-HCl, 1 mM EDTA and protease inhibitor (1 tablet) in 50 ml distilled water. The pH was adjusted to 7.5.

Reaction buffer was prepared by dissolving 10 mM Hepes-KOH, 40 mM β - glycerophosphate, 50 mM NaCl, 2 mM MgCl₂, 5 mM EGTA, 0.1 % CHAPS, 100 μ g / ml BSA and 10 mM DTT (add before used). The pH was adjusted to 7.0.

2.1.2.5 Fluorescent Dyes Used for Flow Cytometry

5,5',6,6'-tetrachloro-1,1',3,3'-tetraethylbenzimidazolylcarbocyanine Iodide (JC-1), 5-(and 6-)-carboxy-2',7-dichlorodihydrofluorescein diacetate (DCF) and Fluo-3/AM (Molecular Probes) were prepared by dissolving in (DMSO) (excess water was absorbed by molecular sieve) to give a concentration of 2.5 mM stock solution. Tetramethylrhodamine, ethyl ester, perchlorate (TMRE) was prepared by dissolving in DMSO to give a concentration of 125 μ M stock solution. All of the fluorescence dyes were stored at -20 °C.

2.1.3 Chemicals

Hong Kong 18 (HK18) is a white solid which is organic synthesized by Prof. Biao Yu, Shanghai Institute of Organic Chemistry, Chinese Academy of Science (Deng *et al.*, 1999; Li *et al.*, 2001). It was stored at 4 °C and was dissolved in

DMSO to prepare a 50 mM stock solution.

Doxorubicin (Sigma) was prepared by dissolving in 1 ml autoclaved distilled water and was then diluted into 1 mM stock with PBS. It was stored at -20 °C and protected from light.

Vincristine (Sigma) was prepared by dissolved in 1ml autoclaved PBS and was stored at -20 °C and protected form light.

3-(4,5-dimethylthiazol-2-yl)-2,5-diphenyltetrazoliumbromide (MTT) Solution (Sigma) was prepared by dissolving in PBS at a concentration of 5 mg/ml. The solution was filtered by a 0.22 µm filter (Kitman) and was stored at 4 °C.

Ionomycin (Calbiochem) was prepared by dissolving in DMSO to give a concentraion of 1mg/ml stock solution and was stored at -20 °C.

Valinomycin (Calbiochem) was prepared by dissolving in DMSO to give a concentration of 1 mM stock solution and was stored at -20 °C.

Bongkreki acid, Triammonium salt (Calbiochem) was prepared by dissolving in 2N NH₄OH and diluted with PBS to 1 mM stock solution. It was stored at -20°C and protected from light.

z-Asp(OME)-Glu(OME)-Val-Asp(OME)-CH₂F (z-DEVD-fmk)

(Calbiochem) was prepared by dissolving in DMSO to give a concentration of 1 mM stock solution and was stored at -20 °C.

z-Ile-Glu(OME)-Thr-Asp(OME)-CH₂F (z-IETD-fmk) (Calbiochem)

was prepared by dissolving in DMSO to give a concentration of 10 mM stock solution and was stored at -20 °C.

z-Leu-Glu(OME)-His-Asp(OME)-fmk (z-LEHD-fmk) (Calbiochem) was prepared by dissolving in DMSO to give a concentration of 10 mM stock solution and was stored at -20 °C.

Acetyl-Asp-Glu-Val-Asp-7-amido-4-methylcoumarin (Ac-DEVD-AMC)

(Sigma) was prepared by dissolving in DMSO to give a concentration of 2 mM stock solution and was stored at -20 °C.

N-Acetyl-Ile-Glu-Thr-Asp-7-amido-4-methylcoumarin

(Ac-IETD-AMC) (Sigma) was prepared by dissolving in DMSO to give a concentration of 1 mM stock solution and was stored at -20 °C.

N-Acetyl-Leu-Glu-His-Asp-7-amido-4-trifluoromethylcoumarin

(Ac-LEHD-AFC) (Sigma) was prepared by dissolving in DMSO to give a concentration of 5 mM stock solution and was stored at -20 °C.

AMC calibrator (7-amido-4-methylcoumarin) was prepared by dissolving in DMSO to give a concentration of 100 μM stock solution and was stored at 4 °C.

AFC calibrator (7-amido-4-trifluoromethylcoumarin) was prepared by dissolving in DMSO to give a concentration of 80 μM stock solution and was stored at 4 °C.

3 % thioglycolate (w/v) was prepared by dissolving 3 g of thioglycolate powder in 100 ml distilled water and autoclaved to sterile.

The name, chemical formula, molecular weight and source of the materials used are listed in Table 2.1.

Table 2.1 List of the chemicals being used in this research project.

Name and formula of chemical	Molecular Weight	Source
5, 5', 6, 6'-tetrachloro-1, 1', 3, 3'-tetraethylbenzimidazolcarbocyanine iodide (JC-1)	652	Molecular Probes
Ac-DEVD-AMC Acetyl-Asp-Glu-Val-Asp-7-amido-4-methylcoumarin	675.7	Sigma
Acetic acid (CH ₃ COOH)	60.05	Merck
Ac-IETD-AMC N-Acetyl-Ile-Glu-Thr-Asp-7-amido-4-methylcoumarin	675.7	Sigma
Ac-LEHD-AFC N-Acetyl-Leu-Glu-His-Asp-7-amido-4-trifluoromethyl coumarin	765.7	Sigma
Acrylamide / bis-acrylamide (30% solution, mix ratio 37.5:1)	/	Sigma.
Agarose	/	Sigma
Albumin, Bovine	/	Sigma
Ammonium persulfate	228.2	Bio-Rad
Aprotinin	6500	Sigma.
Bicinchoninic acid solution (BCA)	/	Sigma
CHAPS	614.89	USB
Chloroform	/	BDH
Commassie brilliant blue R-250	826.0	USB
Copper (II) sulfate pentahydrate (CuSO ₄ . 5H ₂ O)	249.68	Sigma
Digitonin (C ₂₂ H ₂₆ N ₂ O ₄ S)	1228.0	Merck
Dimethylsulfoxide (DMSO) CH ₃ SOCH ₃	78.13	Riedel-de-Haen

DNA marker (100 base pair)	/	Invitrogen
EGTA	380.4	Sigma
Enhanced chemiluminescence reagents (ECL)	/	Amersham
Ethanol (C ₂ H ₅ OH)	46.07	Riedel-de-Haen
Ethidium bromide	394	Molecular Probes
Ethylenediaminetetraacetic acid (EDTA) (C ₁₀ H ₁₆ N ₂ O ₈)	292.2	Sigma
Fetal Bovine Serum (FBS)	/	Invitrogen
Fluo-3, acetoxymethyl ester Fluo-3/AM	1130	Molecular Probes
Glycine (H ₂ NCH ₂ CO ₂ H)	75.07	USB
Hepes-KOH	238.3	Sigma
Igepal-CA	/	Sigma
Ionomycin (C ₄₁ H ₇₂ O ₉)	709	Calbiochem
Isopropanol	/	BDH
Leupeptin (C ₂₀ H ₃₈ N ₆ O ₄)	463	Sigma
Methanol (CH ₃ OH)	/	BDH
Molecular sieve (potassium, sodium alumino-silicate) (normal pore diameter: 3 angstrom)	/	Sigma
MTT (3-[4, 5-dimethylthiazol-2-yl]-2, 5-diphenyltetrazolium bromide; thiazoyl blue) (C ₁₈ H ₁₆ N ₅ SBr)	414.3	Sigma
N, N, N'-tetramethyl-ethylene diamine (TMRE)	116.21	Sigma
Non-fat milk powder	/	Carnation, Nestle
Penicillin-streptomycin	/	Invitrogen
Phenylmethyl-sulphonyl fluoride (PMSF) (C ₇ H ₇ FO ₂ S)	174.2	Sigma
Potassium phosphate (monobasic anhydrous) (KH ₂ PO ₄)	136.1	Sigma

Propidium iodide (PI)	668.4	Sigma
Protease Inhibitor tablet	/	Roche
Proteinase K (16U/mg protein)	/	Sigma
Rainbow marker (low range)	/	Bio-Rad
Ribonuclease A (RNase) (102 U/mg protein)	/	Sigma
Roswell Park Memorial Institute tissue culture medium 1640 (RPMI-1640) (with phenol red)	/	Invitrogen
Roswell Park Memorial Institute tissue culture medium 1640 (RPMI-1640) (without phenol red)	/	Invitrogen
Sheath Fluid	/	USB
Sodium chloride (NaCl)	58.44	USB
Sodium dodecyl sulphate (SDS) (CH ₃ (CH ₂) ₁₁ SO ₄ Na)	288.38	USB
Sucrose (C ₁₂ H ₂₂ O ₁₁)	342.3	Sigma
Thioglycolate	/	Boppard
Tris base (NH ₂ C(CH ₂ OH) ₃)	121.14	USB
TRIzol	/	Invitrogen
Trysin-EDTA	/	Invitrogen
Tween-20 (Polyoxyethylene-sorbitan monolaurate)	/	Sigma
z-DEVD-fmk (Caspase-3 inhibitor) (z-Asp(OME)-Glu(OME)-Val-Asp-(OME)-CH ₂ F)	668.7	Calbiochem
z-IETD-fmk (Caspase-8 inhibitor) z-Ile-Glu(OME)-Thr-Asp(OME)-CH ₂ F)	654.7	Calbiochem
z-LEHD-fmk (Caspase-9 inhibitor) Leu-Glu(OME)-His-Asp(OME)-CH ₂ F	690.7	Calbiochem
β -glycerophosphate	216	Sigma

2.2 Methods

2.2.1 MTT Assay

MTT assay was used to assess the cytotoxicity of HK18. For HepG2 and R-HepG2 cells, 100 μl of 1.5×10^5 cells / ml or 2×10^5 cells / ml were seeded to each well of 96-well flat bottom microtiter plates respectively. The plates were incubated at 37 °C, 5 % CO₂ humidified incubator overnight to allow the cells to grow. The medium was then removed and 100 μl of various concentrations of HK18 were added to the cells. Medium without drug was added to act as the negative control. The cells were incubated for various periods. After treatment, the medium in each well was discarded and washed by PBS. Thirty microliters of MTT solution (5 mg/ml) was added. The plate was incubated at 37 °C for 2 hours. Then, the MTT solution was discarded and 100 μl of DMSO was added to dissolve the crystals. The plate was allowed to stand for 30 minutes at room temperature. The absorbance at 540 nm was read by ELISA plate reader (Bio-Rad). Blank was set by adding 100 μl of DMSO only. Negative control was set as 100 % of cell survival.

2.2.2 Determination of Cell Viability

Tryphan blue exclusion assay was employed to study the viability of HK18 on cells. After treatments, 10 μl of cell suspension was mixed with 10 μl of 0.4 % tryphan blue solution (Sigma). 10 μl of the mixture was then used for cell counting by hemocytometer. Dead cells would be stained blue while viable cell would exclude the dye. The amount of unstained viable cells and total cells were counted. Percentage of viability can be calculated as follows:

$$\% \text{ Viability} = (\text{no. of viable cells} / \text{no. of total cells}) \times 100 \%$$

2.2.3 Purification of Macrophages from balb/c Mice

1.5 ml of 3 % thioglycolate was intra-peritoneally injected into 6 – 8 weeks, 20 – 25 g balb/c mouse. After 3 days, the mouse was killed and peritoneal cells including macrophages were collected by washing the peritoneal cavity with about 10 ml PBS. Cells pellet was collected by centrifugation at 800 x g for 3 minutes. The cells pellet was washed twice with 0.5 X PBS to remove any red blood cells present.

The cells pellet was then resuspended in complete RPMI. The cell density was adjusted into 5×10^6 cells /ml and were seeded into a 96 well plate for cytotoxicity assay. The plate was then incubated at 37 °C, 5 % CO₂ humidified incubator for 3 hours to allow the macrophages to attach to the well bottom. After 3 hours incubation, the wells were washed with PBS twice and 100 µl of complete medium or with various concentrations of drugs were added and incubated for 48 hours. MTT was performed to examine cytotoxicity of drugs.

2.2.4 Hemolysis Assay

The hemolytic activity of HK18 was studied by red blood cell (RBC) hemolysis assay model. Around 12 ml of blood was collected from 300-320 g male SD rat from the dorsal vein by vacuum puncture. The blood collected was centrifuged at 1,500 x g for 10 minutes at 4 °C. The supernatant (serum) was carefully removed. The pellet which contain mostly RBC was then rinsed with 0.15

M NaCl and centrifuge at 1,500 x g for 10 minutes at 4 °C two times. After that, the pellet was rinsed again with 0.15 M NaCl and centrifuged at 1,000 x g for 10 minutes at 4 °C. The pellet obtained was resuspended in PBS to obtain 20 % RBC suspension. 0.5 ml of the 20 % RBC suspension was then mixed with 0.25 ml of PBS and 0.25 ml of various concentration of HK18. 0.25 ml of PBS was used instead of HK18 for the negative control. The reaction mixture was incubated at 37 °C for 3 hours with gentle shaking. After incubation, 0.1 ml of each of the reaction mixture was added to 1.9 ml of distilled water and PBS respectively and were centrifuged at 1,500 x g for 10 minutes at 4 °C. The supernatant was measured at absorbance 540 nm with a 96 well plate by ELISA plate reader (Bio-Rad). The percentage of hemolysis was directly proportional to the absorbance. The percentage of hemolysis would be calculated as follows:

$$\% \text{ Hemolysis} = \{ 1 - [(\text{Abs of H}_2\text{O} - \text{Abs of PBS}) / \text{Abs of H}_2\text{O}] \} \times 100\%$$

2.2.5 *In vivo* Studies of the Toxicity of HK18

The toxicity of HK18 was examined by *in vivo* study. Male Balb/c mice aged 6 to 8 weeks with 20 to 25 grams were employed in this experiment. The mice were divided into 3 groups and 8 mice per group. One group was regarded as control group in which saline was administrated. Another group was regarded as solvent control group in which 0.4 % γ -cyclodextrin was administrated. The last group was regarded as treatment group in which 342 μg / kg mice (equivalent to 5 μM of final concentration in the circulation of mouse) of HK18 was administrated. Saline, 0.4 % cyclodextrin and 5 μM HK18 were injected into the mice intravenously via the tail

vein every alternate day and lasted for 2 weeks. After treatments, the mice were sacrificed and serum was collected. The enzymatic activities of the serum were measured by enzymatic diagnostic kits (Sigma). Four enzymes were examined which are the indicators of heart tissue or liver damage. They are creatine kinase (CK) and lactate dehydrogenase (LDH), which are indicators of heart tissue damage as well as alanine transaminase (ALT) and aspartate transaminase (AST), which are indicators of liver tissue damage.

The procedures of measuring the enzymatic activities were according to the protocol of the enzymatic kits. In brief, for measuring CK and LDH activities, 20 μ l and 50 μ l of serum was mixed with 1 ml of CK reagent or LDH reagent respectively. The mixture were then incubated at 30 °C at dark for 3 minutes or 30 seconds and absorbance were taken at 340 nm by spectrophotometer (Beckman) for 2 minutes or 1 minutes for CK and LDH respectively. For measuring AST and ALT, 100 μ l of serum was mixed with 1 ml AST reagent or ALT reagent at 37 °C at dark for 1 minute. Absorbance was then taken at 340 nm for 2 minutes.

The enzymatic activities were calculated as follows:

$$\text{Enzymatic activity (U/L)} = (\Delta A \text{ per min} \times TV \times 1000) / (6.22 \times LP \times SV)$$

where	ΔA per min	= change in absorbance per minute at 340 nm
	TV	= total reaction volume (ml)
	LP	= light path
	6.22	= millimolar absorptivity of NADPH at 340 nm
	SV	= sample volume
	1000	= conversion of units per ml to per liter

$$\begin{aligned}\text{thus, CK (U/L)} &= \Delta A \text{ per min} \times 8200 \\ \text{LDH (U/L)} &= \Delta A \text{ per min} \times 3376 \\ \text{AST (U/L)} &= \Delta A \text{ per min} \times 1768 \\ \text{ALT (U/L)} &= \Delta A \text{ per min} \times 1768\end{aligned}$$

One unit of activity is defined as the amount of enzyme, which produces 1 μ mole of NADH per minute under the condition of assay procedure.

The mean value of the enzymatic activities of the same group was then plotted against the corresponding treatments. The largest and the smallest values were eliminated.

2.2.6 DNA Fragmentation Assay

DNA fragmentation assay was used to examine apoptosis. 3 ml of 1.5×10^5 cells/ml or 2×10^5 cells/ml of HepG2 or R-HepG2 cells were seeded in 60 mm culture dish respectively. Cells were allowed to grow overnight at 37 °C, 5 % CO₂ humidified incubator. Medium was then removed and various concentrations of HK18 were added. The cells were incubated for various periods. After treatment, cells were harvested and washed twice with PBS. Cells at 1×10^6 were lysed with 400 μ l of DNA lysis buffer. The mixture was vortexed until no cell debris was left. Twenty microliter of proteinase K (10 mg/ml) was added and incubated at 37 °C for at least 2 hours. After cooling down the sample to room temperature, 150 μ l of saturated NaCl was added and the sample was shaken vigorously. The microcentrifuge tubes were centrifuged at 6,500 x g for 15 minutes. The supernatant was collected and 1 ml of cold absolute ethanol was added. The mixture was then

subjected to centrifugation at 15,000 x g for 20 minutes. One ml of cold 75 % ethanol was used to wash the pellet. After centrifuge at 7,000 x g for 5 minutes, the pellet was allowed to dry. Finally, 20 μ l of RNase A (0.2 mg/ml) was added to each sample and further incubated at 37 °C for 90 minutes. The dissolved DNA was then subjected to electrophoresis on 1.5 % (w/v) agarose gel (Sigma).

2.2.7 Detection of Apoptotic and Necrotic / Late Apoptotic Cells by Flow Cytometry with Annexin V-FITC/PI

TACS™ Annexin V-FITC kit (Trevigen) was used to examine early apoptosis and necrosis / late apoptosis of HK18 treated cells. 10 ml of 1.5×10^5 cells/ml or 2×10^5 cells were seeded in 100 mm tissue culture dish. Cells were incubated at 37 °C, 5 % CO₂ humidified incubator overnight. Medium was then removed and various concentrations of HK18 were added and medium without drug was added as negative control. The cells were incubated for various periods. After treatment, both floating dead cells and adherent cells were harvested and washed twice with plain non-phenol red containing RPMI. Cells at 1×10^6 were used for the assay. 2 mg/ml of digitonin was added to permeabilize the plasma membrane of untreated cells to serve as positive control. 100 μ l of Annexin V incubation reagent including 10 μ l of 10X binding buffer, 10 μ l of PI, 2 μ l of Annexin-V conjugate and 78 μ l of distilled water was added and the sample was incubated in the dark at 37 °C for 15 minutes. Then, 400 μ l of 1X binding buffer was added to the sample and the sample was analyzed by FACSort flow cytometry (Becton Dickison) by using 'Cell Quest' software. The cell population was chosen by forward scatter (FSC) light and side scatter (SSC) light. The signal was detected by FL1 channel for the detection of

Annexin V-FITC and FL3 channel for PI with log scale.

2.2.8 Detection of Mitochondrial Membrane Potential by JC-1 Fluorescent Dye

The mitochondrial membrane potential (ϕ_m) was examined by flow cytometry with fluorescent JC-1 dye. 2 ml of 1.5×10^5 cells/ml or 2×10^5 cells/ml of HepG2 or R-HepG2 cells respectively were seeded to each well of a 6 well plate. Cells were incubated at 37 °C, 5 % CO₂ humidified incubator overnight. Medium was removed and various concentrations of HK18 were added and medium without drug was added as negative control. 500 nM of Valinomycin was added to act as the positive control. The cells were incubated for various periods. After treatment, floating dead cells were discarded; adherent cells were harvested and washed twice with plain non-phenol red containing RPMI. Cells at 0.25×10^6 were resuspended in 500 μ l of medium with 10 μ M JC-1. The samples were incubated in the dark at 37 °C for 15 minutes and then were analyzed by FACSort flow cytometry (Becton Dickison) by using ‘Cell Quest’ software. The cell population was chosen by FSC light and SSC light. The signal was detected by FL1 and FL3 channels in log scale.

2.2.9 Detection of Intracellular Ca²⁺ Level by Flow Cytometry with Fluo-3 Fluorescent Dye

The intracellular concentration of Ca²⁺ was examined by flow cytometry with fluorescence dye Fluo-3. 2 ml of 1.5×10^5 cells/ml or 2×10^5 cells/ml of HepG2 or R-HepG2 cells respectively were seeded to each well of a 6 well plate. Cells were

incubated at 37 °C, 5 % CO₂ humidified incubator overnight. Medium was removed and various concentrations of HK18 were added and medium without drug was added as negative control. The cells were incubated for various periods. After treatment, floating dead cells were discarded; adherent cells were harvested and washed twice with plain non-phenol red containing RPMI. Cells at 0.25 x 10⁶ were used for analysis. 40 µg/ml Ionomycin was added to untreated cells for 15 minutes to act as the positive control. The cells were resuspended in 500 µl of medium with 10 µM Fluo-3. The samples were incubated at 37 °C for 30 minutes in dark and then were analyzed by flow cytometry by using “Cell Quest” software. The cell population was chosen by FSC light and SSC light. The signal was detected by FL1 channel in log scale.

2.2.10 Detection of Intracellular Hydrogen Peroxide Level by Flow Cytometry with DCF Fluorescent Dye

The intracellular hydrogen peroxide level was examined by flow cytometry with fluorescence dye DCF. 2 ml of 1.5 x 10⁵ cells/ml or 2 x 10⁵ cells/ml of HepG2 or R-HepG2 cells respectively were seeded to each well of a 6 well plate. Cells were incubated at 37 °C, 5 % CO₂ humidified incubator overnight. Medium was removed and various concentrations of HK18 were added and medium without drug was added as the negative control. Cells were incubated for various periods. After treatment, floating dead cells were discarded; adherent cells were harvested and washed twice with plain non-phenol red containing RPMI. Cells at 0.25 x 10⁶ were resuspended in 500 µl of medium with 10 µM DCF. The samples were incubated at 37 °C for 30 minutes in dark and then were analyzed by flow cytometry by using

“Cell Quest” software. The cell population was chosen by FSC light and SSC light. The signal was detected by FL1 channel in log scale.

2.2.11 Simultaneous Detection of Mitochondrial Membrane Potential and Intracellular Ca²⁺ or Mitochondrial Membrane Potential and Intracellular Hydrogen Peroxide

Change of mitochondrial membrane potential (φ_m) could be analyzed with change of intracellular Ca²⁺ or hydrogen peroxide level simultaneously by flow cytometry with TMRE and Fluo-3 or DCF. 2 ml of 1.5×10^5 cells/ml or 2×10^5 cells/ml of HepG2 or R-HepG2 cells respectively were seeded to each well of a 6 well plate. Cells were incubated at 37 °C, 5 % CO₂ humidified incubator overnight. Medium was removed and various concentrations of HK18 were added and medium without drug was added as negative control. Cells were incubated for various periods. After treatment, floating dead cells were discarded; adherent cells were harvested and washed twice with plain non-phenol red containing RPMI. Cells at 0.25×10^6 were resuspended in 500 μ l of medium with 500 nM TMRE and 10 μ M Fluo-3 or 10 μ M DCF. The samples were incubated at 37 °C for 30 minutes in dark and then were analyzed by flow cytometry by using “Cell Quest” software. The cell population was chosen by FSC light and SSC light. The signal was detected by FL-3 channel for TMRE and FL-1 channel for Fluo-3 or DCF in log scale.

2.2.12 Western Analysis

2.2.12.1 Total Protein Extraction

- *Protein Extraction*

10 ml of 1.5×10^5 cells/ml or 2×10^5 cells/ml HepG2 and R-HepG2 cells were seeded in a 100 mm tissue culture dish and incubated at 37 °C, 5 % CO₂ humidified incubator overnight. Medium was removed and various concentrations of HK18 were added. Cells were incubated for various periods. After treatment, both floating dead cells and adherent cells were collected and were washed twice with PBS. 100 µl of lysis buffer (2% SDS, 10% glycerol, 0.0625 M Tris-HCl pH 6.8, β-mercaptoethanol (5 % v/v), 0.002 % bromophenol blue) was added and was allowed to stand in ice for 1 hour. Subsequently, samples were boiled for 10 min. The extracts were then centrifuged at 11,000 x g for 10 minutes at 4 °C. After centrifugation, supernatant was collected and stored at -70 °C.

- *Determination of Protein Amount*

The amount of total protein extracted by SDS lysis buffer was determined by BCA protein assay. 1 µl of each sample was mixed with 9 µl PBS in a 96 well plate. A standard bovine serum albumin (BSA) curve was obtained as 0, 2, 4, 6, 8 and 10 mg/ml BSA in the 96 well plate. Both protein samples and BSA standard were done in triplicate. BCA mixture was composed of mixing BCA (bicinchoninic acid) solution and CuSO₄ . 5H₂O solution in the ratio of 50:1. 200 µl of BCA mixture was added to each well and incubate at 37 °C for 30 min. BCA mixture only was used as blank. Fig 2.1 showed a standard BSA curve.

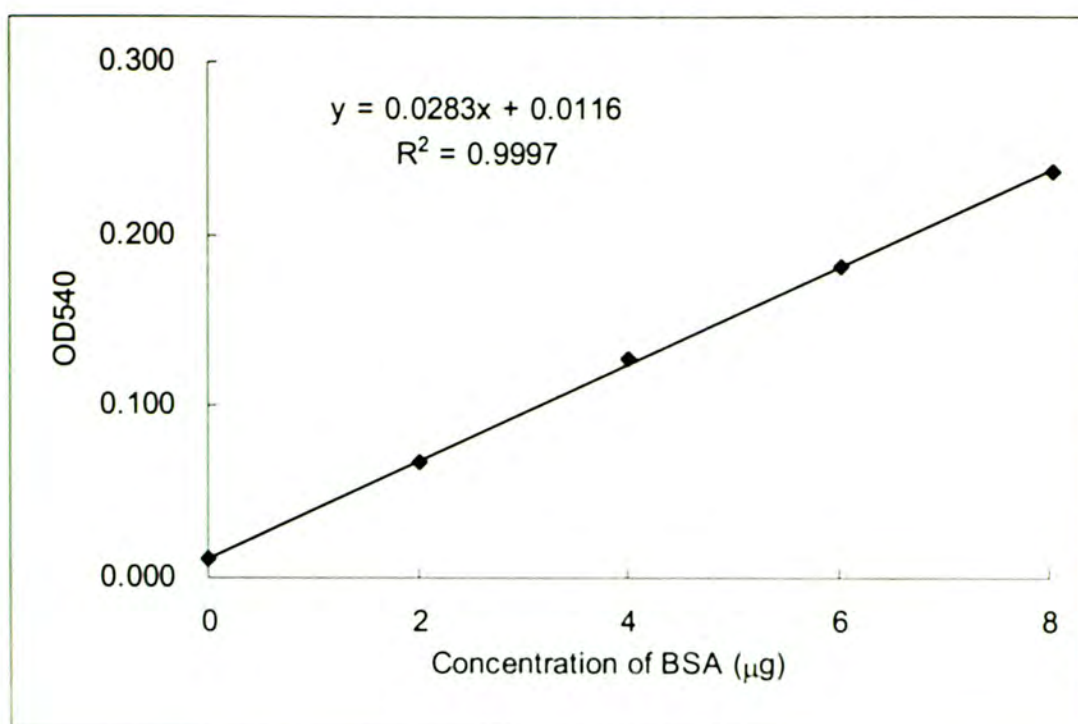


Fig 2.1 BSA protein standard curve used for protein concentration determination.

- ***SDS Polyacrylamide Gel Electrophoresis***

The apparatus of 3D vertical electrophoresis system (BioRad) was set referring to the steps in user manual.

According to the molecular weight of the target protein, different percentages of stacking and separating gel were used. The composition was as follows:

	Separating gel			Stacking gel
	8 %	12 %	15 %	4.5 %
Distilled water	1.9 ml	1.375 ml	0.975 ml	1.2 ml
30% Acrylamide	1.07 ml	1.6 ml	2 ml	0.3 ml
4 x lower gel buffer	1 ml	1 ml	1 ml	/
4 x upper gel buffer	/	/	/	0.5 ml
TEMED	4.65 μ l	4.65 μ l	4.65 μ l	2.65 μ l
10 % APS	20 μ l	20 μ l	20 μ l	15 μ l

Table 2.2 The compositions of various percentage of SDS gel.

According to the BSA standard curve, equal amount of protein samples (25-50 μ g) were used for electrophoresis. Protein samples were mixed with equal amount of 2 x SDS loading dye and boiled for 10 minutes. Then samples were loaded to the well of the polyacrylamide gel with rainbow low range marker (Amershan). The gel was run under constant voltage of 100 V for 2-3 hours.

- ***Electroblotting of Protein***

The apparatus of Semi-Dry Electrophoretic Transfer Cell (semi-dry blotter, Bio-Rad) was set referring to the steps in manual.

0.45 μ m PVDF (polyvinylidene fluoride) membrane (Immobilon, Millipore) was used for electroblotting. The dry PVDF membrane was soaked in absolute methanol for re-hydration. Membrane was then put in the electroblotting buffer

(E-blot buffer) for 15 minutes. 3 pieces of blotter paper were soaked in E-Blot buffer and put onto the platinum anode. The membrane was put onto the blotter papers following with the acrylamide gel (the upper stacking gel was cut and removed). Air bubbles were excluded by rolling. Another 3 pieces of E-blot buffer-soaked blotter paper were put onto the gel. The proteins were transferred at constant current at 150 mA for 2 gels for 20-50 minutes. After blotting, the gel was stained with commassie blue staining solution and destaining solution to check the completeness of transfer.

- ***Probing of Proteins with Antibodies***

The membrane was then soaked in 10 % non-fat milk (in TBS-T) at 4 °C overnight for non-specific blocking. It was washed with TBS-T for 10 minutes 3 times. Then, primary antibody in 10 % non-fat milk was added for probing at room temperature for 1 hour. After that, the membrane was washed with TBS-T for 10 minutes 3 times and probed with second antibody (conjugated with horseradish peroxidase) at room temperature for 1 hour. The membrane was washed again with TBS-T for 10 minutes 3 times and it was ready for ECL detection. The anti-bodies which had been used in this project were listed at Table 2. 3.

- ***Enhanced Chemiluminescence (ECL) Assay***

After probing antibody, the target protein can be detected by using ECL assay. Reagent 1 and 2 and ECL (Amersham) were mixed in the ratio of 1:1 and the membrane was immersed in the mixture for 90 seconds. Then the membrane was wrapped and put into the Hypersensitive film cassette (Amersham) following with

Fuji Medical x-ray film (Super Rx, Fuji) at dark with various exposure period. The film was developed by a film processor (M35 X-OMAT, Kodak) and the band intensity was analyzed by ImageQuaNT software (Molecular Dynamics).

Anti-bodeis	Molecular weight of the target protein	Ratio	Company
Anti- β -actin	42	1 : 1000	Sigma
Anti-AIF	65	1 : 1000	Santa Cruz
Anti-Bcl-2	25	1 : 1000	Santa Cruz
Anti-cytochrome c	15	1 : 1000	Santa Cruz
Anti-PARP	116, 85	1 : 1000	Santa Cruz
Anti-Pro-caspase 3	35	1 : 1000	Santa Cruz
Anti-mouse-HRP	/	1 : 1000	ZYMED
Anti-rabbit-HRP	/	1 : 1000	Santa Cruz

Table: 2.3 List of the anti-bodies used in this project with the corresponding target protein molecular weight, dilution ratio and purchasing companies.

2.2.12.2 Extraction of Cytosolic Proteins

- *Extraction of Protein*

20 ml of 1.5×10^5 cells/ml or 2×10^5 cells/ml of HepG2 or R-HepG2 cells were seeded into a 75 cm² tissue culture flask and incubated at 37 °C, 5 % CO₂ humidified incubator overnight. Medium was discarded and various concentrations of HK18 were added and medium without drug was added as the negative control.

Cells were incubated for various periods. After treatment, cells were harvested and washed with plain medium 2 times. 4×10^6 cells of each sample were used for assay. 50 μ l of lysis buffer (75 mM NaCl, 1 mM NaH_2PO_4 , 8 mM Na_2HPO_4 , 250 mM sucrose, 21 μ g/ml aprotinin, 5 μ g/ml leupeptin, 1 mM PMSF and various concentration of digitonin) was added to 4×10^6 cells and vortexed vigorously for 30 seconds following with centrifugation at 8,000 x g for 1 minute at room temperature immediately. The supernatant was collected and mixed with equal volume of 2X SDS loading dye and boiled for 10 minutes. Then, the samples were subjected to centrifugation at 11,000 x g for 7 minutes at 4 °C (Single *et al.*, 1998). The supernatant collected was used to run SDS electrophoresis or store at -70 °C. For running electrophoresis, the samples were boiled for 5 minutes and 20 μ l of each sample was loaded to the well of a 12 % SDS gel. The following procedures of electrophoresis were as same as total protein extraction mentioned above.

• ***Determination of the Dosage of Digitonin***

Since digitonin was used to cause plasma membrane permeabilization, the dosage of digitonin was very critical. Insufficient amount of digitonin may lead to incomplete plasma membrane permeabilization while in excess digitonin may lead to disruption of mitochondrial membrane and release of mitochondrial proteins and hence lead to incorrect and misleading result. Thus, the dosage of digitonin was determined first with untreated cells. Various concentrations of digitonin (12.5, 25, 50, 100, 200 and 400 μ g / 4×10^6 cells) were used to lyse cells and the extracts were subjected to SDS electrophoresis. From the film (Fig 2.2), the band intensity of cytochrome c was similar for 12.5, 25, 50 and 100 μ g digitonin / 4×10^6 cells while

the band intensity of 200 and 400 μg digitonin was much higher. This indicated that 200 and 400 μg digitonin did not only permeabilize the plasma membrane but also permeabilize the outer mitochondrial membrane and hence release the cytochrome c of mitochondrial inter-membrane space. From the gel (Fig 2.2), at 12.5 and 25 μg / 4×10^6 cells, the total protein amount was less than other digitonin concentrations. This indicated that these two concentrations of digitonin could not permeabilize the plasma membrane of all cells. Thus, 50 μg digitonin / 4×10^6 cells was chosen to be used which was able to permeabilize the plasma membrane fully but did not affect mitochondrial membrane.

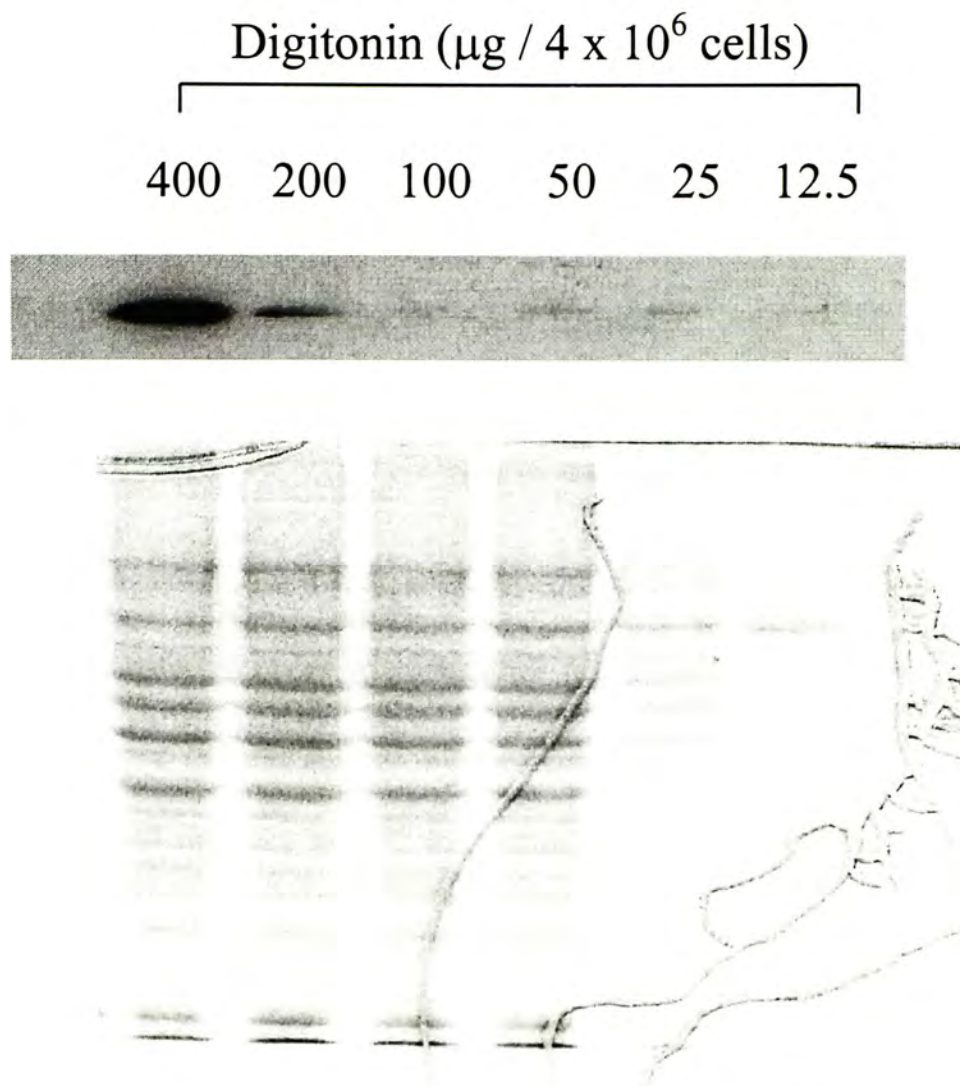


Fig 2.2 Determination of digitonin concentration. 4×10^6 untreated HepG2 cells were lysed with $50 \mu\text{l}$ lysis buffer in the presence of 12.5, 25, 50, 100 or 200 μg digitonin. The protein extracts obtained were mixed with equal volume of 2 X SDS loading dye and $20 \mu\text{l}$ of each sample was loaded to SDS gel electrophoresis. One of the gel was stained with Commassie brilliant blue while another was transferred and probed with anti-cytochrome c anti-bodies.

2.2.13 Determination of Caspases Enzymatic Activity

- *Extraction of proteins*

20 ml of 1.5×10^5 cells/ ml or 2×10^5 cells/ ml of HepG2 or R-HepG2 cells were seeded to a 75 cm² tissue culture flask and incubated at 37 °C, 5 % CO₂ humidified incubator overnight. Medium was removed and HK18 was added. Cells were incubated for various periods. After treatment, both of the floating dead cells and adherent cells were collected and were washed twice with plain medium. Cells were counted and were centrifuge at 400 x g for 10 minutes to collect cell pellet. The pellet can be store at -70 °C for later use. 50 µl of chilled lysis buffer was added to each 2×10^6 cells in order to resuspend and lyse the cell pellet. The cells were allowed to stand on ice for 10 minutes. Then the cell lysate was centrifuge at 11, 000 x g for 3 minutes at 4 °C to precipitate cell debris (Mack *et al.*, 2000). The supernatant was collected for use. The protein concentration of each sample was determined by BCA assay as mentioned above.

- *Assessment of caspases enzymatic activities*

- **Caspase-3 activity**

50 µg of protein of each sample was used for measuring caspase-3 activity. 90 µl of reaction buffer supplemented with 10 mM DTT were added to wells of a 96 well plate. In order to confirm that the increase of substrate signal is due to caspase-3 activity, caspase-3 specific inhibitor z-DEVD-fmk was added before addition of substrate. Lysate containing 50 µg of protein sample was added and 1 µl of 1 mM z-DEVD-fmk was added to the wells and incubated at 37 °C for 30 minutes

at dark. During this incubation period, the other lysate were kept on ice. After incubation, lysate containing 50 μg of protein was added to wells. Then 0.5 μl of 2 mM fluorescent AMC conjugated caspase-3 specific substrate Ac-DEVD-AMC was added to each well (including the wells with inhibitor) and the plate was incubated at 37 $^{\circ}\text{C}$ for 1 hour at dark. A well without cell lysate but containing reaction buffer and substrate was set to act as blank. A standard curve of AMC was set as the following concentrations 0, 0.625, 1.25, 2.5 and 5 μM . After incubation, the fluorescent intensity was measured by a fluorescence microplate reader (CytoFluoTM, Millipore). The excitation and emission filters were 390 nm and 460 nm respectively. The sensitivity of the scanning was maximized. According to the standard AMC fluorescent curve (Fig 2.3), the amount of AMC released from the conjugated substrate can be calculated.

Caspase-8 activity

For measuring caspase-8 activity, 100 μg of protein was used. Similarly, 90 μl of reaction buffer supplemented with 10 mM DTT were added to wells of a 96 well plate. In order to confirm the increase of substrate signal is due to caspase-8 activity, caspase-8 specific inhibitor z-IETD-fmk was added before addition of substrate. Lysate containing 100 μg of protein sample was added and 2 μl of 10 mM z-IETD-fmk was added to the wells and incubated at 37 $^{\circ}\text{C}$ for 30 minutes at dark. During this incubation period, the other lysate were kept on ice. After incubation, lysate containing 100 μg of protein was added to wells. Then 5 μl of 1 mM fluorescent AMC conjugated caspase-8 specific substrate Ac-IETD-AMC was added to each well (including the wells with inhibitor) and the plate was incubated at 37 $^{\circ}\text{C}$

for 1 hour at dark. A well without cell lysate but containing reaction buffer and substrate was set to act as blank. A standard curve of AMC was set as the following concentrations: 0, 0.625, 1.25, 2.5 and 5 μM . After incubation, the fluorescent intensity was measured by a fluorescence microplate reader (CytoFluoTM, Millipore). The excitation and emission filters were 390 nm and 460 nm respectively. The sensitivity of the scanning was maximized. According to the standard AMC fluorescent curve (Fig 2.3), the amount of AMC released from the conjugated substrate can be calculated.

Caspase-9 activity

For measuring caspase-9 activity, 200 μg of protein was used. Similarly, 90 μl of reaction buffer supplemented with 10 mM DTT were added to wells of a 96 well plate. In order to confirm the increase of substrate signal is due to caspase-9 activity, caspase-9 specific inhibitor z-LEHD-fmk was added before addition of substrate. Lysate containing 100 μg of protein sample was added and 2 μl of 10 mM z-LEDH-fmk was added to the wells and incubated at 37 $^{\circ}\text{C}$ for 30 minutes at dark. During this incubation period, the other lysate were kept on ice. After incubation, lysate containing 100 μg of protein was added to wells. Then 5 μl of 1 mM fluorescent AFC conjugated caspase-9 specific substrate Ac-IETD-AFC was added to each well (including the wells with inhibitor) and the plate was incubated at 37 $^{\circ}\text{C}$ for 1 hour at dark. A well without cell lysate but containing reaction buffer and substrate was set to act as blank. A standard curve of AFC was set as the following concentrations: 0, 0.5, 1, 2 and 4 μM . After incubation, the fluorescent intensity was measured by a fluorescence microplate reader (CytoFluoTM, Millipore). The

excitation and emission filters were 400 nm and 505 nm respectively. The sensitivity of the scanning was maximized. According to the standard AFC fluorescent curve (Fig 2.3), the amount of AFC released from the conjugated substrate can be calculated.

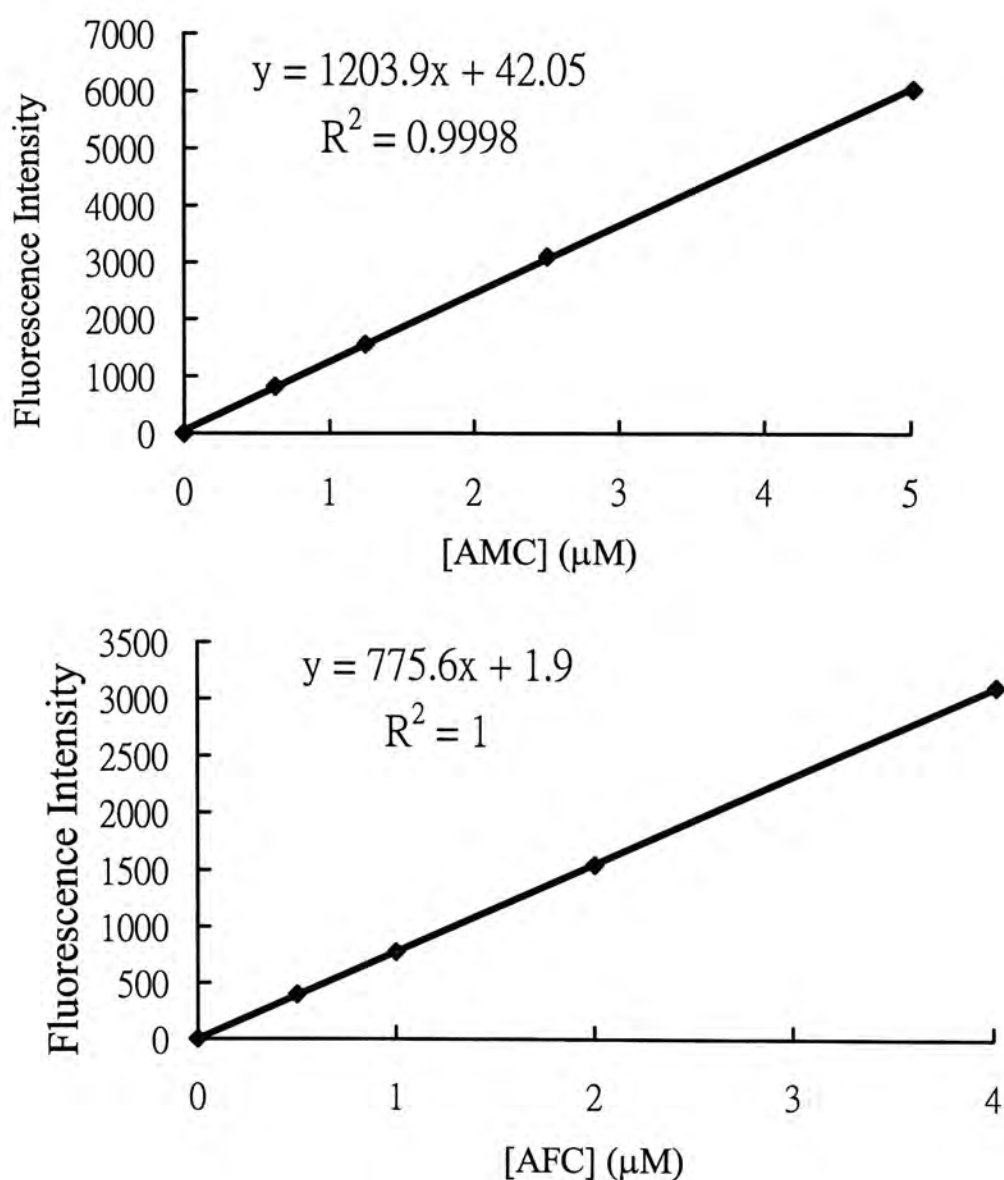


Fig 2.3 Standard curves of AMC and AFC for the determination of caspases enzymatic activities.

2.2.14 Reverse Transcriptase Polymerase Chain Reaction (RT-PCR)

2.2.14.1 RNA Extraction by TRIzol Reagent

1.5 x 10⁶ cells of HepG2 or 2 x 10⁶ cells of R-HepG2 were seeded to 6 wells plate and incubated at 37°C, 5 % CO₂ humidified incubator overnight. The cells were then treated with HK18 or medium with various time periods. After treatment, medium was discarded and 1 ml TRIzol reagent (Invitrogen) was added to each well and was incubated at room temperature for 5 minutes. The lysate was then transferred to 1.5 ml micro-centrifuge tube and 200 µl of chloroform was added. The mixture was mixed by vortex vigorously for 15 seconds and stand at room temperature for 2 to 3 minutes. The mixture was then centrifuged at 12,000 x g for 15 minutes at 4 °C. After centrifugation, 3 layers: a lower red phenol-chloroform layer, an interphase layer and a colorless upper aqueous layer were observed. RNA remains exclusively in the aqueous layer. The upper aqueous layer was transferred to a new micro-centrifuge tube on ice. 0.5 ml isopropanol was added and incubated at room temperature for 10 minutes for RNA precipitation. After that, the sample was centrifuge at 12,000 x g for 10 minutes at 4°C. The supernatant was discarded and 1 ml of 75 % EtOH was added to wash the pellet. The sample was further centrifuge at 7,500 x g for 5 minutes at 4°C and the supernatant was discarded. The pellet was allowed to air-dry for 5 to 10 minutes and then 20 – 30 µl of DEPC-treated dH₂O was added to dissolve the pellet. The RNA samples were then stored at –80°C. The purity of the RNA samples was then checked by measuring OD at 260 and 280 nm by UV-visible spectrophotometer (UV-1601, Shimadzu). 1 µl of RNA sample was diluted with 499 µl DEPC-treated dH₂O for measurement. The ratio of OD 260/280 should be within 1.6 – 1.8. The concentration of RNA (µg/µl) was calculated by (OD

at 260 nm / 0.1) x (4 / 1000) x (500 / 1). Besides, the RNA samples were subjected to gel electrophoresis to check integrity. One μl of RNA samples were mixed with 1 μl 2 X RNA loading dye and incubated at 65 °C for 5 minutes. The mixture was then loaded to 1 % agarose gel for electrophoresis.

2.2.14.2 Reverse Transcription

The RNA samples were then subjected to reverse transcription by ThermoScript™ RT-PCR kit (Invitrogen) for cDNA synthesis. 3 μg of each RNA sample was mixed with 1 μl of oligo(dT) primer (50 μM), 2 μl dNTP (10 mM) and DEPC-treated dH₂O was added to adjust the volume to 12 μl in a 0.5 ml micro-centrifuge tube. The mixture was incubated at 65 °C for 5 minutes and then placed on ice for RNA and primer denaturation to take place. After that, 8 μl of reaction mixture (composed of 4 μl of 5 X cDNA Synthesis Buffer, 1 μl of 0.1 M DTT, 1 μl of 40 U / μl RNasOUT™, 1 μl DEPC-treated dH₂O and 1 μl of 15 units / μl ThermoScript™ RT) was added. RT reaction was carried out in a thermal cycler at 50°C for 60 minutes and terminated at 85°C for 5 minutes. Then 1 μl of RNase H was added and incubated at 37°C for 20 minutes. The cDNA synthesized was diluted 5 folds with autoclaved dH₂O and can be stored at -20°C or used for PCR immediately.

2.2.14.3 Polymerase Chain Reaction

For polymerase chain reaction, 5 μl of diluted cDNA was mixed with 45 μl reaction mixture which composed of 5 μl of 10X PCR buffer. 5 μl of dNTP (2 mM),

5 μl of forward primer (2.5 μM), 5 μl reverse primer (2.5 μM), 28.5 μl autoclaved dH_2O and 0.5 μl of *Taq* polymerase (1.25 units). The sample mixture was then subjected to PCR in a thermal cycler (Progene). The initial denaturing temperature was 94 $^\circ\text{C}$ for 3 minutes and the final elongation temperature was 72 $^\circ\text{C}$ for 10 minutes. While the cycling conditions were set according to the nature of the primer pairs. After finishing the PCR reaction, 2 μl of the PCR product was then mixed with 10 μl of 6X DNA loading dye and then subjected to 1 % agarose gel electrophoresis along with 100 bp DNA marker. Table 2.4 showed the primer sequences used in this project with the corresponding sizes of PCR product as well as the conditions used.

Gene	Sequence / Conditions	Size of PCR Product (bp)
GADPH	Forward: 5'ACCACAGTCCATGCCATCAC3' Reverse: 5'TCCACCACCCTGTTGCTGTA3' Denature: 95 °C, 1 minute Annealing: 50 °C, 1 minute Amplification: 72 °C, 1 minute 27 cycles	400
bcl-2	Forward: 5'AGCTGCACCTGACGCCCTT3' Reverse: 5'CAGCCAGGAGAAATCAAACAGAGG3' Denature: 94 °C, 45 seconds Annealing: 65 °C, 45 seconds Amplification: 72 °C, 2 minute 27 cycles	293
bcl-x	Forward: 5'TGGCAACCCATCCTGGCACCT3' Reverse: 5'ACTGAAGAGTGAGCCCAGCAGAAC3' Denature: 95 °C, 45 seconds Annealing: 61 °C, 45 seconds Amplification: 72 °C, 1 minute 27 cycles	538
bak	Forward: 5GCCCAGGACACAGAGGAGGTTTTTC3' Reverse: 5'AAACTGGCCCAACAGAACCACACC3' Denature: 95 °C, 45 seconds Annealing: 61 °C, 45 seconds Amplification: 72 °C, 1 minute 27 cycles	528

Table 2.4 List of the sequences of primers used in this project and their corresponding PCR conditions and size of PCR products.

2.3 Statistic Analysis

All experiments were performed in triplicate unless otherwise noted. The results were expressed as mean \pm standard derivation. Student's T-test was performed in the experiment indicated and $p < 0.05$ or $p < 0.001$ was considered as statistically significant.



Chapter 3

Cytotoxicity of HK18

3 Cytotoxicity of HK18

3.1 Cytotoxicity of HK18 on HepG2 Cells

First of all, the cytotoxicity of HK18 on the human hepatocellular carcinoma cell line HepG2 was studied by MTT and tryphan blue exclusion assays.

3.1.1 Study of the Cytotoxic Activity of HK18 on HepG2 Cells by MTT Assay

HepG2 cells were incubated with HK18 with the following concentrations: 0, 1, 2, 3, 4, 5, 6, 7, and 10 μM . From Fig. 3.1a, HK18 was found to have cytotoxic effect on HepG2 cells. The percentage of survival decreased when concentrations of HK 18 increased. Most of the HepG2 cells died at the concentration around 10 μM for 24 hours incubation while most of the cells died at the concentration around 7 μM for 48 hours incubation. The IC_{50} of HK18 on HepG2 cells were around 3.5 μM and 2.5 μM for 24 hours and 48 hours respectively. Thus, HK18 was cytotoxic to HepG2 cells in a dose and time dependent manner. A solvent control was carried out to check whether DMSO itself could induce cytotoxic effect. At 10 μM of HK18, the solvent content was 0.02 %. We found that at 0.02 % DMSO, there was around 100 % survival, so the cytotoxic effect was contributed by HK18.

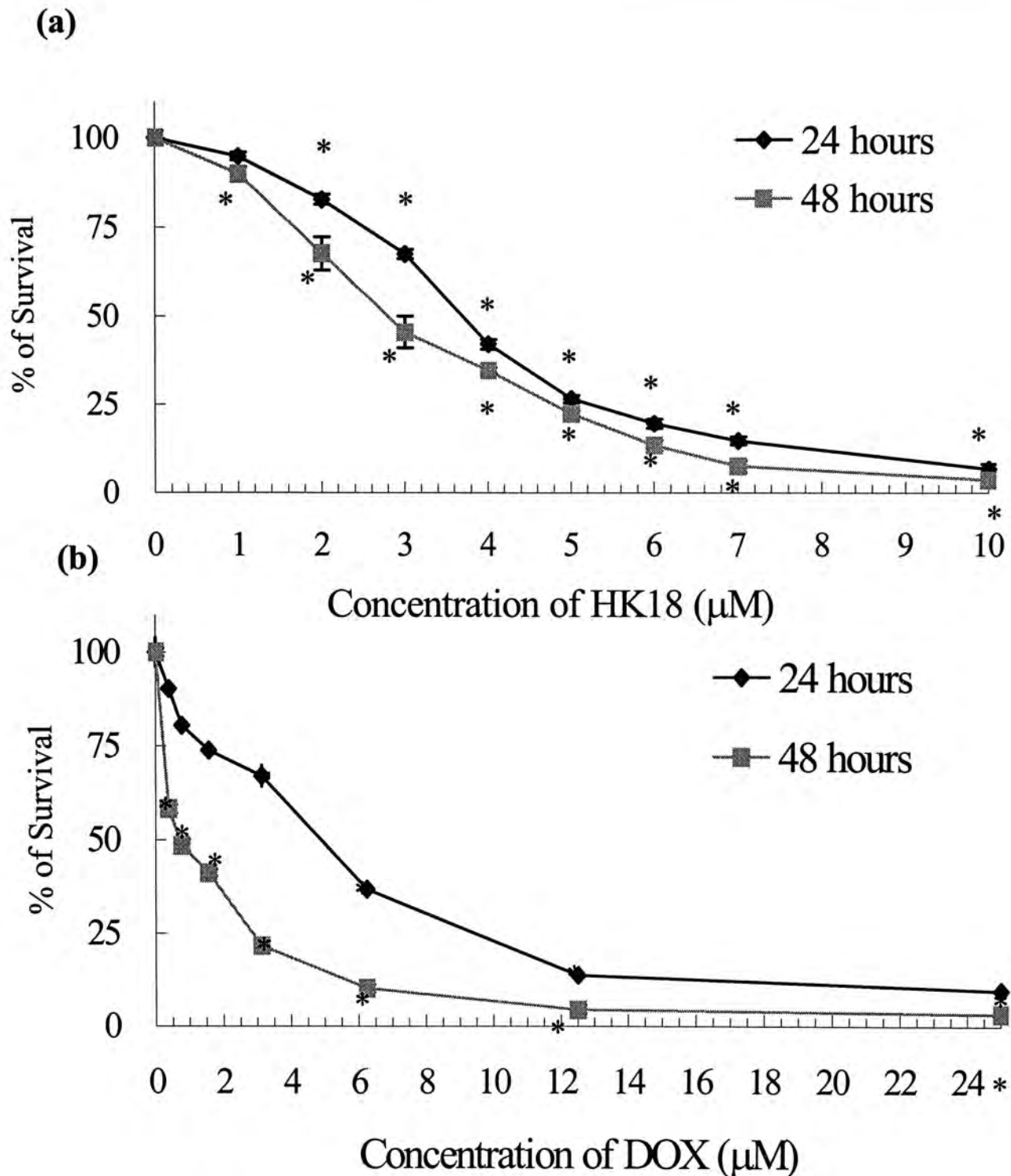


Fig 3.1 Study of cytotoxicity of HK18 and DOX on HepG2 cells for 24 and 48 hours by MTT assay. 1.5×10^5 cells / ml were incubated with various concentrations of HK18 or DOX in a 96 well plate for 24 or 48 hours. After treatment, MTT assay was carried out. Percentage of survival was plotted against concentration of drug added. (a) Percentage survival of HepG2 upon various concentration of HK18. (b) Percentage survival of HepG2 upon various concentration of DOX. Percentage survival was calculated relative to the control that is expressed as 100 %. Mean marked with (*) are significantly ($*P < 0.001$) lower than the control.

As mentioned before, HepG2 is a hepatocellular carcinoma (HCC) cell line. Doxorubicin (DOX) is a commonly prescribed chemotherapeutic drug for treating HCC. Thus, MTT assay was also carried out to study the cytotoxic effect of DOX on HepG2 cells so that it can be used to compare with HK18. Various concentrations were used to incubate with HepG2 cells for 24 and 48 hours. As shown in Fig 3.1b, the percentage of survival decreased with increasing concentrations of DOX. Most of the cells died at the concentration 25 μM and 12.5 μM for 24 and 48 hours incubation respectively. The IC_{50} were around 4.5 μM and 1 μM for 24 and 48 hours. Thus, DOX also possesses cytotoxic effect on HepG2 cells in a dose and time dependent manner. And our data also indicated that HK18 was a high potency anti-tumor drug and had a comparable IC_{50} with this promising chemotherapeutic drug, DOX. The following table summarizes the IC_{50} of HK18 and DOX on HepG2 cells with different incubation time intervals.

Time \ Drug	HK18	DOX
24 hours	3.5 μM	4.5 μM
48 hours	2.5 μM	1 μM

Table 3.1 Summary of the IC_{50} of HK18 and DOX on HepG2 cells treating for 24 and 48 hours by MTT assay.

3.1.2 Study of the Cytotoxic Activity of HK18 on HepG2 Cells by Tryphan Blue Exclusion Assay

Apart from MTT assay, tryphan blue exclusion assay was also performed to study the cytotoxicity of HK18 on HepG2 cells. After treating HepG2 cells with various concentrations of HK18 for 24 and 48 hours, cells were collected and loaded with tryphan blue and cell counting was performed. As indicated in Fig 3.2, HK18 was shown to have cytotoxic effect on HepG2 cells in a dose and time dependent manner.

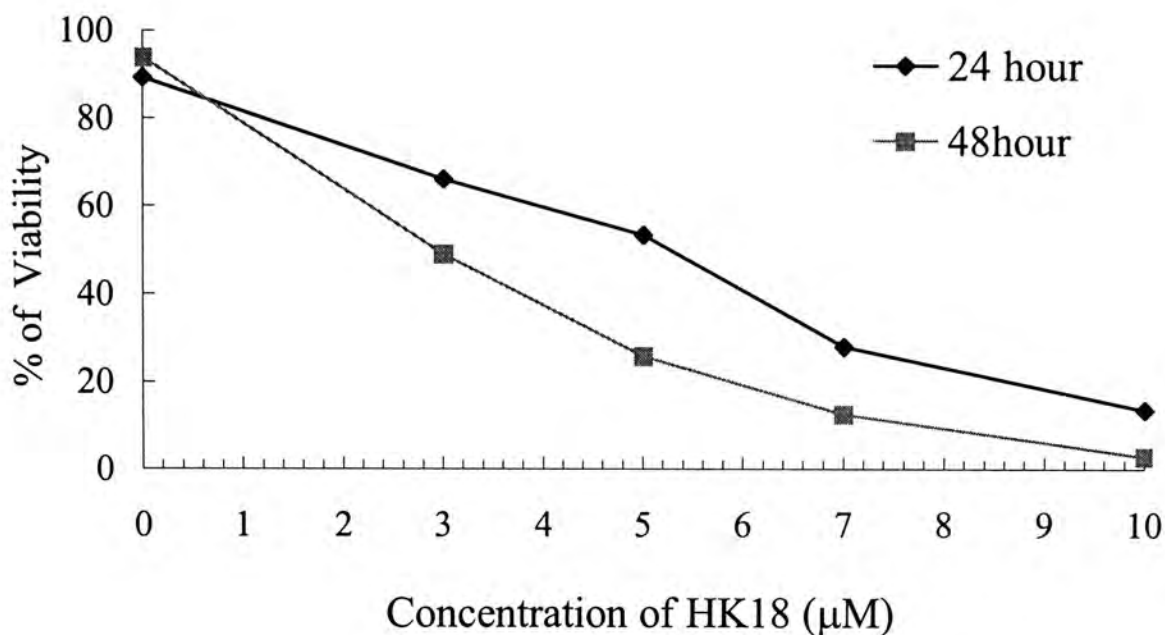


Fig 3.2 Study of the cytotoxicity of HK18 on HepG2 cells by trypan blue exclusion assay. 1.5×10^5 cells / ml of HepG2 cells were seeded into a 6 well plate and incubated with 0, 3, 5, 7 and 10 µM of HK18 for 24 and 48 hours respectively. After treatments, cells were collected and loaded with trypan blue then cell counting was performed. Cells stained blue were dead cell while cells remain unstained were regarded as viable cells. Data are from a representative of three separate experiments. Percentage viability was calculated as: no. of viable cells / no. of total cells x 100 % and was plotted against concentration of HK18.

3.2 Cytotoxicity of HK18 on R-HepG2 Cells

R-HepG2 cells were derived from HepG2 cells incubated with stepwise increased concentrations of DOX. They have acquired the over-expression of P-glycoprotein and thus are multidrug resistant. In this research project, the activities of HK18 on R-HepG2 cells were studied. First of all, its cytotoxicity on R-HepG2 cells were studied by MTT assay and tryphan blue exclusion assay.

3.2.1 Study of the Cytotoxic Activity of HK18 on R-HepG2 Cells by MTT Assay

Various concentrations of HK18 were incubated with R-HepG2 cells for 24 and 48 hours. The concentrations used were 0, 1, 2, 3, 4, 5, 6, 7, and 10 μM . As shown in Fig 3.3 a, HK18 was cytotoxic to R-HepG2 cells in a dose and time dependent manner. Most of the cells died at the concentration 6 μM and 10 μM for 24 and 48 hours respectively. The IC_{50} was around 3.5 μM for 24 hours treatment and 2.5 μM for 48 hours treatment. There was around 100 % survival for 0.02 % DMSO solvent control.

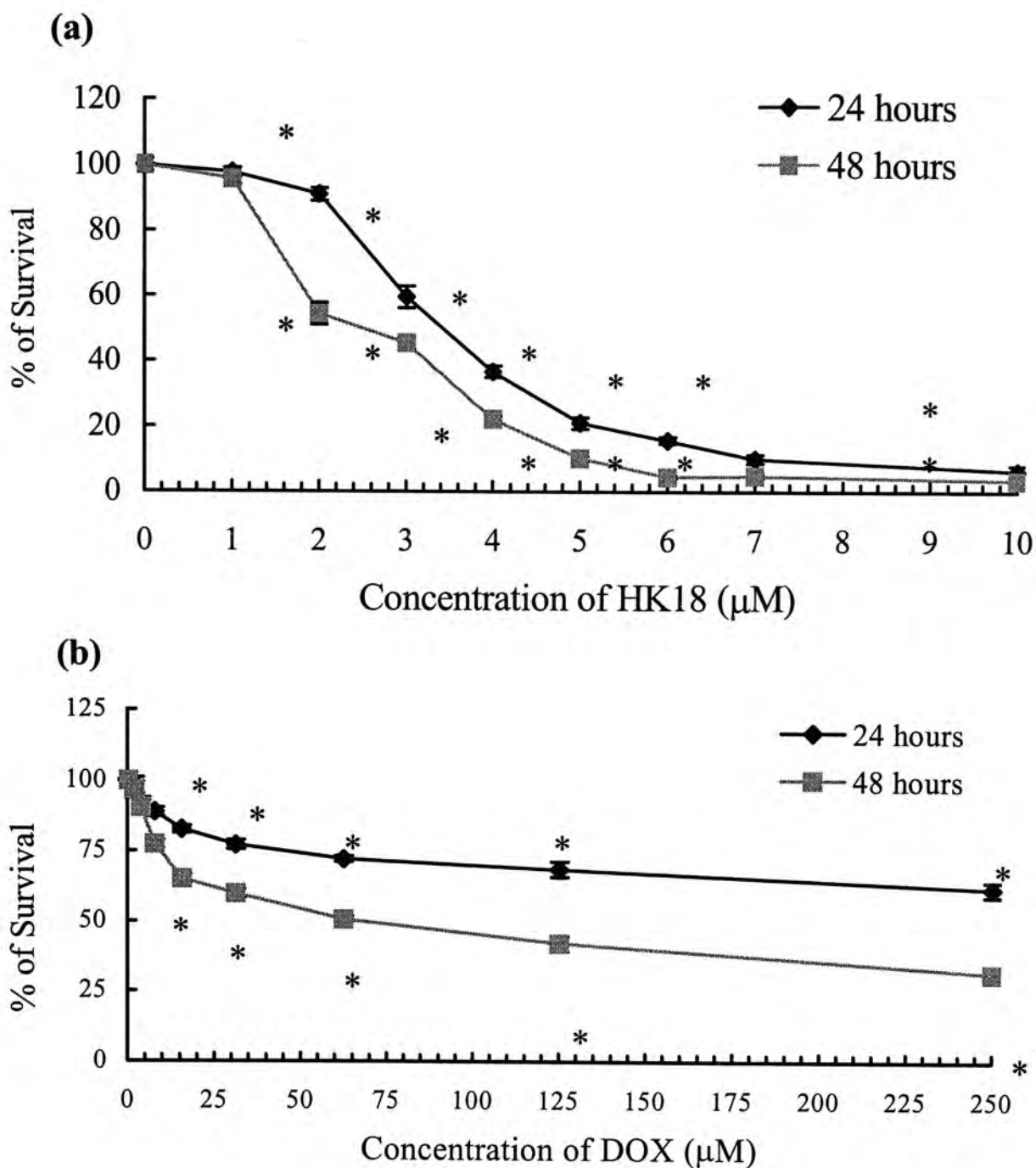


Fig 3.3 Study of cytotoxicity of HK18 and DOX on R-HepG2 for 24 and 48 hours by MTT assay. 2×10^5 cells / ml were incubated with various concentration of HK18 or DOX in a 96 well plate for 24 or 48 hours. After treatment, MTT assay was carried out. Percentage of survival was plotted against concentration of drug added. (a) Percentage survival of R-HepG2 upon various concentration of HK18. (b) Percentage survival of R-HepG2 upon various concentration of DOX. The percentage of survival was calculated as relative to the control that is expressed as 100 %. Mean marked with (*) are significantly ($*P < 0.001$) lower than the control.

Besides, the cytotoxic effect of DOX was also examined on R-HepG2 cells by MTT assay. Various concentrations of DOX (up to 250 μM) were used for 24 and 48 hours treatment. Since there was over-expression of p-glycoprotein in R-HepG2 cells, they are more resistant to the action of DOX. As shown in Fig 3.3 b, DOX was cytotoxic to R-HepG2 cells in a concentration and time dependent manner. However the IC_{50} were much higher than its parental cells HepG2. The IC_{50} of DOX on R-HepG2 cells were around 68 μM for 48 hours and greater than 250 μM for 24 hours treatment. The IC_{50} of HK18 and DOX on R-HepG2 cells with different incubation time intervals was summarized in Table 3.2.

Time \ Drug	HK18	DOX
24 hours	3.5 μM	> 250 μM
48 hours	2.5 μM	68 μM

Table 3.2 Summary of the IC_{50} of HK18 and DOX on R-HepG2 cells treating for 24 and 48 hours by MTT assay.

3.2.2 Study of the Cytotoxic Activity of HK18 on R-HepG2 Cells by Tryphan Blue Exclusion Assay

Tryphan blue exclusion assay was also carried out to study the cytotoxicity of HK18 on R-HepG2 cells. The following concentrations of HK18: 3, 5, 7 and 10 μM were used to incubate with R-HepG2 cells for 24 and 48 hours. As shown in Fig 3.4, HK18 was cytotoxic to R-HepG2 cells on a dose and time dependent manner.

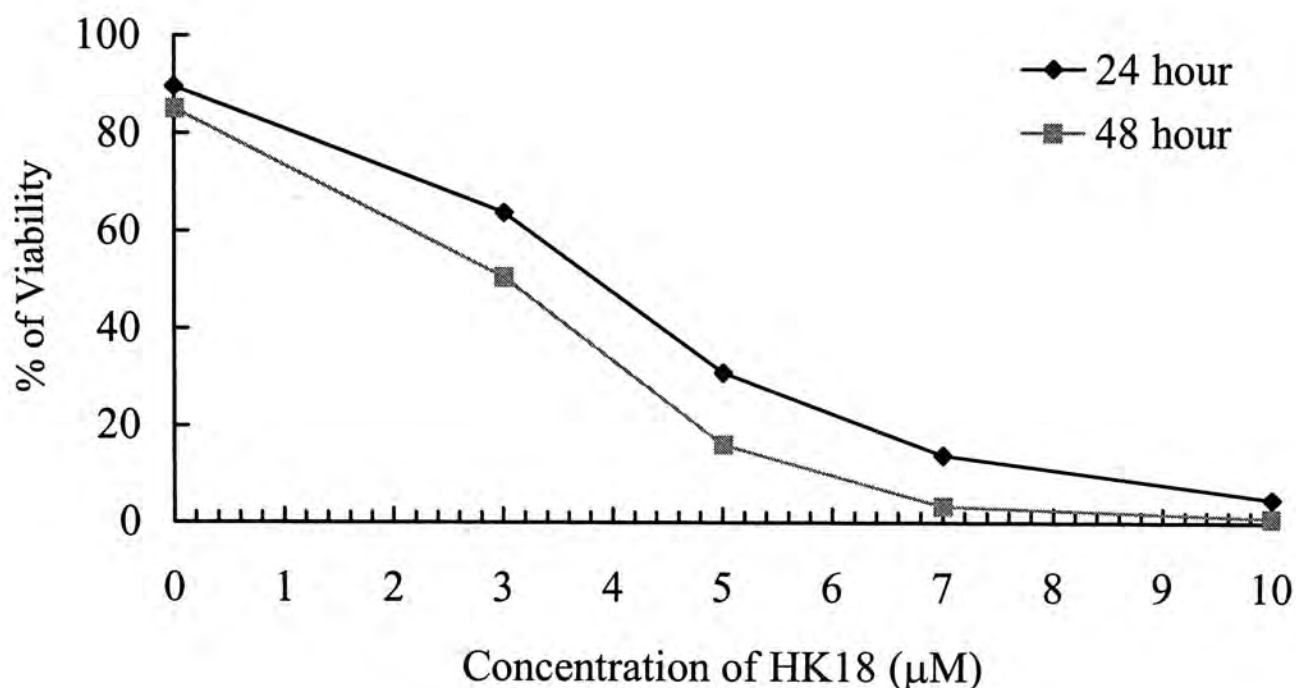


Fig 3.4 Study of the cytotoxicity of HK18 on R-HepG2 cells by Trypan blue exclusion assay. 2×10^5 cells / ml of R-HepG2 cells were seeded into a 6 well plate and incubated with 0, 3, 5, 7 and 10 μM of HK18 for 24 and 48 hours respectively. After treatments, cells were collected and loaded with trypan blue and then cell counting was performed. Cells stained blue were dead cells while cells remain unstained were regarded as viable cells. Data are from a representative of three separate experiments. Percentage viability was calculated as: $\text{no. of viable cells} / \text{no. of total cells} \times 100 \%$ and was plotted against concentration of HK18.

3.3 Cytotoxicity of HK18 on Macrophages

The cytotoxicity of HK18 on normal primary cells, using macrophages as a model, was also studied. Macrophages ($M\Phi$) were collected from balb/c mice as mentioned in the chapter of Materials and Methods. $M\Phi$ obtained were seeded to a 96 well plate and 2.5 μM and 5 μM of HK18 were added for 48 hours incubation. 2.5 μM was used since the IC_{50} obtained from MTT assay for HepG2 and R-HepG2 cells for 48 hours treatment were 2.5 μM . Apart from 2.5 μM , 5 μM was used since it induced around 80 % cytotoxicity on both cell lines for 24 hours treatment. This concentration, 5 μM would further used for the mechanistic studies of HK18 on HepG2 and R-HepG2 cells. After treatment, MTT assay was carried out. The percentage survivals were plotted against the concentration of HK18. Along with $M\Phi$, the percentage survivals of HepG2 and R-HepG2 cells against 2.5 μM and 5 μM of HK18 were also plotted for comparison. As shown in Fig 3.5, the percentage survivals of $M\Phi$, HepG2 and R-HepG2 cells upon 2.5 μM HK18 were around 90 %, 52 % and 48 % respectively. While at 5 μM HK18, the percentage survival were around 70 %, 10 % and 12 % for $M\Phi$, HepG2 and R-HepG2 cells respectively.

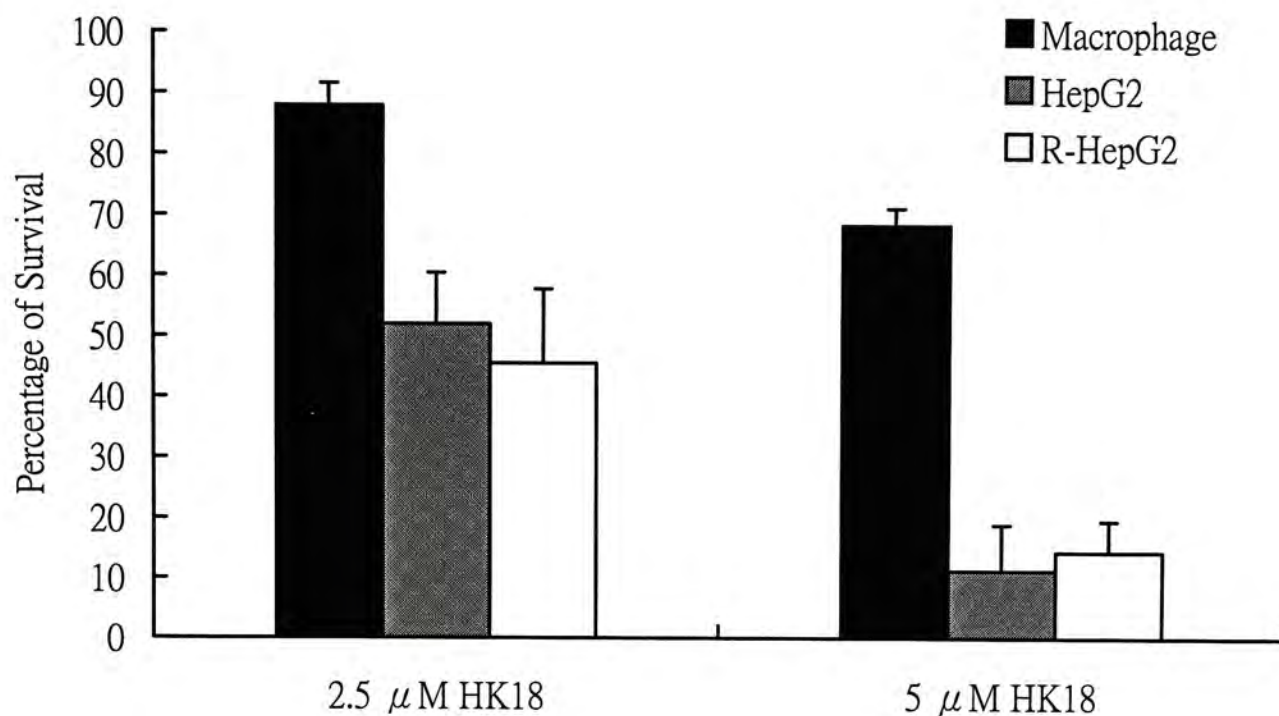


Fig 3.5 Comparison of the cytotoxicity of HK18 on macrophages, HepG2 and R-HepG2 cells. Macrophages collected from balb/c mice, HepG2 and R-HepG2 cells were incubated with 2.5 and 5 μ M of HK18 for 48 hours. After treatment, MTT assay was carried out. Percentage survival was calculated as relative to the control that is expressed as 100 % and was plotted against concentration of HK18 according to the cells.

3.4 Hemolytic Activity of HK18

As mentioned in the Introduction chapter, hemolysis is a common feature of saponins. Thus, the hemolytic ability of HK18 was studied. HK18 was used to incubate with red blood cells collected from SD rat with the concentrations of 3, 5, 7, 10, 20, 40, 80 and 120 μM . From Fig 3.6, it showed that HK18 induce hemolysis in a dose dependent manner with LD_{50} around 70 μM and about 80 % hemolysis at the concentration of 120 μM . However, only a small proportion of red blood cells were lysed (< 3 %) at the concentration of IC_{50} (i.e. 3.5 μM for 24 hours) obtained from the MTT assay on HepG2 cells as well as R-HepG2 cells and around 7 % hemolysis observed at the maximum concentration (10 μM) applied on HepG2 cells and R-HepG2 cells for studies.

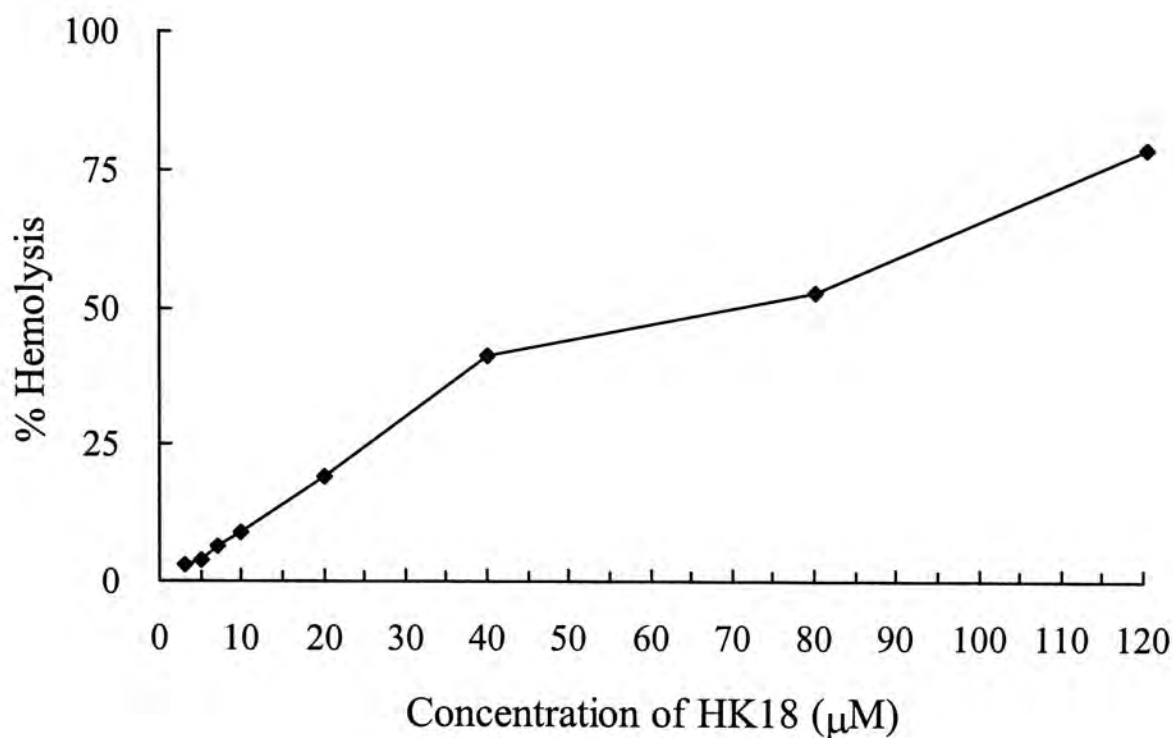


Fig 3.6 Study of the hemolytic activity of HK18. Red blood cells were collected from 200-220 g SD rat and were incubated with various concentrations of HK18. After incubation, absorbance was measured by spectrometer. The readings indicated the extent of hemolysis. The percentage of hemolysis was plotted against the concentration of HK18.

3.5 *In vivo* Study of the Toxicity of HK18

The toxicity of HK18 was further investigated by *in vivo* study. 342 $\mu\text{g} / \text{kg}$ of HK18 which is equivalent to 5 μM final circulation concentration was injected to a group of balb/c mice via intravenous injection. In parallel with HK18, a group of mice were treated with saline only as control and 0.4 % γ -cyclodextrin as solvent control. γ -cyclodextrin was used instead of DMSO as solvent since γ -cyclodextrin is a commonly used clinical solvent. The treatments last for two weeks with intravenous injection applied every alternative day. After treatments, the mice were sacrificed and serum was collected. The enzymes levels were then measured to examine tissues damage. Creatine kinase (CK) and lactate dehydrogenase (LDH) are the biomarkers of heart tissue damage while aspartate transaminase (AST) and alanine transaminase (ALT) are the hallmarks of liver damage. The enzyme levels are directly proportional to the degree of corresponding tissues damage and was measured by their enzymatic activities.

It has been found that 342 $\mu\text{g} / \text{kg}$ of HK 18 was non-toxic to both heart and liver tissues since the levels of all the four enzymes were more or less similar to the control and solvent control (Fig 3.7 and 3.8).

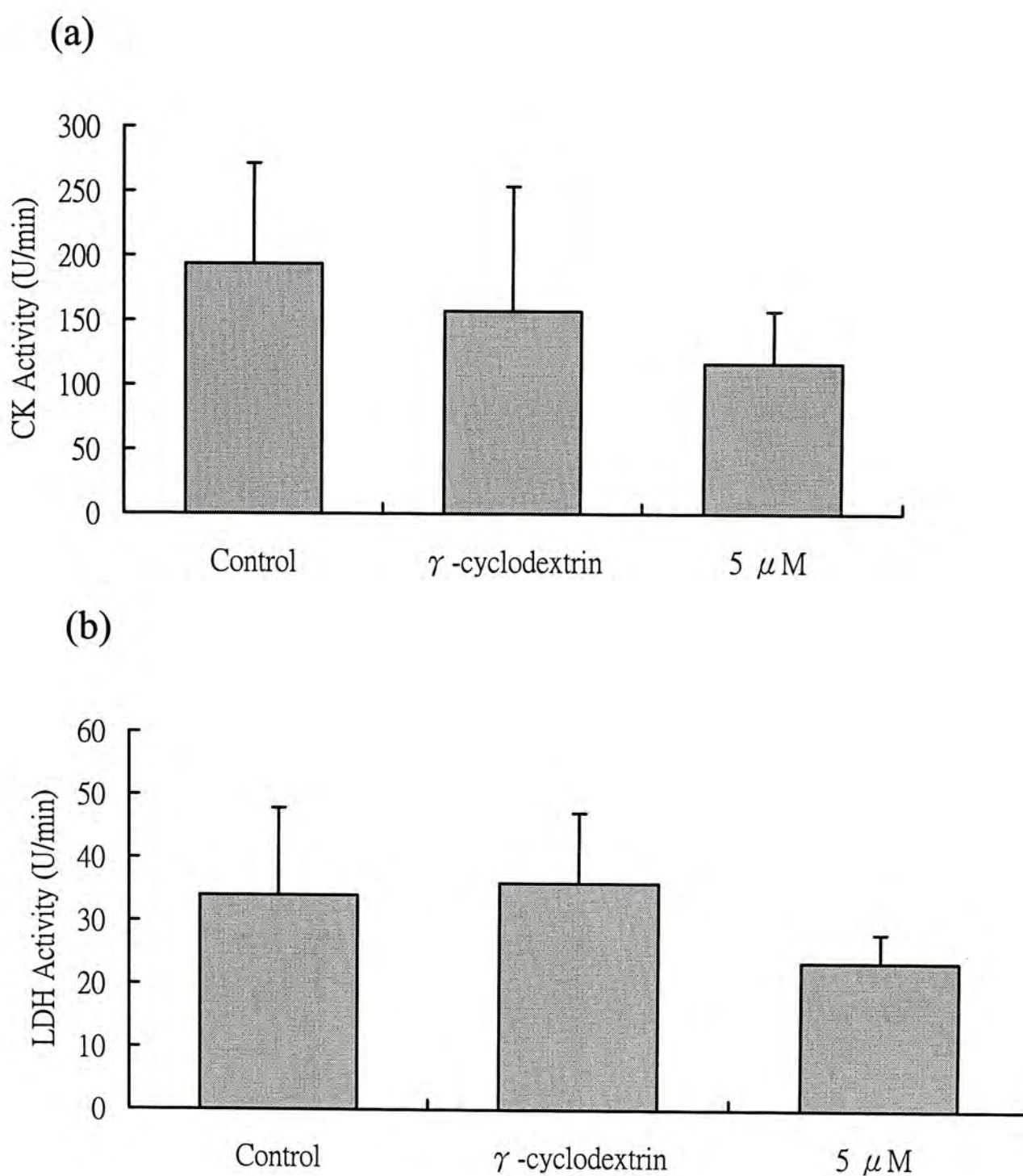


Fig 3. 7 *In vivo* studies of the toxicity of HK18 by measuring the heart tissue specific enzymes CK and LDH. 3 groups of mice were treated with saline, 0.4 % γ -cyclodextrin or 342 μ g / kg HK18 via intravenous injection every alternate day for 2 weeks. After treatments, mice were killed and serum was collected. The serum enzyme levels were then measured based on their enzymatic activities. (a) CK enzymatic activity. (b) LDH enzymatic activity. n = 6.

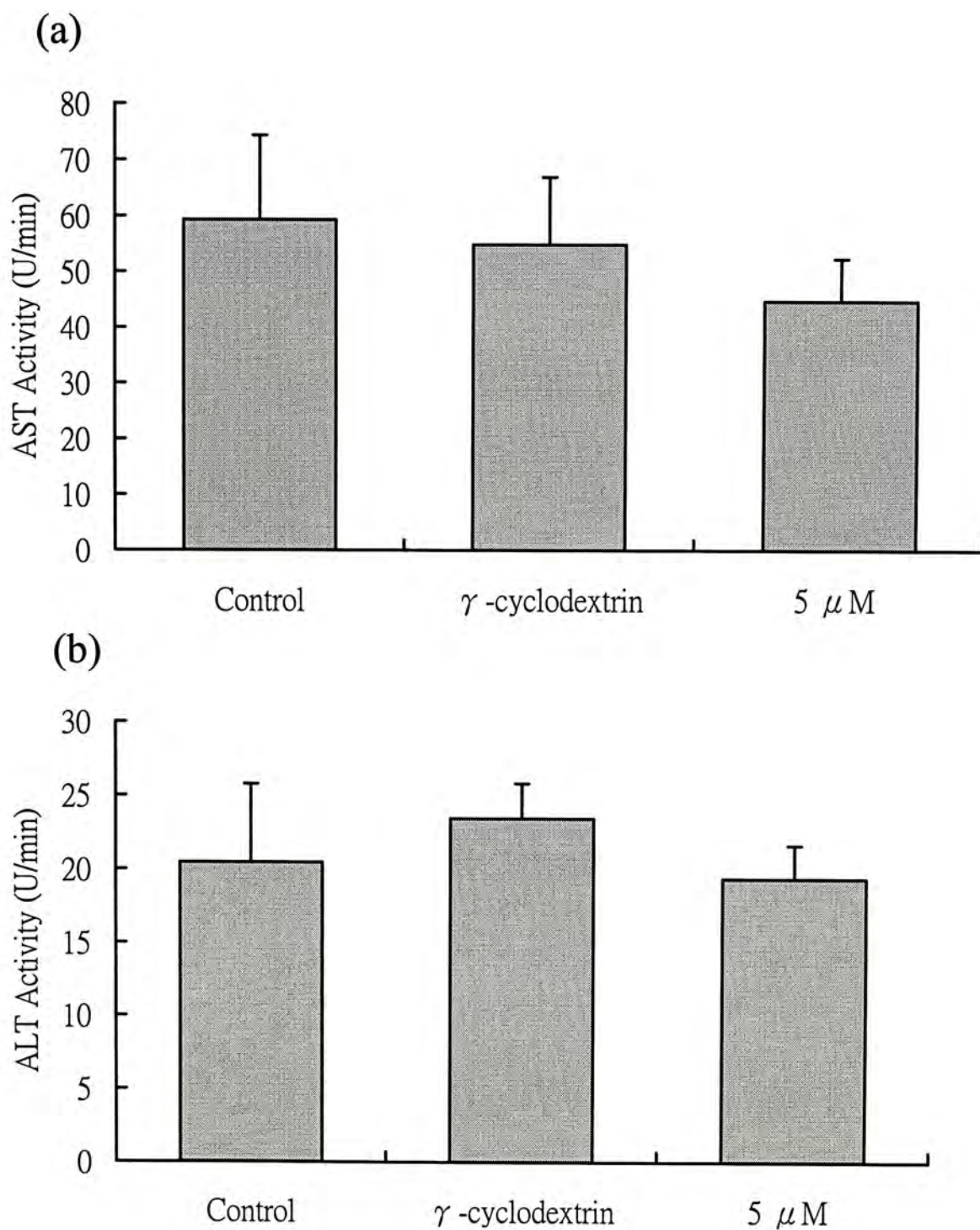


Fig 3. 8 *In vivo* studies of the toxicity of HK18 by measuring the liver tissue specific enzymes AST and ALT. 3 groups of mice were treated with saline, 0.4 % γ -cyclodextrin or 342 μ g / kg HK18 via intravenous injection every alternate day for 2 weeks. After treatments, mice were killed and serum was collected. The serum enzyme levels were then measured based on their enzymatic activities. (a) AST enzymatic activity. (b) ALT enzymatic activity. n = 6.

Chapter 4
Mechanistic Study of
HK18 on HepG2 Cells

4 Mechanistic Study of HK18 on HepG2 Cells

4.1 Hallmarks of Apoptosis Induced by HK18 on HepG2

Cells

Nowadays, there are several approaches in treating cancer. One of them is the induction of cell cycle arrest. Tumor cells are cells undergoing uncontrollable cell division. Thus an agent, which obstructs the cell cycle progression, can be used for cancer treatment. Besides, the induction of cell differentiation is another approach. The principle of this approach is the induction of active proliferating progenitor cells into non-proliferating or less active proliferating cells such as promyelocytic leukemia cells into monocytic cells. Apart from cell cycle arrest and cell differentiation, induction of apoptosis is another important approach. Since HK18 was found to be cytotoxic to HepG2 cells, its apoptotic inducing ability was investigated in this project.

There are several hallmarks observed during apoptosis, such as morphological changes including chromatin condensation, cellular shrink and apoptotic bodies formation. Biochemical changes also resulted including plasma membrane alternation as indicated by externalization of phosphatidylserine (PS), DNA fragmentation and caspases activation (Webb *et al.*, 1997).

4.1.1 Induction of Phosphatidylserine Externalization by HK18 on HepG2 Cells

Phosphatidylserine (PS) is a phospholipid normally restricted to the inner

leaflet of the plasma membrane. However, during apoptosis, PS usually flipped from the inner to the outer membrane. This externalization property is one of the biochemical events occur during apoptosis and is usually precedes other morphological changes. It is a critical property for the maintenance of homeostasis of an organism. It is because exposure of PS on cell surface is a stigma for phagocytosis by macrophages. Thus, the dying cells can be removed before they lose membrane integrity and leakage of cellular substances into surrounding and cause inflammation (Spactor *et al.*, 1998).

This property can be made use to study early apoptosis and necrosis / late apoptosis in the combination of FITC conjugated Annexin V and propidium iodide (PI). Intact cell membrane of viable and early apoptotic cells can exclude a number of substances such as PI. On the contrary, necrotic and late apoptotic cells usually lose membrane integrity and thus allow PI to enter. Annexin V binds tightly with PS in the presence of calcium. Thus fluorescence FITC conjugated Annexin V can be used to stain the PS existing in the outer leaflet of plasma membrane of apoptotic cells (Spactor *et al.*, 1998)(Fig 4.1 a).

By combining these changes of membrane integrity and PS localization, early apoptosis and necrosis / late apoptosis can be distinguished by using flow cytometry. Annexin V-FITC intensity can be detected at the FL-1 channel while PI intensity can be detected at the FL-3 channel. For normal viable cells, both fluorescence dyes are excluded from the cells. Therefore, both of the Annexin V and PI intensity were low which can be observed at the lower left quadrant of the density

plot of FL-1 against FL-3 (Fig 4.1 b). While during early apoptosis, Annexin V binds to the exposed PS but PI was excluded. This was indicated as a cell population at the lower right quadrant. On the other hand, for cells undergoing necrosis or late apoptosis, the cells will be stained with both dyes, which appeared as a cell population at the upper right quadrant. The percentage of cell populations in each quadrant can be analyzed and so it allows quantification of apoptosis.

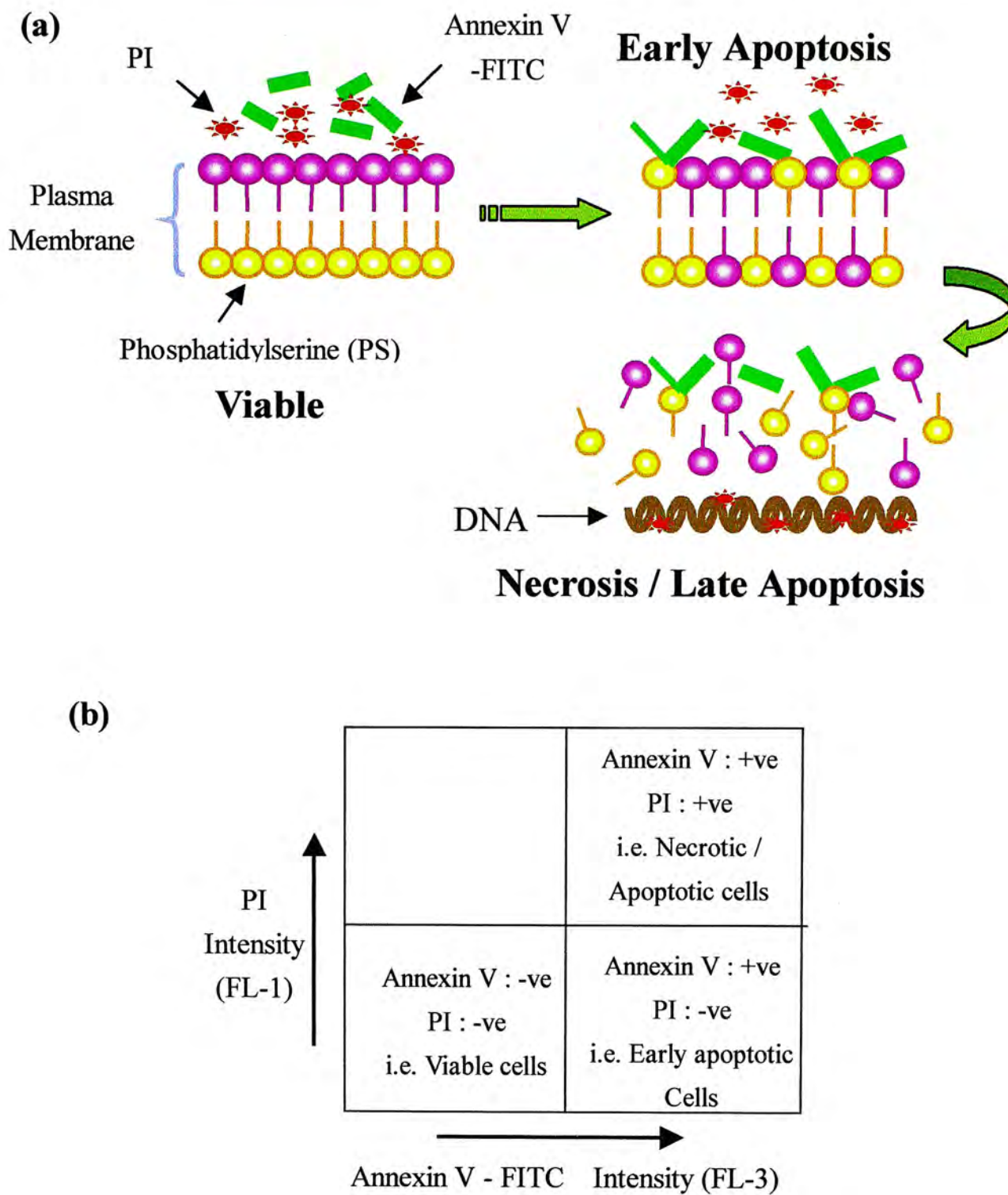


Fig 4.1 Quantification of apoptosis by Annexin V-FITC conjugate and PI by flow cytometry. (a) Schematic diagram showing the binding of Annexin V-FITC and PI to apoptotic or necrotic cells. (b) The density plot can be divided into four quadrants for distinguish and quantification of viable, early apoptotic and later apoptotic / necrotic cells.

Externalization of PS of HK18 treated HepG2 cells were studied by Annexin V – FITC and PI staining, in this assay, 3, 5 and 7 μM of HK18 were used to incubate with HepG2 cells for 24 hours. From the density plots (Fig 4.2), two additional cell populations were observed in the lower right and upper right quadrants of HK18 treated cells. The percentage of cells in the lower left quadrant, which represent the percentage of viable cells, decreased from 86.6 % of control to 53.7, 40.6 and 36.3 % of treatments at 3, 5 and 7 μM of HK18 respectively. On the other hand, the percentage of cells in the lower right quadrant, which indicate the percentage of early apoptotic cells, increased from 7.9 % of control to 28.4, 34.7 and 38.9 % for treatments of 3, 5 and 7 μM of HK18 respectively. The folds of increase were 3.6, 4.4 and 4.9 folds respectively. The percentage of cells in the upper right quadrant also increased from 5.3 % of control to 16.2, 21.3 and 19 % for 3, 5 and 7 μM of HK18 which indicate the percentage of necrotic / late apoptotic cells. Therefore, HK18 could induce apoptosis in a dose-dependent manner. At the concentration of 7 μM , the percentage of DMSO was 0.014 % and it was used to incubate with HepG2 cells as a solvent control. The density plot of solvent control was similar to the control one; thus, the changes of distribution of cells for HK18 treated HepG2 cells were contributed by HK18 solely. Besides, a positive control was performed to verify this experiment, by adding 20 mg/ml digitonin which binds with cholesterol of plasma membrane and hence increase cell permeability. From the result, most of the cells of the positive control were located at the necrotic / late apoptotic region.

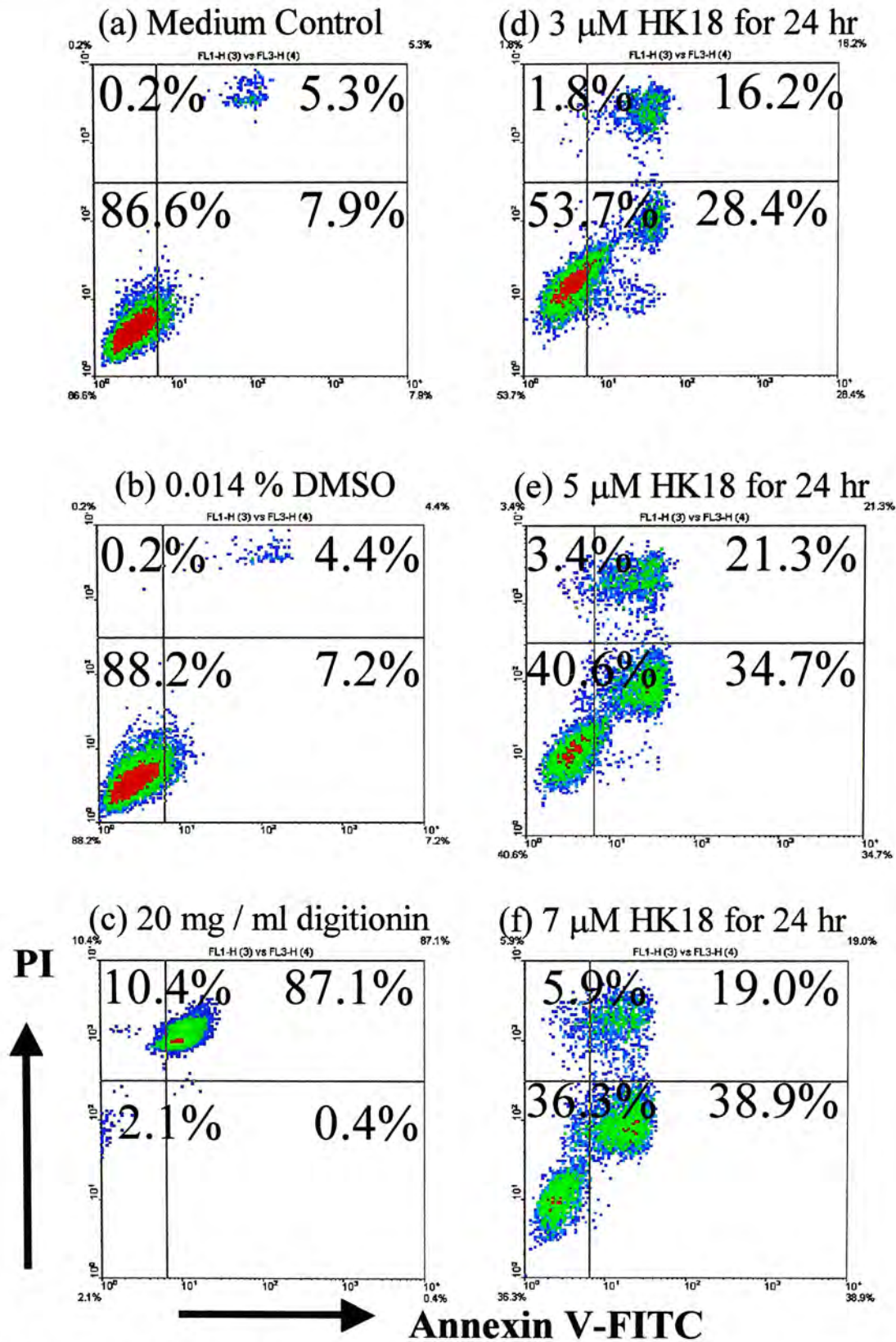


Fig 4.2 Phosphatidylserine externalization induced by HK18 on HepG2 cells. 1.5×10^5 cells / ml of HepG2 cells were seeded into a 6 well plate and 3, 5 and 7 μ M of HK18 were added to incubate for 24 hours. After treatment, cells were collected and loaded with Annexin V-FITC and PI for staining and followed by flow cytometric analysis. 20mg / ml digitonin was added to act as a positive control. Data are from a representative of five separate experiments.

4.1.2 Induction of DNA Fragmentation by HK18 on HepG2 Cells

DNA fragmentation is a common feature of apoptosis in most, though not all, cell types. During apoptosis, endonuclease was activated which cleave the genomic DNA first into large fragments of 30-50 kilobases and further cleave at the linker regions between nucleosomes (Webb *et al.*, 1997). The resulted oligonucleosomal fragments can be detected as multiples of 180 – 200 base pairs, which can be assessed by agarose gel electrophoresis. The fragmented DNA would appear as a ladder after electrophoresis and so this method is called DNA-ladder development (Spactor *et al.*, 1998).

The ability of HK18 to induce DNA fragmentation on HepG2 cells was studied. HepG2 cells were incubated with various concentrations of HK18 as 1, 3, 5, 7 and 10 μM for 24 and 48 hours. Cells without HK18 and with 0.02 % DMSO were also carried out to act as medium control and solvent control respectively. From the result of 24 hours incubation, DNA ladder developed at the concentration of 5, 7 and 10 μM but not in the control, solvent control, 1 and 3 μM of HK18 (Fig 4.3). This indicated that HK18 could induce DNA fragmentation at the concentration above 5 μM after 24 hours incubation. For 48 hours, DNA ladder was observed at a lower concentration of 3 μM apart from 5, 7 and 10 μM . Thus, HK18 could induce DNA fragmentation in a time dependent manner. However, since DNA fragmentation only gives a qualitative assessment, we cannot conclude HK18 induce DNA fragmentation of HepG2 cells in a dose-dependent manner.

Lane 1 2 3 4 5 6 7 8

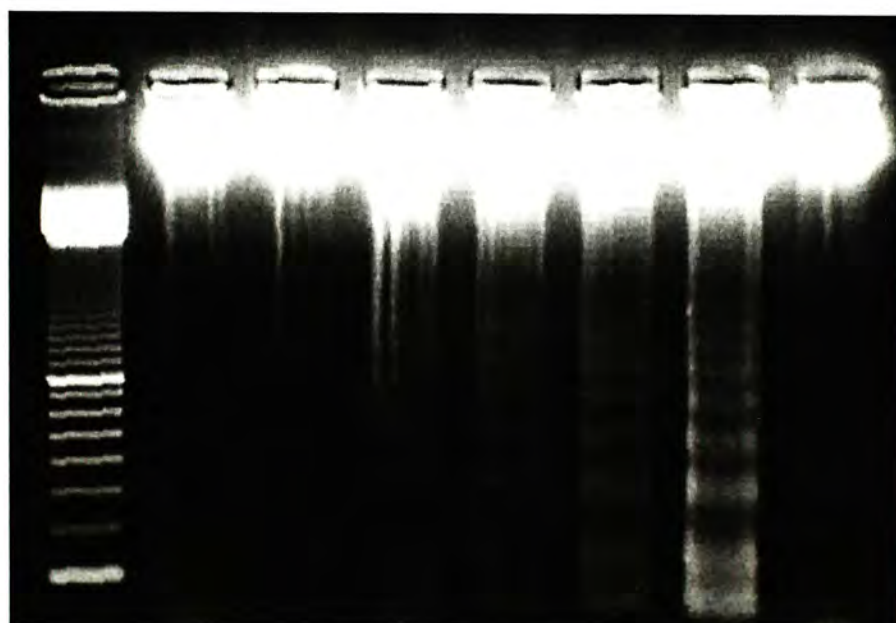
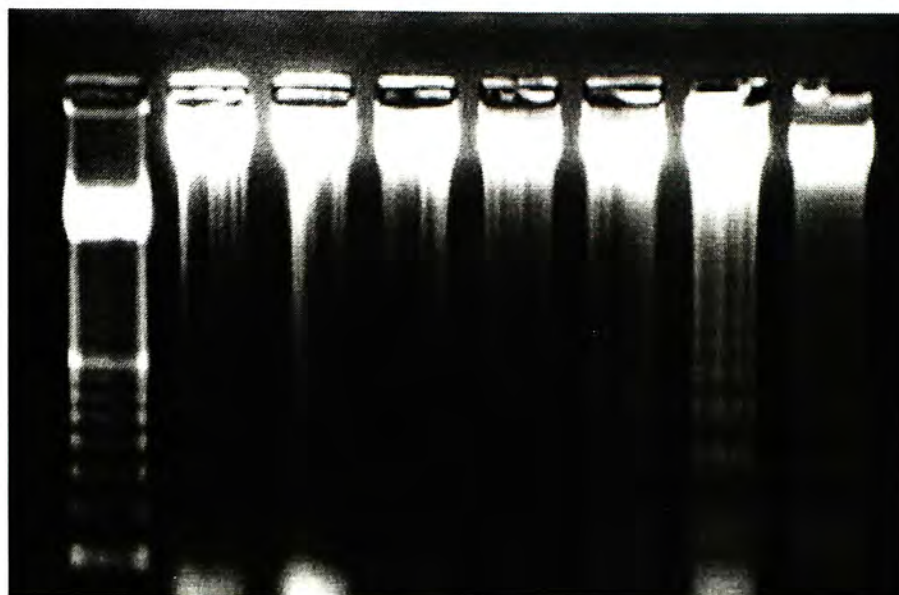


Fig 4.3 Induction of DNA fragmentation in HK18 treated HepG2 cells. 1.5×10^5 cells/ml of HepG2 cells were seeded into a 6 well plate and various concentrations of HK18 were added for 24 or 48 hours incubation. After treatments, cells were collected and DNA was extracted and subjected to gel electrophoresis. (a) 24 hr incubation. Lane 1: 100 base pairs marker. Lane 2: Medium control. Lane 3: 0.02 % DMSO solvent control. Lanes 4 – 8: 1, 3, 5, 7 and 10 μM of HK18. (b) 48 hr incubation. Lane 1: 100 base pairs marker. Lane 2: Medium control. Lanes 3 –7: 1, 3, 5, 7 and 10 μM HK18. Lane 8: 0.02 % DMSO solvent control. Data are from a representative of five separate experiments.

4.2 Study of the Underlying Mechanisms of HK18 Induced Apoptosis in HepG2 Cells

From the above assays, it can be concluded that HK18 was able to induce apoptosis in HepG2 cells. After that, the mechanisms of its apoptosis-inducing ability were studied in this research project.

4.2.1 The Role of Mitochondria in HK18 Induced Apoptosis of HepG2 Cells

Recently, more and more studies have given evidences that mitochondria play an important role in regulating apoptosis. Mitochondrial permeability transition (MPT) plays an active role in apoptosis (Zamzami *et al.*, 1996; Marchetti *et al.*, 1996; Green and Reed, 1998). The proposed MPT pore composed of several components, which form a complex, spans both the inner and outer mitochondrial membrane. They are the voltage-dependent anion channel (VDAC) (located at outer membrane), the adenine nucleotide translocator (ANT) (located at the inner membrane), the peripheral benzodiazepin receptor (located at the outer membrane), cyclophilin D (located at the matrix), creatine kinase (located at the intermembrane space) and hexokinase (located at the outer surface of outer membrane) (Kroemer and Reed, 2000; Crompton, 1999). The proposed schematic diagram of MPT pore complex was shown in Fig 4.4 (Costantini *et al.*, 2000).

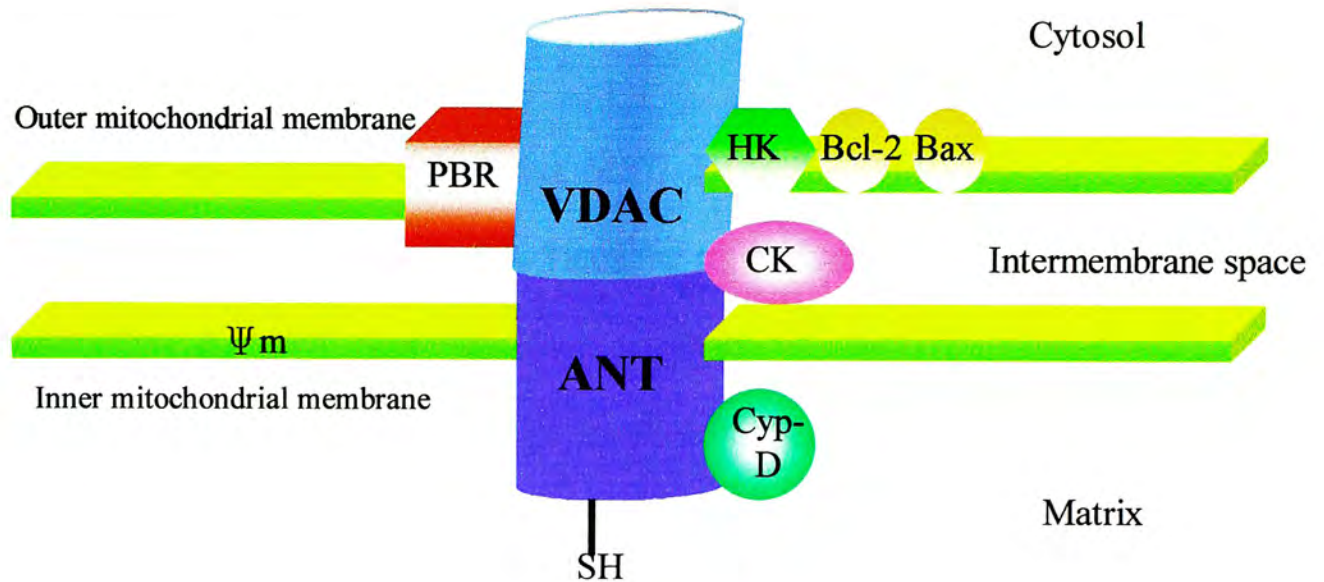


Fig 4.4 Proposed schematic diagram of MPT pore complex. VDAC: voltage dependent anion channel; ANT: adenine nucleotide translocator; PBR: peripheral benzodiazepin receptor; HK: hexokinase, Bcl-2 and Bax: anti-apoptotic and pro-apoptotic Bcl-2 family proteins; CK: creatine kinase; Cyp-D: cyclophilin D; SH: thiol group and Ψ_m : mitochondrial membrane potential. (Modified from (Costantini *et al.*, 2000)).

There are several well known conditions, which are able to induce MPT. They are oxidative stress, high intracellular calcium concentration, low ATP, high ADP, high pH and mitochondrial membrane potential depolarization (Lemasters *et al.*, 1998; Crompton, 1999). Once the MPT pores open, solute with molecular weight smaller than 1,500 Da will escape from the boundary of mitochondria into cytoplasm and the mitochondrial membrane potential may be collapsed (Crompton, 1999).

It was proposed that during MPT, the highly folded mitochondrial inner membrane was allowed to expand. Since the surface area of the inner membrane is greater than the outer membrane, such expansion was thought to cause membrane rupture and release of intermembrane apoptogenic protein such as cytochrome c and apoptosis inducing factor (AIF) to trigger apoptosis. There are many researches proving that cytochrome c and AIF are released into cytosol before apoptotic alternation observed. And studies have found that inhibition of MPT would inhibit apoptosis (Kroemer and Reed, 2000; Crompton, 1999).

In view of this, the involvement of mitochondria in HK18-induced HepG2 cells apoptosis was carried out in this research project.

4.2.1.1 HK18 Induced Mitochondrial Membrane Depolarization in HepG2 Cells

Mitochondria are regarded as the powerhouses of a cell. Under normal physiological conditions, the transmembrane potential difference is around 180 mV with negative charge on the matrix side and positive charge on the cytosolic side. The maintenance of potential difference is contributed by the proton gradient across

the membrane, which is critical for energy production (Stryer, 1995b). However, during apoptosis, the mitochondrial membrane potential (Ψ_m) may collapse .

To measure the potential difference, cationic lipophilic fluorescent dyes can be used. In this project, JC-1 was used. The uptake of this dye by mitochondria is driven by the negative charge. They will aggregate to form dimer in the inner mitochondrial membrane and give out red fluorescence (Cossarizza *et al.*, 1993; Reers *et al.*, 1995), which can be measured by flow cytometry at the FL-3 channel. However, when the mitochondria become depolarize, the dimerized JC-1 dye will break down into monomer and give out green fluorescence as measured at the FL-1 channel. Thus, increase of green fluorescence with decrease of red fluorescence implies Ψ_m depolarization.

Effect of HK18 on the mitochondria potential of HepG2 cells was studied. As shown in Fig.4.5, 3, 5 and 7 μM of HK18 were used to incubate with HepG2 cells for 12 and 24 hours. The x-axis of the contour plot shows the green fluorescence of monomeric JC-1 while the y-axis shows the red fluorescence of dimeric JC-1. The contour plots were divided into two regions. The region R1 indicated the cell population with higher green but lower red fluorescence which reflect Ψ_m depolarization. For 12 hours incubation, the cell population in R1 increased from 9.3 % of control to 22.6 % and 23.5 % for 5 and 7 μM of HK18 respectively. The increment was more significant for 24 hours incubation. The cell population in R1 increased to 22.4, 35.6 and 41.3 % for 3, 5 and 7 μM respectively which were around 2.4, 3.8 and 4.4 folds of the control. Therefore, it was obvious that HK18 was able to

induce Ψ_m depolarization in a dose and time dependent manner. Besides, a solvent control (0.014 % DMSO) and a positive control (500nM Valinomycin) were performed. Valinomycin is a chemical, which could induce MPT (Furlong *et al.*, 1998). For the solvent control, the percentage in the R1 region is similar to the control one. Thus the Ψ_m depolarizing activity was attributed to HK18. For the positive control, almost all cells fell in the region R1.

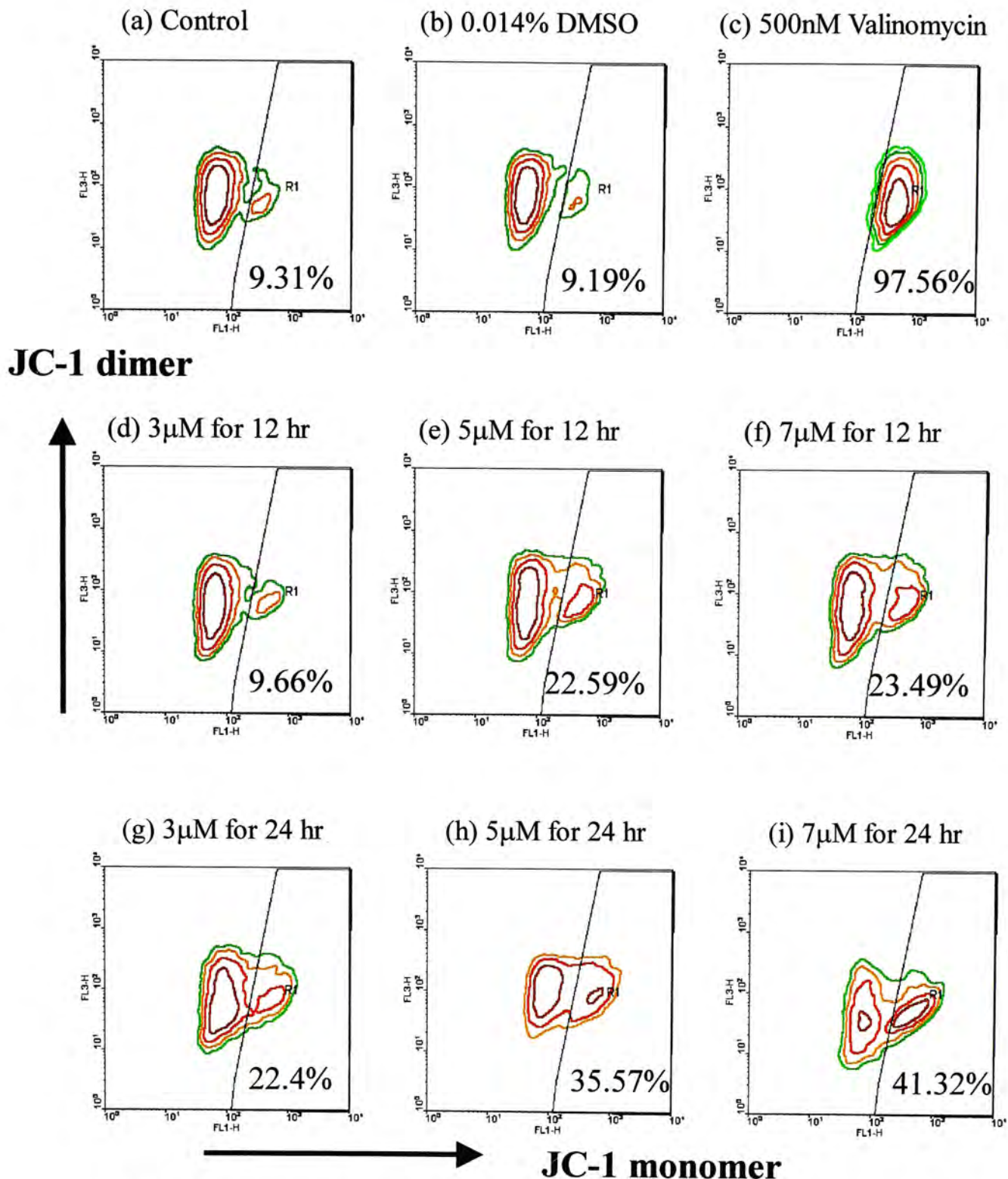


Fig 4.5 Induction of mitochondrial membrane potential depolarization in HK18 treated HepG2 cells. 1.5×10^5 cells / ml were seeded into a 6 well plate and various concentrations of HK18 were added as indicated for 24 and 48 hours. After treatments, cells were loaded with JC-1 and fluorescence intensity was recorded by flow cytometry. (a) and (b) control and 0.014 % DMSO solvent control. (c) 500 nM valinomycin as positive control. Plots (d)-(f) 3, 5 and 7 μ M HK 18 for 24 hr incubation. Plots (g)-(i) 3, 5 and 7 μ M of HK18 for 48 hr incubation. Data are from a representative of five separate experiments.

4.2.1.2 Addition of Bongkreikic Acid Reduced HK18 Cytotoxicity on HepG2 cells

To study the requirement of MPT in HK18 treated-apoptotic cells, MPT inhibitors were added. The most widely used MPT inhibitors are cyclosporin A and Bongkreikic acid (Crompton, 1999; Zamzami *et al.*, 1996; Marchetti *et al.*, 1996).

Bongkreikic acid (BA) is an unsaturated fatty acid produced by *Pseudomonas cocovenans* on partially defatted coconut. Its name has been derived from “bongkreck”, a moulded coconut product from Banjoemas (Indonesia) (Lijmbach *et al.*, 1970).

BA was used to study MPT since it is an MPT inhibitor via binding with the adenine nucleotide translocator (ANT), one of the components of the MPT pore complex. ANT is the transporter, which transports ADP / ATP across the mitochondria membrane. When binding with its substrate, it oscillates between two conformations in which the ADP / ATP binding site is either on the matrix side or on the cytosolic side. By such conformational change, the ADP and ATP will be transported across the membrane. However, when ANT is binding with its ligand, which stabilizes the matrix-side conformation, MPT will be prohibited (since it has been found that the cytosolic-side conformation is critical for MPT). BA is the ligand which stabilizes the matrix-side conformation, thus it can inhibit MPT (Crompton, 1999; Zamzami *et al.*, 1996; Marchetti *et al.*, 1996).

In order to study whether MPT was involved in HK18 induced HepG2 cells apoptosis, HK18 was added in the presence of BA and then MTT assay was

performed. For 24 hours incubation, 5 μM of HK18 induced around 80 % cytotoxicity on HepG2 cells from MTT assay. Thus, 5 μM of HK18 was used for study.

In this experiment, 5 μM of HK18 was used to incubate with HepG2 cells in the presence or absence of 50 μM BA for 24 hours. 50 μM BA alone was also incubated for 24 hours to study its effect on HepG2 cells. After incubation, MTT assay was performed. The result was shown as Fig 4.6.

From the result, it has been found that addition of BA could reduce the cytotoxicity of HK18 on HepG2 cells. The percentage survival rose from around 15.8 % to 42.2 % in the presence of BA which was significantly higher ($p < 0.001$) than the cells under 5 μM HK18 alone (Fig 4.6 a). Actually, BA has shown to have a dose-dependent inhibitory effect on HK18 induced apoptosis in HepG2 cells. As demonstrated by incubating HepG2 cells with 5 μM HK18 in the presence of 25, 50 and 100 μM of BA (Fig 4.6 b). From the result of this experiment, MPT has been shown to play an important role in HK18 induced apoptotic cell death.

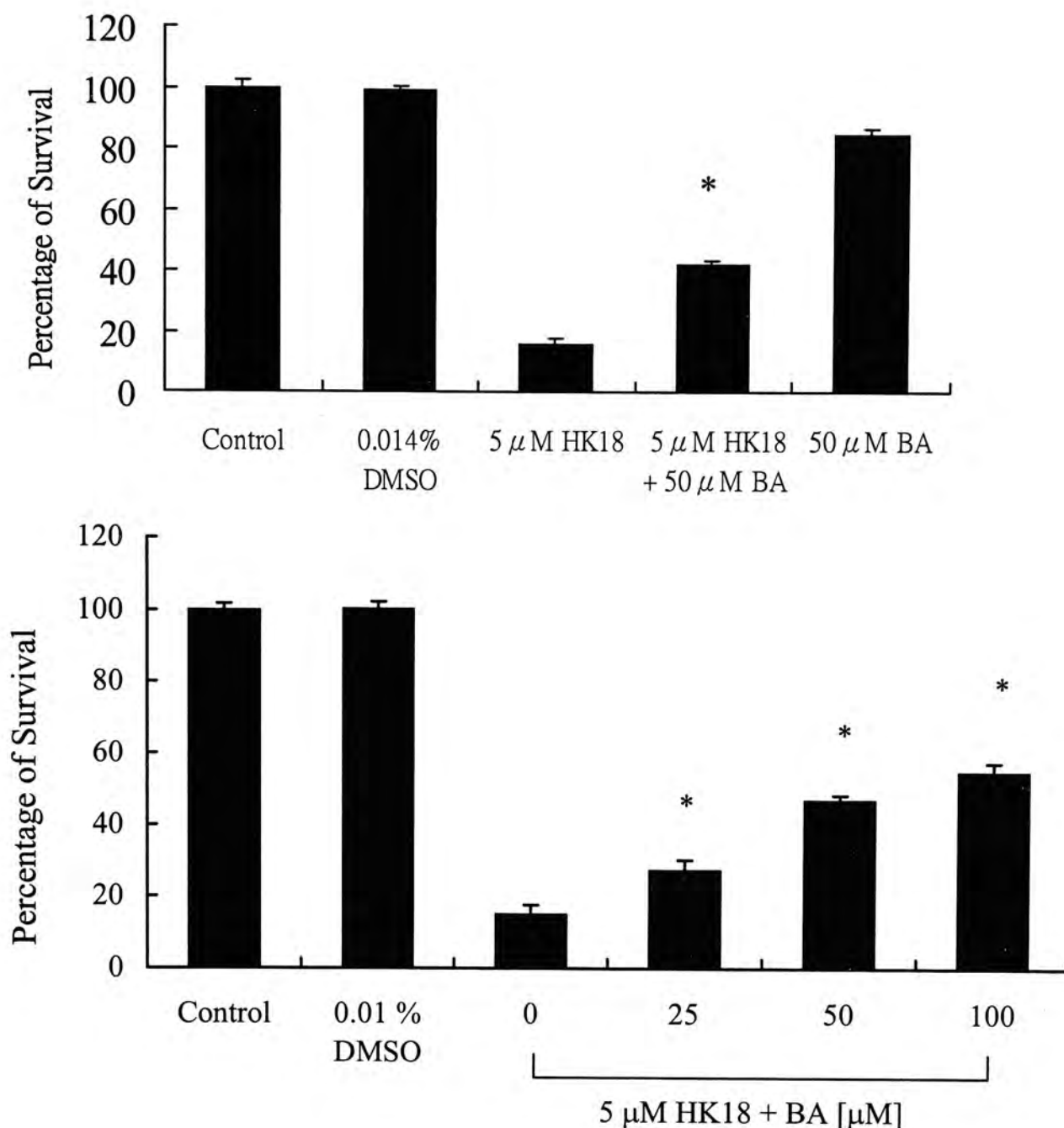


Fig. 4.6 Addition of BA would reduce the cytotoxicity of HK18 toward HepG2 cells. 1.5×10^5 cells / ml of HepG2 cells were seeded to a 96 well plate for 24 hours treatment. (a) Cells were treated with 5 μ M of HK18 in the presence or absence of 50 μ M BA for 24 hours. (b) Cells were treated with 5 μ M HK18 with 0, 25, 50 or 100 μ M BA for 24 hours. After treatments, MTT assay was carried out to find out the percentage of survival. The percentage survival was calculated as relative to the control that is expressed as 100 %. Mean marked with (*) indicated that the value is significantly higher (* $p < 0.001$) than the percentage survival of 5 μ M HK18 treatment.

4.2.1.3 Elevation of Intracellular Hydrogen Peroxide Level in HK18 Treated HepG2 Cells

There are increasing studies showing that intracellular free radicals level is a modulator of apoptosis. Mitochondria are the most abundant source of reactive oxygen species (ROS). During oxidative phosphorylation, electrons are transferred through the electron transport chain, which localized in the inner mitochondrial membrane. In most circumstances, four electrons are funneled into one O_2 molecule to completely reduce it into H_2O and concomitantly pump protons from the matrix to the cytosolic side of the inner mitochondrial membrane (Stryer, 1995b).

However, a small amount of superoxide anion $O_2^{\cdot-}$ is unavoidable to form if only one electron was funneled to a O_2 molecule. This superoxide anion is highly destructive, thus must be removed. Our bodies have developed some defense mechanism to work against the accidentally formed ROS. The defense system can be divided into enzymatic dependent and independent systems. For the enzymatic dependent system, several enzymes are included. Superoxide dismutase (SOD) which exists as two isoforms: mitochondrial SOD (Mn-SOD) and cytosolic SOD (Cu-dependent SOD). They scavenge two superoxide anions into one hydrogen peroxide H_2O_2 and one O_2 molecule. The H_2O_2 formed will then scavenged by another enzyme, namely catalase, into a water and oxygen molecule or being converted into H_2O by the action of glutathione peroxidase.

The non-enzymatic defense system includes water soluble agents such as glutathione (GSH), ascorbate, uric acid and plasma proteins as well as lipid soluble

agents including α -tocopherol, β -carotene and bilirubin. Despite of these, still some of these ROS escape from the defense systems and leak out from the mitochondria and cause damages to the macromolecules including lipids, proteins and DNA of cells. Therefore, increased intracellular ROS will lead to necrosis of cells.

Although ROS is harmful, recent studies have found that these ROS play an important role in mediating apoptosis (Kroemer and Reed, 2000; Crompton, 1999; Lemasters *et al.*, 1998). But how cells react with ROS for different consequences is still an open question. It has been proposed that a very high intracellular H_2O_2 ($>500 \mu M$) will lead to necrosis while medium intracellular H_2O_2 ($25-500 \mu M$) will end up with apoptosis. On the other hand, low H_2O_2 ($<25 \mu M$) may induce cell proliferation. Some tumors have transformed to over-produce ROS (Pervaiz and Clement, 2002).

Actually the aroused interest towards the apoptotic mediating activity of ROS is due to the discovery of anti-oxidative activity of the anti-apoptotic Bcl-2 protein. Up to now, the mechanisms of ROS induced apoptosis are under elucidation. One of the proposed mechanisms is that the ROS enhance the cytosolic Ca^{2+} (Suzuki *et al.*, 1997) and stimulate some transcriptional factors such as NF κ B, AP-1 and p53, which may up-regulate death proteins or produce inhibitors of survival proteins (Suzuki *et al.*, 1997; Chandra *et al.*, 2000). Another proposed mechanism is that the released H_2O_2 will act on mitochondria to cause MPT and Ψ_m depolarization and subsequently cytochrome c release (Pervaiz and Clement, 2002; Chandra *et al.*, 2000). And studies have found that oxidation of the MPT pore complex under

mitochondrial oxidative stress was able to induce MPT (Costantini *et al.*, 1996). The suspected oxidative modification site was located at the ANT component (Costantini *et al.*, 1996).

In view of this, intracellular H_2O_2 level of HK18 treated HepG2 cells was measured by flow cytometry with fluorescence dye, carboxy- H_2DCFDA . The non-fluorescent carboxy- H_2DCFDA passively diffused into cells, where the acetates are cleaved by intracellular esterases into carboxy- H_2DCF . Oxidation of carboxyl- H_2DCF occurs almost exclusively in cytosol and produces a fluorescent carboxyl-DCF (Cathcart *et al.*, 1983).

In this experiment, 5 μM of HK18 was used to treat HepG2 cells for 12 and 24 hours while 0.01 % DMSO was used as a solvent control. It was found that HK18 was able to induce H_2O_2 accumulation in a time-dependent manner. The maker M1 of the histograms (Fig. 4.7) indicated the percentage of cells with higher DCF intensity (i.e. higher H_2O_2 level). The higher the intracellular H_2O_2 level, the greater the shift of the fluorescence peak. From the histograms, 0.01 % DMSO had similar M1 percentage with control (11.5 % vs 11.2 %) while at 12 and 24 hours, the percentage of cells with higher H_2O_2 was 23.9 and 35.3 % respectively. That meant the intracellular H_2O_2 level for 12 and 24 hours treatment were around 2 and 3 folds of the control.

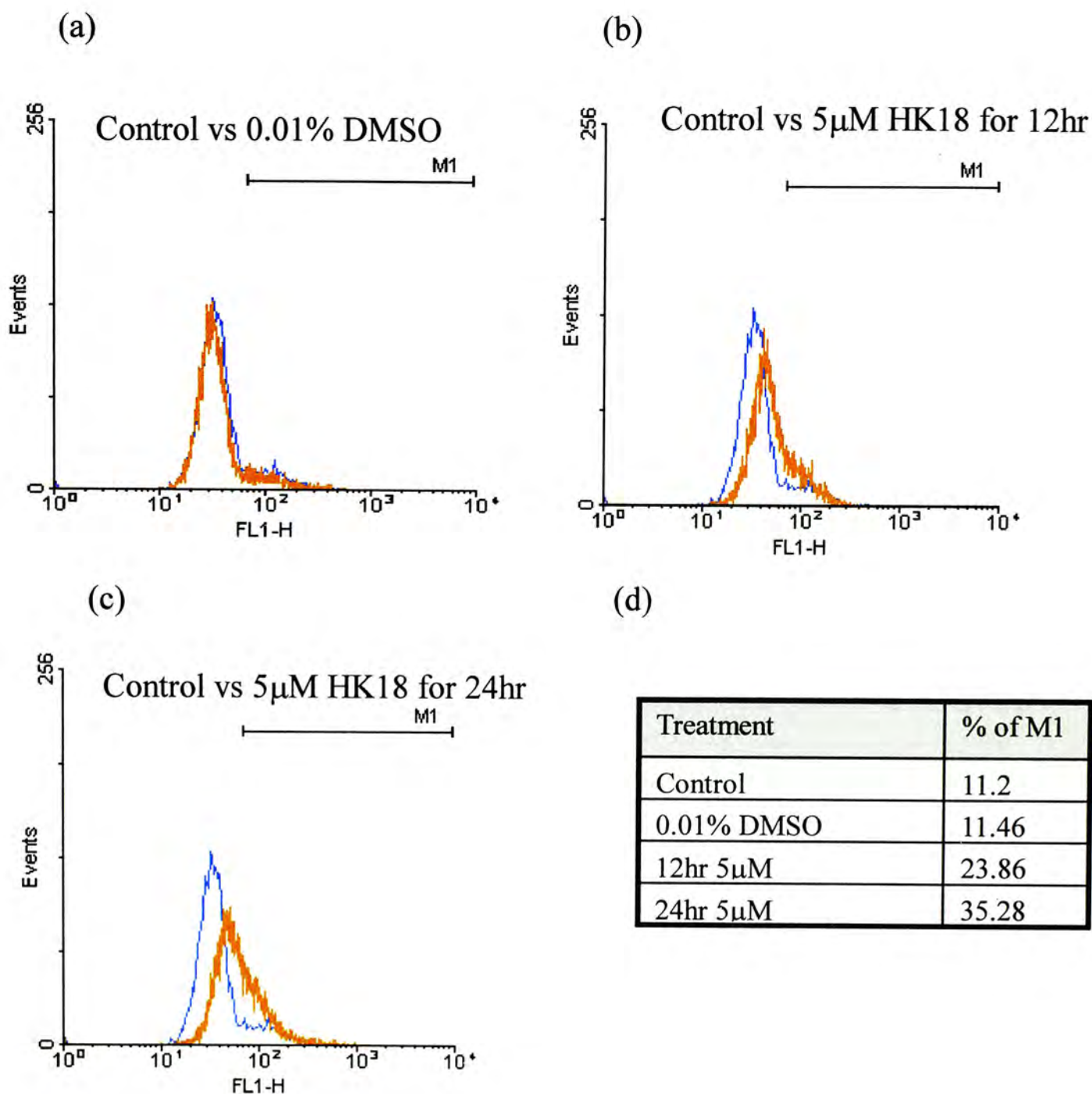


Fig 4.7 Intracellular H_2O_2 level of HepG2 cells was enhanced by HK18. 1.5×10^5 cells / ml of HepG2 cells were seeded into a 6 well plate with 5 μ M of HK18 for 12 or 24 hours incubation. After treatments, cells were collected and loaded with DCF. The marker M1 showed the percentage of cells with higher DCF intensity, which reflects cells with higher intracellular H_2O_2 level. (a) Histogram plotting control against 0.01% DMSO solvent control. (b) Histogram plotting control against 5 μ M of HK18 for 12 hours. (c) Histogram plotting control against 5 μ M of HK18 for 24 hours. (d) The table summarizes the percentage of cells in M1. The data are from a representative of five separate experiments.

As it was proposed that increased intracellular level of ROS would induce Ψ_m depolarization (Chandra *et al.*, 2000), the changes of both H_2O_2 and Ψ_m were measured simultaneously by flow cytometry with two compatible fluorescence dyes TMRE for Ψ_m and DCF for H_2O_2 . TMRE is a positively charged fluorescence dye and is uptaken by the negatively charged Ψ_m . The fluorescence intensity would decrease when the cells become depolarized.

Similarly, 5 μM of HK18 was used to incubate with HepG2 cells for 12 and 24 hours and 0.01 % DMSO was used as solvent control. The x-axis of the contour plot (Fig. 4.8) shows the green fluorescence of DCF while the y-axis shows the red fluorescence of TMRE. The region R2 indicates the percentage of cells having higher DCF but lower TMRE fluorescence (i.e. higher H_2O_2 level but lower membrane potential). From the result, treating HepG2 cells with 5 μM HK18 for 12 hours would increase the percentage of cells in the R2 from 11.8 % of control to 28.6 % (i.e. around 2.4 folds). The percentage of cells in the R2 region further increased to 35.7 %, which is around 3 folds of the control at 24 hours. The percentage of cells in R2 of solvent control was similar to the control one. Therefore, HK18 was able to induce intracellular H_2O_2 level accumulation with declined membrane potential simultaneously in a time dependent manner.

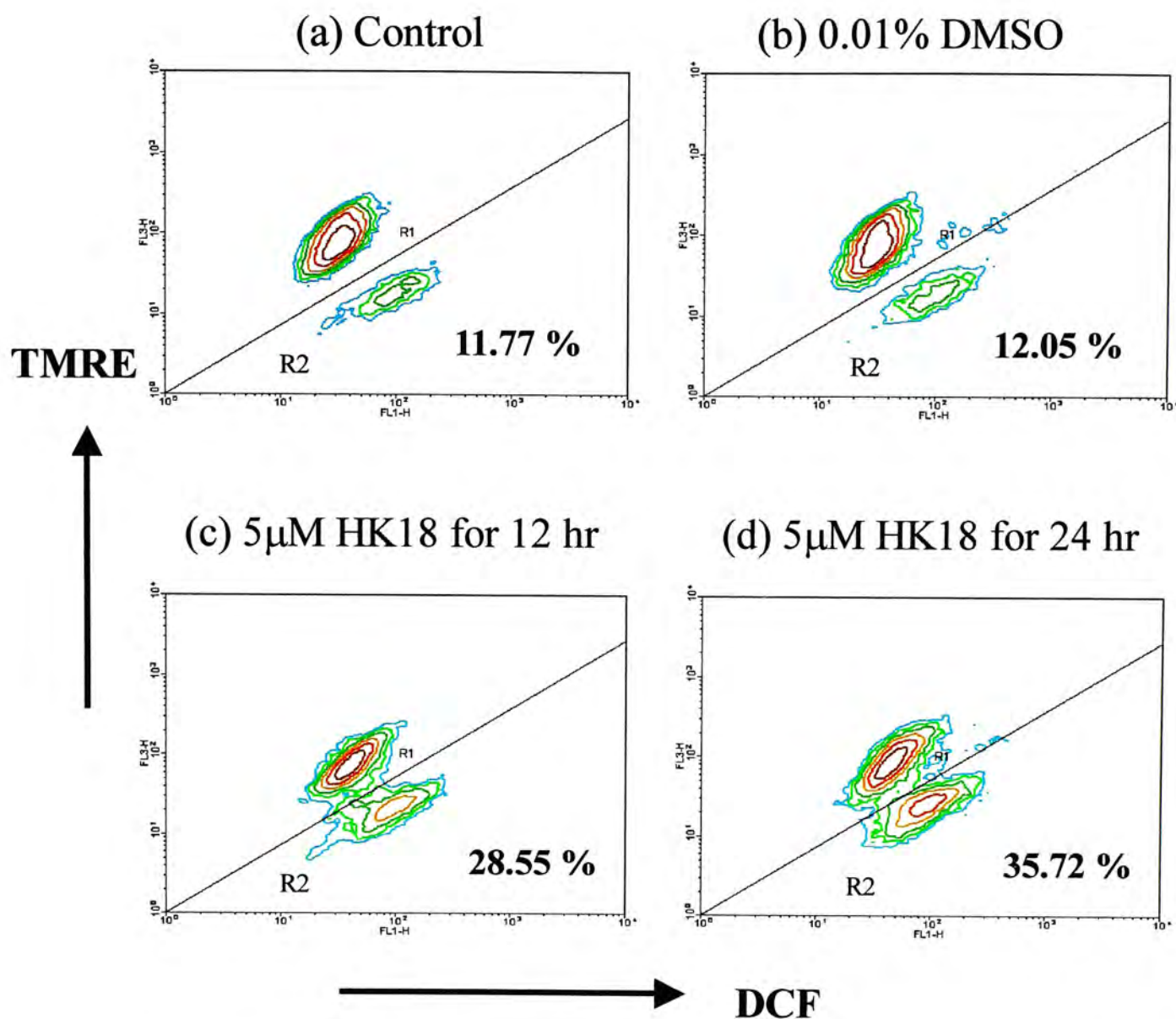


Fig 4.8 Study of the intracellular H_2O_2 level and Ψ_m simultaneously of HK18 treated HepG2 cells. 1.5×10^5 cells / ml of HepG2 cells were seeded into a 6 well plate and 5 μ M HK18 was added for 12 and 24 hours incubation. After treatments, cells were collected and loaded with both DCF and TMRE. Fluorescence intensity of DCF was measured at the x-axis while TMRE was measured at the y-axis. (a) Control. (b) 0.01 % DMSO solvent control. (c) 5 μ M HK18 for 12 hours and (d) 5 μ M for 24 hours. Region R2 indicated the cells with higher DCF but lower TMRE intensity. Data are from a representative of five separate experiments.

4.2.1.4 Elevation of Intracellular Ca^{2+} Level in HK18 Treated HepG2 Cells

Recently, studies have found that intracellular Ca^{2+} homeostasis was upset during apoptosis. It is well known that Ca^{2+} is an important physiological ion since it is a key intracellular messenger in many eukaryotic signaling pathways and is a mediator of many metabolic pathways. Thus, maintaining its homeostasis is very important. In a normal resting cell, the cytosolic Ca^{2+} level is maintained at around 100 nM while the Ca^{2+} in extracellular, endoplasmic reticulum and mitochondria is maintained at the millimolar level (Stryer, 1995a). To maintain the low cytosolic Ca^{2+} level against the electrochemical gradient to ensure normal cell functions, several transporting systems exist for exclusion of Ca^{2+} from the cytosol. They are the ATP-dependent Ca^{2+} pump located in the plasma, ER and mitochondrial membranes as well as the $\text{Na}^+ / \text{Ca}^{2+}$ exchanger located in plasma and mitochondrial membranes. Another one is the Ca^{2+} uniporter located in mitochondrial membrane (Suzuki *et al.*, 1997). Mitochondria and ER are the major stores of intracellular Ca^{2+} . The large electrochemical gradient favors the influx of Ca^{2+} from extracellular space or outflow of Ca^{2+} from internal stores thermodynamically.

Studies have found that increased intracellular ROS may act on the mitochondria, ER and plasma membranes. It has been proposed that increase of intracellular ROS will enhance cytosolic Ca^{2+} level, which come from intracellular and / or extracellular stores (Suzuki *et al.*, 1997). It has been found that ROS would induce Ca^{2+} release from sarcoplasmic reticulum (SR) of smooth muscle cells by inhibiting the ATP-dependent Ca^{2+} pump and hence Ca^{2+} ions were able to passively diffuse from the SR into cytosol (Suzuki *et al.*, 1997). Besides, it have been found

that oxidation of mitochondrial pyridine nucleotide including NAPH (due to the increase of mitochondrial ROS) would induce Ca^{2+} release from mitochondria into cytosol (Suzuki *et al.*, 1997; Chakraborti *et al.*, 1999). The elevated cytosolic Ca^{2+} stimulates the Ca^{2+} -dependent catabolic enzymes such as endonuclease and subsequently leads to apoptosis (Chakraborti *et al.*, 1999; McConkey and Orrenius, 1997). On the other hand, the elevated cytosolic Ca^{2+} would enhance mitochondria to take up Ca^{2+} (Smaili *et al.*, 2000). The resulted mitochondrial Ca^{2+} overload would induce MPT opening and apoptosis (Crompton, 1999; Lemasters *et al.*, 1998; Smaili *et al.*, 2000; Bernardi *et al.*, 1999).

Since there was elevation of intracellular ROS level in HK18 treated HepG2 cells, the intracellular Ca^{2+} concentration was also studied in this project by using flow cytometry with a fluorescence dye, Fluo-3/AM (Fluo-3). On binding with Ca^{2+} , the fluorescence intensity would increase (Fluo-3 is non-fluorescent until binding with Ca^{2+}) which can be recorded at the FL-3 channel.

In this experiment, 5 μM of HK18 was used to incubate with HepG2 cells for 12 and 24 hours. The marker M1 of the histograms indicated the cell population with higher Fluo-3 intensity, which meant higher intracellular Ca^{2+} level. As shown in the histograms (Fig 4.9), intracellular Ca^{2+} level was enhanced by HK18. The percentage of M1 increased from 8.4 % of control to around 36 % of 12 and 24 hours treatments, which was approximately 4 folds of the control. However, the rise was not time dependent since both of the time points showed similar percentage of increment. A positive control with 40 $\mu\text{g/ml}$ ionomycin was performed for

verification. Inomycin would increase the permeability of biological membrane to divalent ions, especially Ca^{2+} . Most of the cells (92 %) of the positive control exhibited higher intracellular Ca^{2+} level.

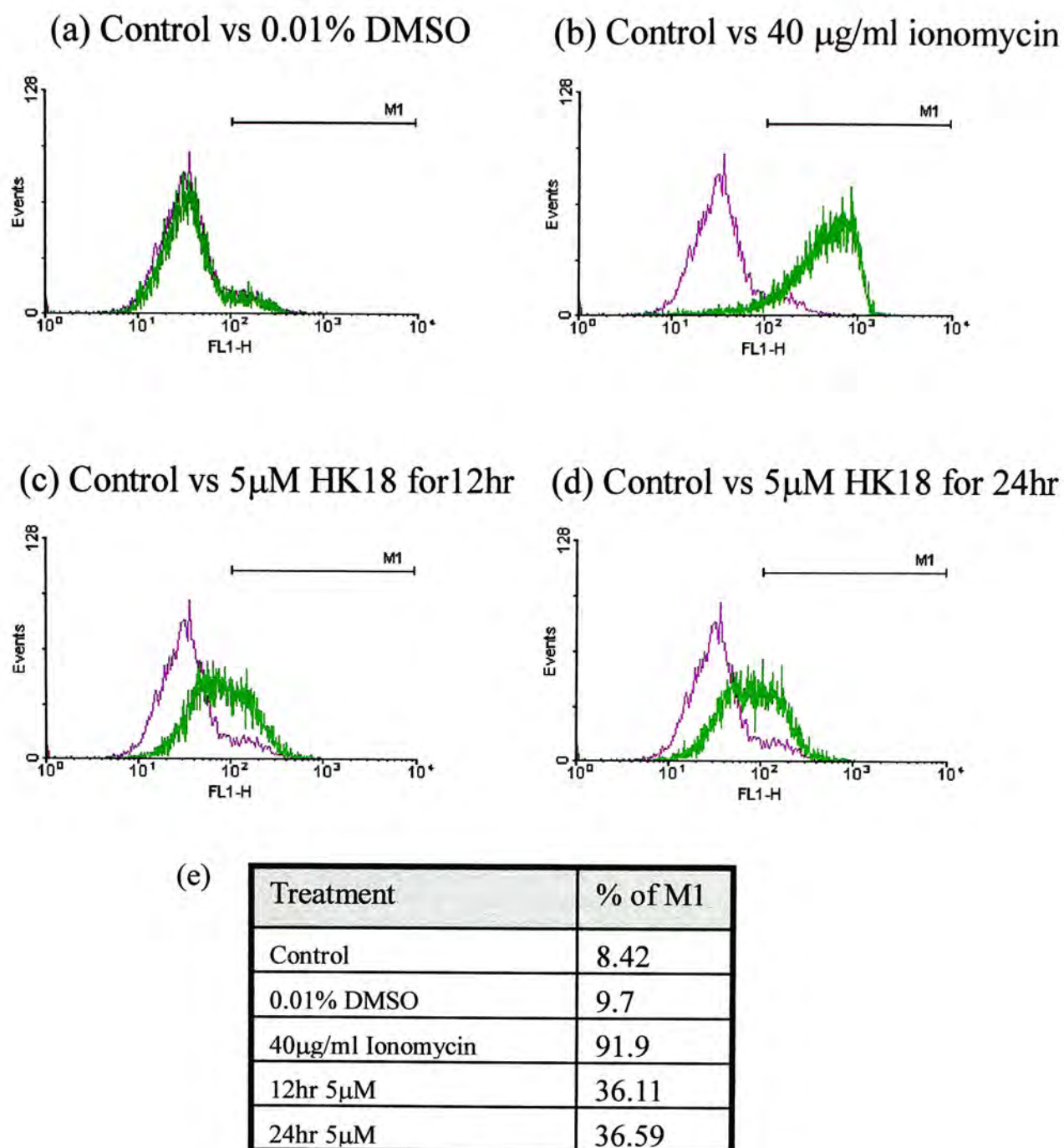


Fig 4.9 Intracellular Ca^{2+} level of HepG2 cells was enhanced by HK18. 1.5×10^5 cells / ml of HepG2 cells were seeded into a 6 well plate and 5 μM of HK18 was added for 12 and 24 hours incubation. After treatment, cells were collected and loaded with Fluo-3. The marker M1 showed the percentage of cells with higher Fluo-3 intensity, which reflects cells with higher intracellular Ca^{2+} level. (a) Histogram plotting control against 0.01% DMSO solvent control. (b) Histogram plotting control against the positive control (40 $\mu\text{g} / \text{ml}$ Ionomycin). (c) Histogram plotting control against 5 μM of HK18 for 12 hours. (d) Histogram plotting control against 5 μM of HK18 for 24 hours. (e) The table summarizes the percentage of cells within M1. Data are from a representative of five separate experiments.

Recent studies have found that Ca^{2+} is one of the triggers of MPT and Ψ_m depolarization. (Crompton, 1999; Lemasters *et al.*, 1998; Smaili *et al.*, 2000; Bernardi *et al.*, 1999). Thus, effects of HK18 on Ψ_m and intracellular Ca^{2+} level were measured simultaneously with TMRE and Fluo-3.

In this experiment, 5 μM of HK18 was incubated with HepG2 cells for 12 and 24 hours. The x- and y-axis of the contour plots showed the Fluo-3 and TMRE fluorescence intensity respectively (Fig 4.10). The region R2 indicated the cells with higher Fluo-3 but lower TMRE intensity implied that the treated cells having higher Ca^{2+} level but with collapsed Ψ_m . Therefore HK18 could induce intracellular Ca^{2+} level elevated from 8.7 % of control to 25.8 % and 29.5 % of 12 and 24 hours treatments respectively, which was around 3 folds of the control.

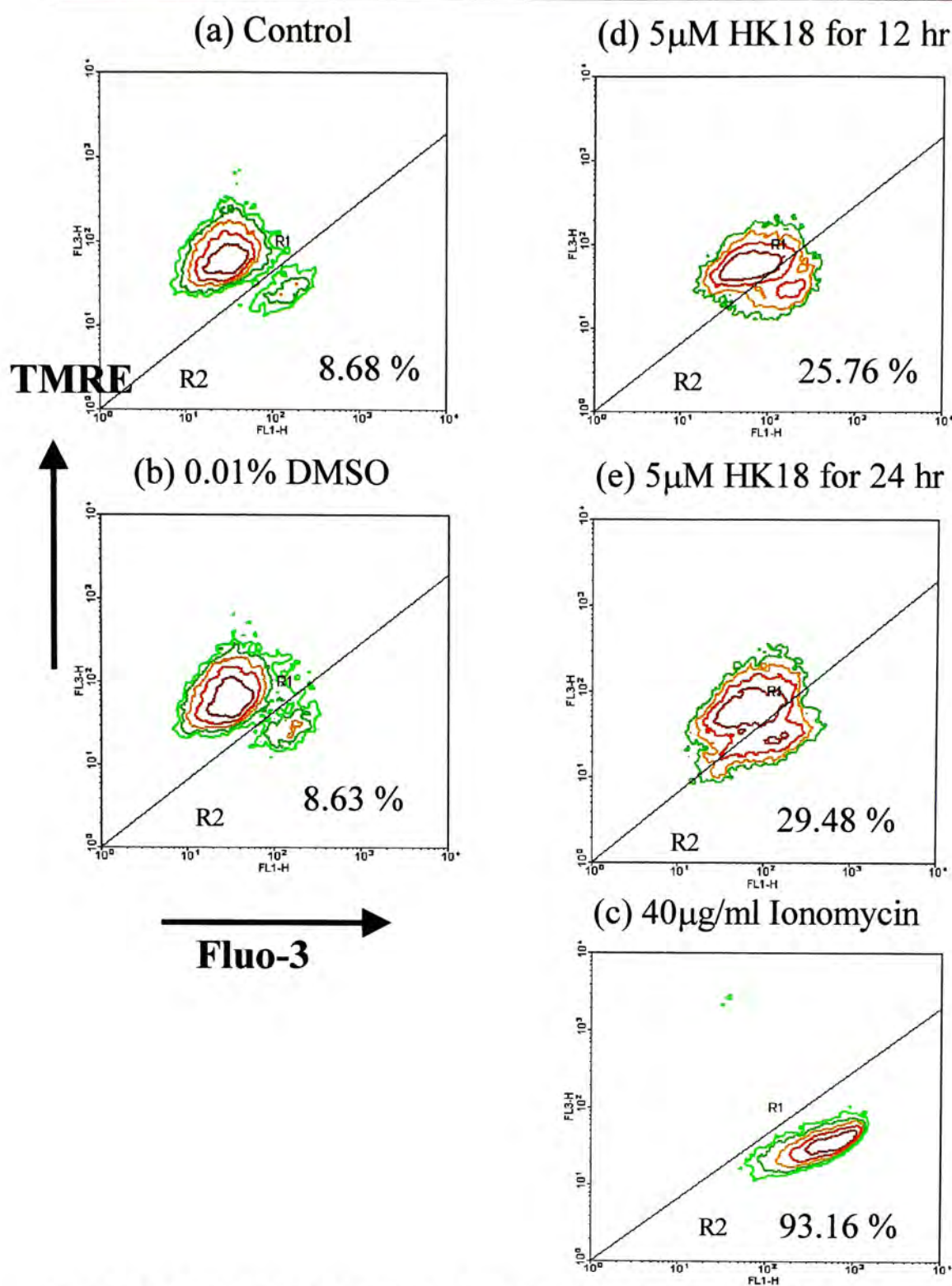


Fig 4.10 Study of the intracellular Ca^{2+} level and Ψ_m simultaneously of HK18 treated HepG2 cells. 1.5×10^5 cells / ml of HepG2 cells were seeded into a 6 well plate and $5 \mu\text{M}$ HK18 was added for 12 and 24 hours incubation. After treatments, cells were collected and loaded with Fluo-3 and TMRE. Fluorescence intensity of Fluo-3 was measured at the x-axis while TMRE was measured at the y-axis. (a) Control. (b) 0.01 % DMSO solvent control. (c) Positive control ($40 \mu\text{g}/\text{ml}$ ionomycin), (d) $5 \mu\text{M}$ HK18 for 12 hours and (e) $5 \mu\text{M}$ of HK18 for 24 hours. Region R2 indicated the cells with higher Fluo-3 but lower TMRE intensity. Data are from a representative of five separate experiments.

4.2.1.5 HK18 Induced Cytochrome c and AIF Released from Mitochondria of HepG2 Cells

Recent studies have found that during early stage of mitochondrial dependent apoptosis, a variety of mitochondrial intermembrane space proteins will be released. These include cytochrome c, apoptosis inducing factor (AIF), adenylate kinase-2 and Smac/DIABLO (Loeffler and Kroemer, 2000; Kohler *et al.*, 1999; Verhagen *et al.*, 2000; Du *et al.*, 2000). Release of these proteins into cytosol will trigger cellular catabolic destruction.

Cytochrome c is a 15 kDa protein which normally located at the inner mitochondrial membrane. It is encoded by nuclear DNA. The protein is synthesized as the precursor apocytochrome c in cytosol and is then translocated to mitochondria spontaneously, which does not require membrane potential or general translocation machinery (Evans and Scarpulla, 1988; Mayer *et al.*, 1995). Inside mitochondria, the precursor incorporates with a heme group and then refolded into functional cytochrome c molecule. Cytochrome c plays an important role in energy production. It transports electrons through the complex III to complex IV of respiratory chain. And most recent studies have found that release of cytochrome c into cytosol would induce caspases activation and subsequent apoptosis (Liu *et al.*, 1996).

Apoptosis inducing factor (AIF) is another apoptogenic protein being released from mitochondria into cytosol (Susin *et al.*, 1996). AIF is a 57 kDa flavoprotein encoded by the gene located on the X chromosome. It is synthesized in the cytosol and then transported into mitochondria and confined in the

intermembrane space (Daugas *et al.*, 2000a). During apoptosis, AIF redistributed from the mitochondria into cytosol and nucleus. In isolated nuclei, addition of AIF would induce chromatin condensation as well as large scale DNA fragmentation (i.e. 50 kbp DNA fragmentation) (Susin *et al.*, 1996). Besides, AIF could induce PS externalization to outer plasma membrane, collapse of Ψ_m and release of cytochrome c (Susin *et al.*, 1999). And its activities have been found to be caspases-independent. That means AIF mediate apoptosis in a different mechanism from cytochrome c (Loeffler *et al.*, 2001; Daugas *et al.*, 2000b).

In this research project, the release of cytochrome c and AIF from mitochondria was examined. HepG2 cells were treated with 5 μ M of HK18 for 12 and 24 hours. After treatment, protein was collected as mentioned in the chapter of Materials and Methods. The protein collected was then subjected to SDS electrophoresis and then probed with anti-cytochrome c or anti-AIF antibodies. Since the amount of protein loaded per sample was normalized by cell numbers, anti- β -actin antibody was used to check the degree of normalization.

As illustrated in Fig 4.11, cytochrome c was being released from mitochondria into cytosol after treating with 5 μ M of HK18 for 12 and 24 hours. The amount of cytochrome c released at 24 hours was greater than that at 12 hours. Apart from this, AIF was also being released from mitochondria into cytosol after treating with 5 μ M of HK18 for 24 hours.

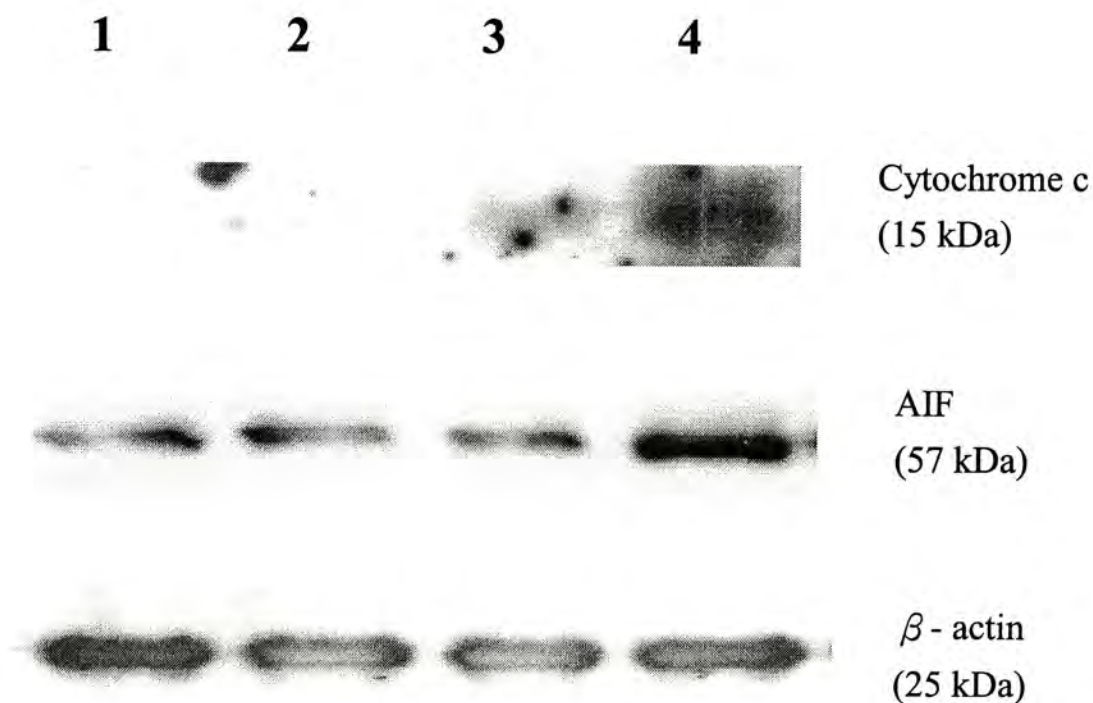


Fig 4.11 HK18 induce mitochondrial cytochrome c and AIF release of HepG2 cells. 1.5×10^5 cells / ml of HepG2 cells were seeded into 75 cm^2 culture flask. Cells were then treated with medium (lane 1), 0.01 % DMSO (lane 2), $5 \mu\text{M}$ HK18 for 12 hours (lane 3) or $5 \mu\text{M}$ HK18 for 24 hours (lane 4). After treatment, cells were collected and cytosolic fraction was extracted as mentioned in the chapter of Materials and Methods. The cytosolic proteins were then subjected to Western analysis and were probed with anti-cytochrome c, anti-AIF or anti- β -actin antibodies. Data are from a representative of three separate experiments.

4.3 Downstream Biochemical Changes Induced by HK18 on HepG2 Cells

Caspases activation is a common biochemical change occurred in most, though not all, apoptotic cells. Activated caspases will act on their substrates, which will then participate in apoptosis to destruct the cells (Zimmermann *et al.*, 2001).

4.3.1 Activation of Caspase 3 of HepG2 Cells by HK18 as Demonstrated by Western Blot

First of all, the participation of caspase 3 was examined by Western blotting. Various concentrations of HK18 were used to incubate with HepG2 cells for 24 and 48 hours. As illustrated in the film, the level of procaspase 3 protein (35 kDa) decreased when the concentration of HK18 increased (Fig 4.12). Thus, HK18 was able to induce caspase 3 activation in a dose-dependent manner.

Besides, the level of PARP (poly(ADP-ribose)polymerase), one of the substrates of catalytically active caspase 3, is regarded to play a role in DNA repair (de Murcia *et al.*, 1997; Soldani and Scovassi, 2002) was also studied. Various concentrations of HK18 were used to treat HepG2 cells for 24 and 48 hours. As indicated in the film (Fig 4.12), the levels of uncleaved intact PARP (116 kDa) decreased while the cleaved PARP (85 kDa) increased when concentration of HK18 increased.

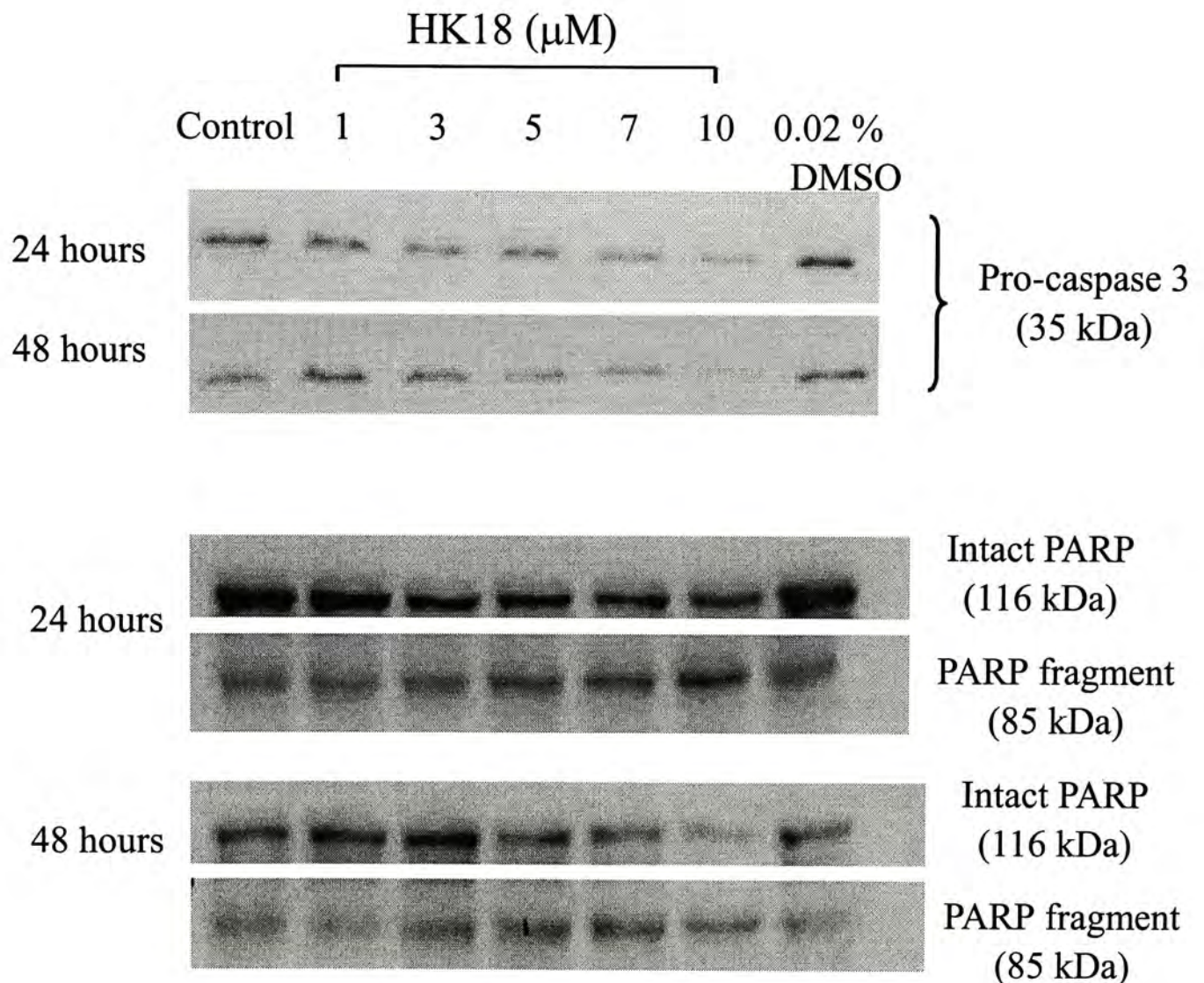


Fig 4.12 Activation of caspase 3 and induction of PARP cleavage by HK18 on HepG2 cells. Cells were treated with various concentrations of HK18 for 24 and 48 hours and were then subjected to Western analysis. (a) Probed with anti-pro-caspase 3 (35 kDa) antibodies. (b) Probed with anti-PARP (116 kDa for intact PARP and 85 kDa for cleaved PARP) antibodies. Data are from a representative of three separate experiments.

4.3.2 Induction of Caspases Activities of HepG2 Cells by HK18 as Demonstrated by Enzymatic Activity Assays

Apart from studying the protein levels of caspase 3 by Western blot analysis, the enzymatic activity of caspase 3 was also studied. 5 μM of HK18 was used to treat HepG2 cells for 12 and 24 hours, and then protein was extracted. The protein extract was incubated with caspase 3 specific fluorescent AMC conjugated substrate Ac-DEVD-AMC. The amount of fluorescent AMC (μM) released from the substrate by the action of caspase 3 was plotted against various treatments, which is directly proportional to its enzymatic activity. To confirm the correlation between the fluorescence signal and caspase 3 activity, caspase 3 specific inhibitor z-DEVD-fmk was added to the protein extract before addition of substrate. In the presence of inhibitor, the increased fluorescence intensity was prohibited. As shown in the bar chart (Fig 4.13), HK18 induced caspase 3 activity in a time dependent manner. The caspase 3 activities were around 6.05 folds and 10 folds of the solvent control for 12 and 24 hours respectively.

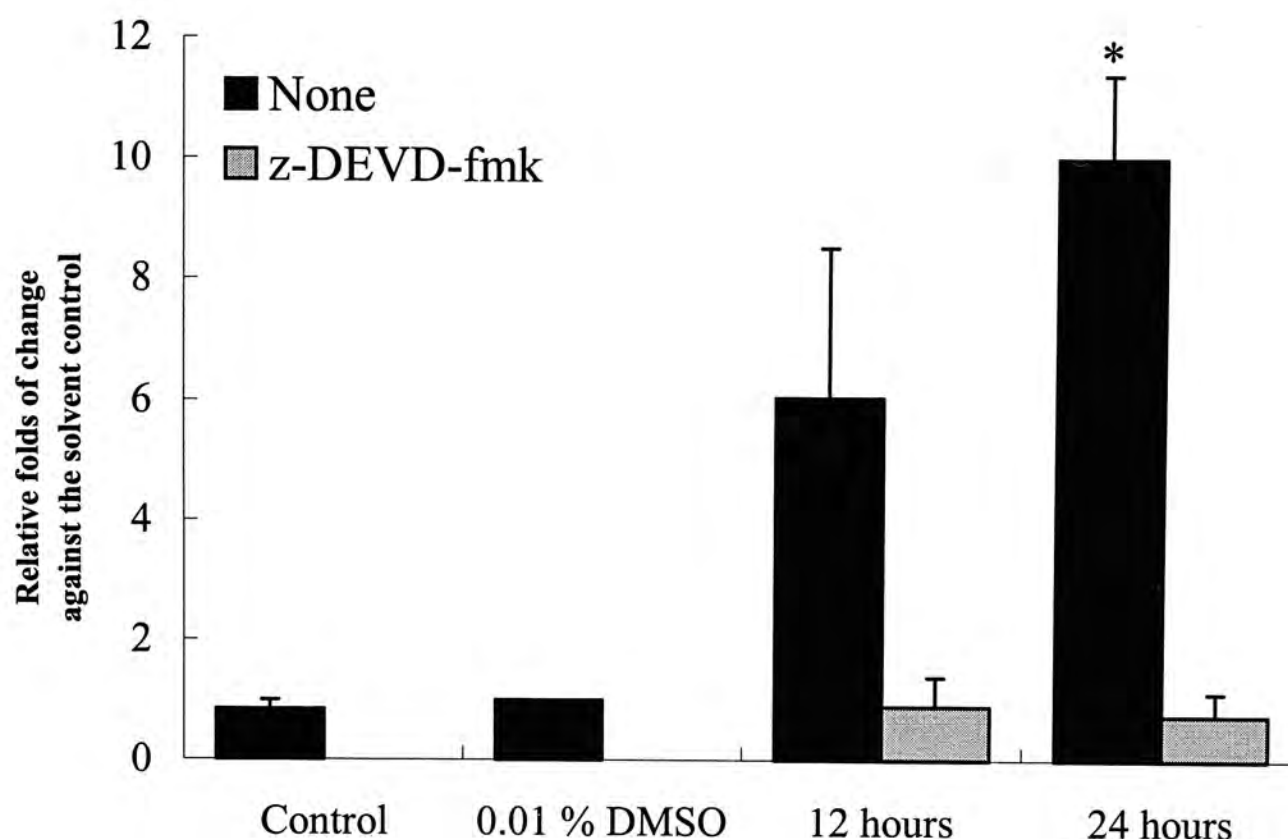


Fig 4.13 Caspase 3 enzymatic activity of HepG2 cells was enhanced by HK18. 1.5×10^5 cells / ml of HepG2 cells were seeded into 75 cm² flask and medium, 0.01 % DMSO control or 5 μ M of HK18 was added for 12 or 24 hours incubation. After treatment, cells were collected and lysed. The protein extracts were incubated with caspase-3 specific substrate Ac-DEVD-AMC in the presence or absence of caspase-3 specific inhibitor z-DEVD-fmk. The fluorescence intensity of AMC released was measured and the amount was calculated according to the standard curve. Data are means of three separate experiments. The folds of change of treatments were calculated as relative to the solvent control that is expressed as 1 fold. Mean marked with (*) is significantly (* $P < 0.05$) higher than the solvent control.

In addition of caspase 3 enzymatic activity, activities of caspase 8 and 9 were also studied. For measuring caspase 8 activity, caspase 8 specific substrate Ac-IETD-AMC was used instead. Similarly, the fluorescence intensity should be directly proportional to caspase 8 activity and caspase 8 specific inhibitor z-IETD-fmk was added before substrate addition for verification. As observed from the bar chart (Fig 4.14 a), there were no significant increase of caspase 8 activity for the HK18 treated HepG2 cells for 12 hours and 24 hours compared with the solvent control.

On the other hand, caspase 9 specific fluorescent AFC conjugated substrate Ac-LEHD-AFC was employed to measure caspase 9 enzymatic activity in the presence or absence of caspase 9 specific inhibitor z-LEDH-fmk. As illustrated in the bar chart (Fig 4.14 b), HK18 would induce caspase 9 activity. The activity of caspase 9 was around 1.5 fold and 1.4 fold of that of solvent control for 12 and 24 hour treatments respectively.

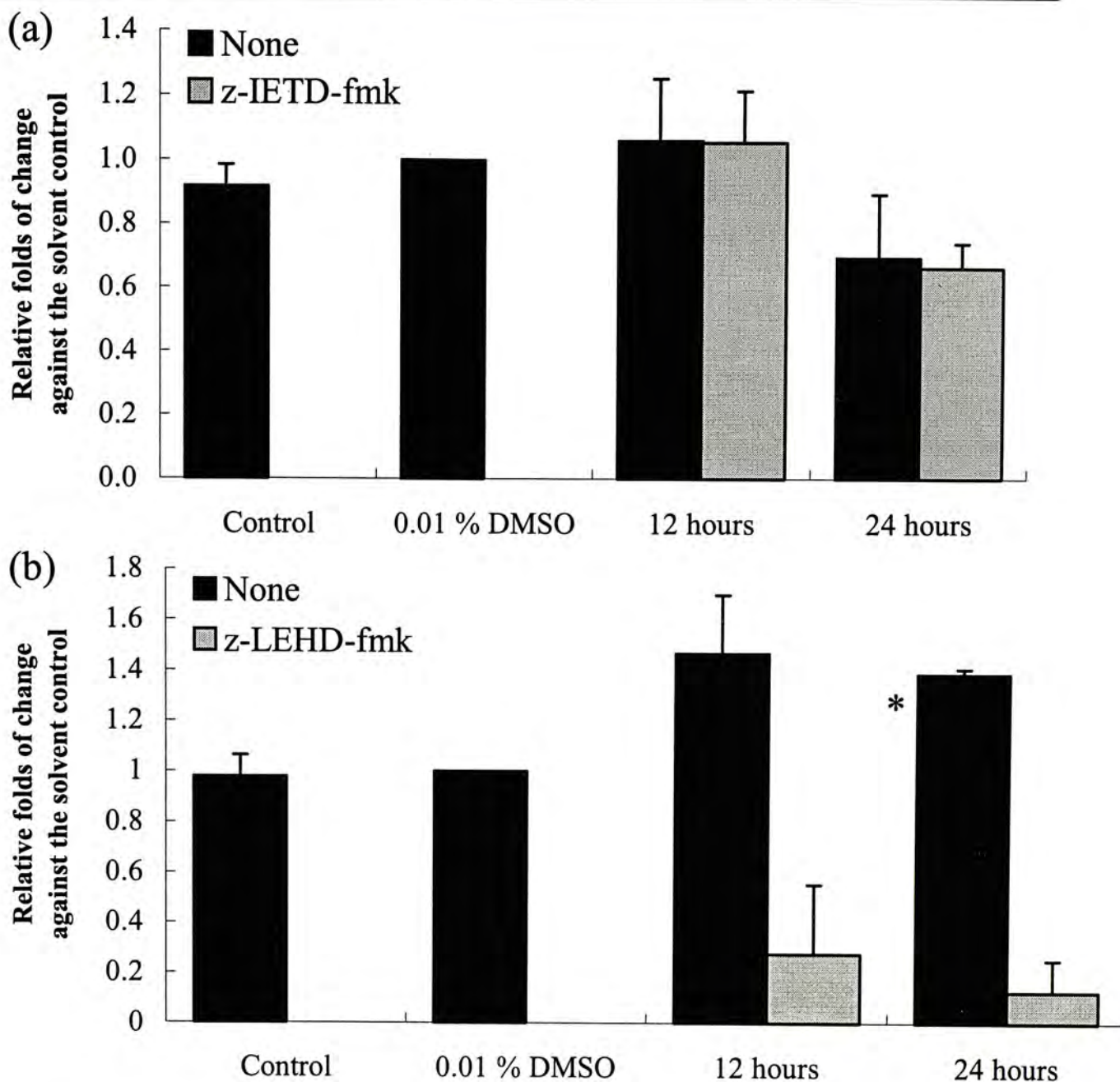


Fig 4.14 Caspase 9 enzymatic activity of HepG2 cells was enhanced by HK18 but not caspase 8. 1.5×10^5 cells / ml of HepG2 cells were seeded into 75 cm^2 flask and medium, 0.01 % DMSO control or $5 \mu\text{M}$ of HK18 was added for 12 or 24 hours incubation. After treatment, cells were collected and lysed. (a) The protein extracts were incubated with caspase 8 specific substrate Ac-IETD-AMC in the presence or absence of caspase 8 specific inhibitor z-IETD-fmk. (b) The protein extracts were incubated with caspase 9 specific substrate Ac-LEHD-AFC in the presence or absence of caspase 9 specific inhibitor z-LEHD-fmk. The fluorescence intensity of AMC or AFC released was measured and the amount was calculated according to the standard curve. Data are means of three separate experiments. The folds of change of treatments were calculated as relative to the solvent control that is expressed as 1 fold. Mean marked (*) is significantly (* $p < 0.05$) higher than the solvent control.

4.4 Down-regulation of Anti-apoptotic Bcl-2 Family Members of HepG2 Cells by HK18

It is well known that the Bcl-2 family members play an important role in apoptosis. Bcl-2 (homologue to CED-3 of *C. elegans*) was first identified from B cell lymphomas, where chromosomal translocations activate its expression at inappropriate high level (Reed, 1997). Overexpression of Bcl-2 has been detected in a wide variety of cancer. Actually Bcl-2 family members can be divided into two groups as anti-apoptotic such as Bcl-2, Bcl-X_L, Bcl-w and Mcl-1 as well as the pro-apoptotic such as Bax, Bcl-X_S, Bak, Bid and Bad. These proteins interact with each other to form homodimers or heterodimers, which decide the fate of the cells. For instant, Bcl-2 can heterodimerize with Bax and their ratio is important for apoptosis. In fact, the anti-apoptotic function of Bcl-2 is depend on, at least in part, of its ability in interacting with pro-apoptotic members especially Bax and inhibiting their apoptotic inducing activities (Reed, 1997).

Therefore, the protein expression level of Bcl-2 of HK18 treated HepG2 cells was examined. HepG2 cells were treated with 3, 5 and 7 μ M of HK18 for 12 and 24 hours. It was found that HK18 inhibited Bcl-2 expression in a dose and time dependent manner (Fig 4.15).

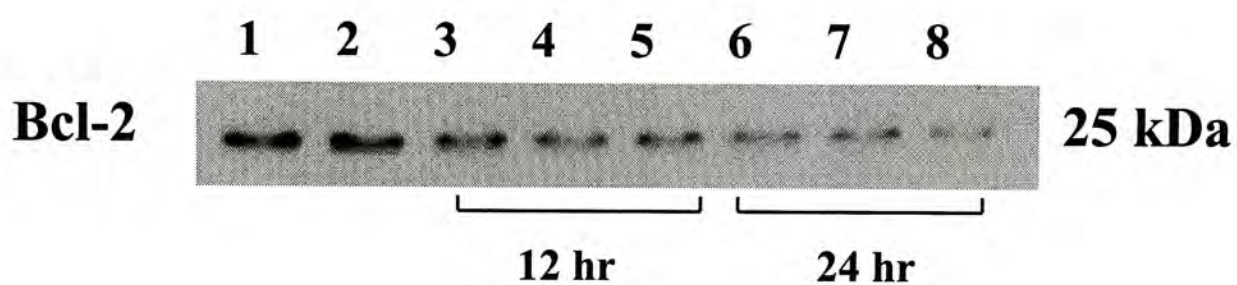


Fig 4.15 Down-regulation of Bcl-2 expression of HepG2 cells by HK18. HepG2 cells were treated with 3, 5 and 7 μM HK18 for 12 and 24 hours. The protein extracted was subjected to Western blot and probed with anti-Bcl-2 antibodies. Lane 1: medium control, lane 2: 0.014 % DMSO, lanes 3 – 5: 12 hours with 3, 5 or 7 μM HK18, lanes 6-8: 24 hours with 3, 5 or 7 μM HK18. Data are from a representative of two separate experiments.

On the other hand, the RNA levels of bcl-2, bcl-X_L and bak genes were studied in order to examine the effect of HK18 at the transcriptional level. 5 μM of HK18 was used to treat HepG2 cells for 12 and 24 hours. Then total RNA was extracted and was subjected to RT-PCR with bcl-2, bcl-X_L or bak primers. It was found that the amount of bcl-2 mRNA of HK18 treated HepG2 cells decreased to around 75 % and 80 % of the control for 12 and 24 hours treatments (Fig 4.16). On the other hand, the amount of bcl-X_L reduced to around 52 % and 68 % of the control for 12 and 24 hours treatments. However, it did not affect the transcription of the pro-apoptotic gene bak.

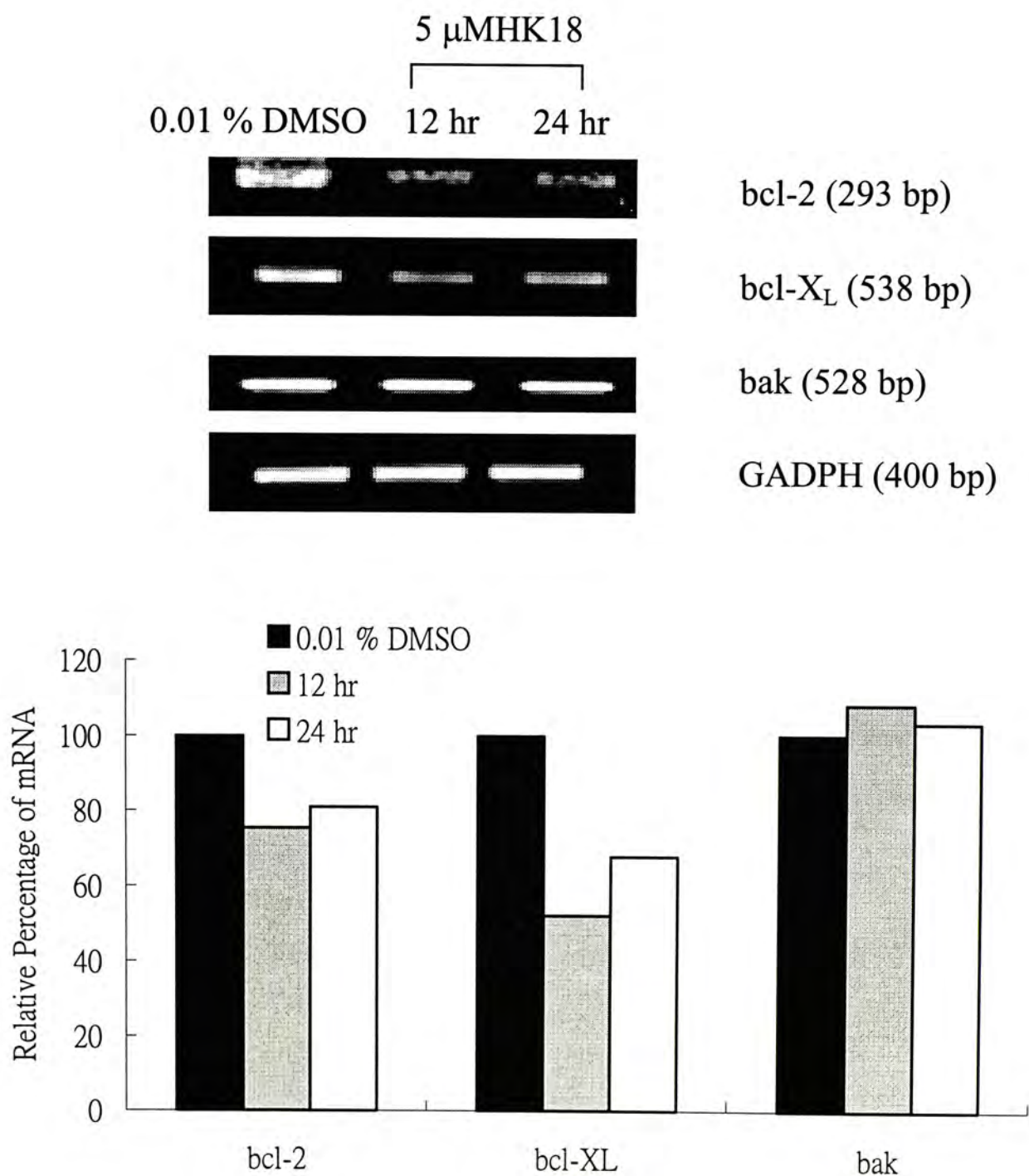


Fig 4.16 Down-regulation of bcl-2 and bcl-X_L genes transcription of HepG2 cells by HK18. HepG2 cells were treated with 0.01 % DMSO solvent control or 5 μM HK18 for 12 or 24 hours. The RNA extracted was subjected to RT-PCR with primers of bcl-2, bcl-X_L, bak or GADPH. Data are from a representative of two separate experiments.

Chapter 5
Mechanistic Study of
HK18 on R-HepG2 Cells

5 Mechanistic Study of HK18 on R-HepG2 Cells

5.1 Hallmarks of Apoptosis Induced by HK 18 on R-HepG2 Cells

It has been found that HK18 was cytotoxic to R-HepG2 cells as demonstrated by MTT assay and tryphan blue exclusion assay. Thus, emerge of apoptosis hallmarks were studied to see whether HK18 induces R-HepG2 cell death via apoptosis or not.

5.1.1 Induction of Phosphatidylserine Externalization by HK18 on R-HepG2 Cells

First of all, externalization of phosphatidylserine (PS) induced by HK18 on R-HepG2 cells was measured and quantified by flow cytometry with Annexin V – FITC and PI staining. In this experiment, 3, 5 and 7 μM of HK18 were used to incubate with R-HepG2 cells for 24 hours. The density plot was divided into 4 quadrants. Cells in the lower left quadrant are viable cells while the cells at lower right quadrant are early apoptotic cells. Necrotic and late apoptotic cells are located at the upper right quadrant.

As shown in the density plots of Fig 5.1, the percentage of viable cells decreased from 82.8 % to 49.8 %, 29.2 % and 16.4 % upon 3, 5 and 7 μM of HK18 respectively. On the other hand, the percentage of cells at the early apoptotic

quadrant increased from 8.6 % to 24.6 %, 44.2 % and 57.7 % upon treatments of 3, 5 and 7 μ M of HK18 respectively. That was around 2.9 folds, 5.1 folds and 6.7 folds of the control respectively. A solvent control with 0.014 % DMSO was performed and the resulted density plot was similar to the control. Besides, 2 mg/ml digitonin was used as positive control and large proportion of cells were located at the necrotic / late apoptotic quadrant.

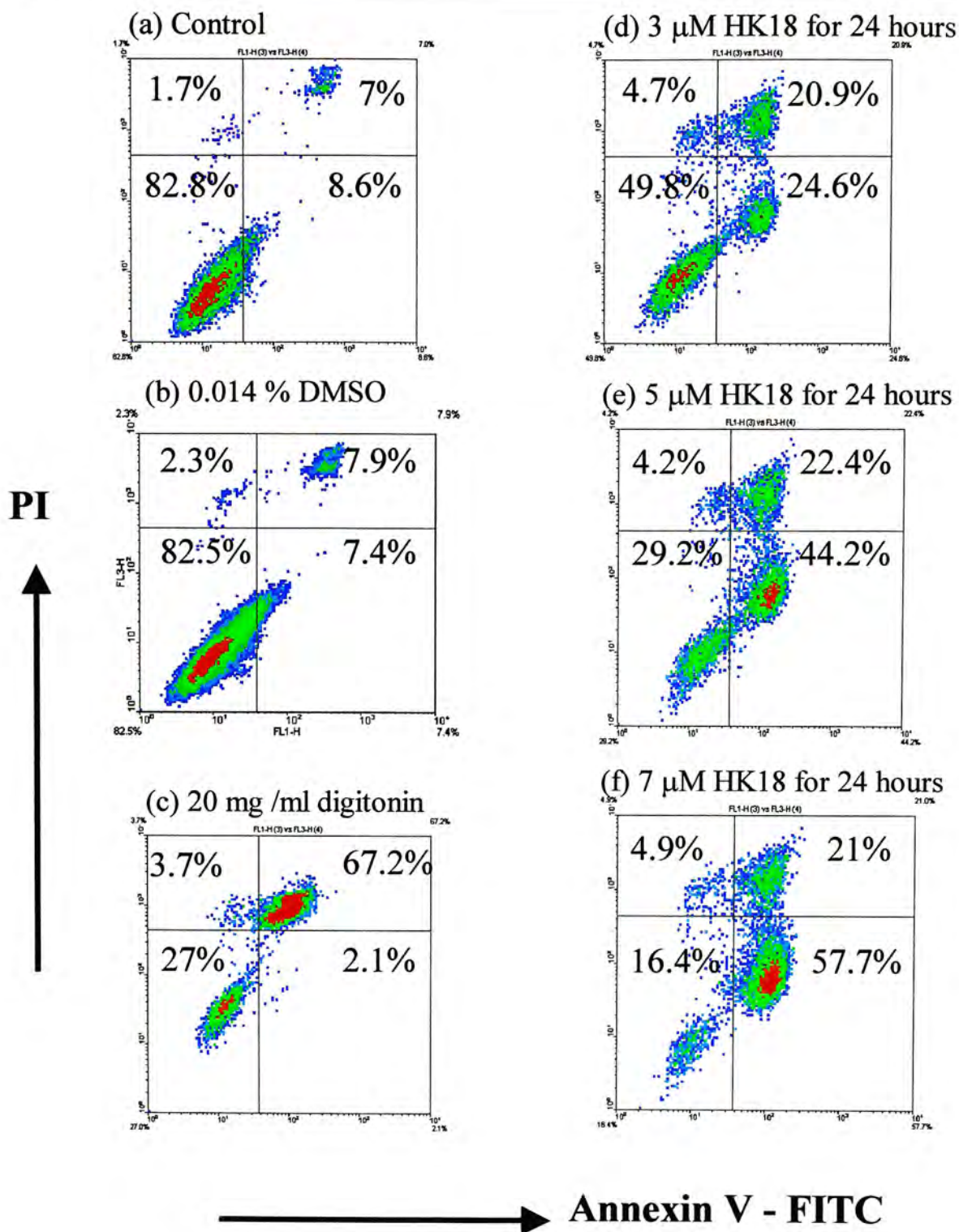


Fig 5.1 Induction of phosphatidylserine externalization by HK18 on R-HepG2 cells. 2×10^5 cells / ml of R-HepG2 were seeded into a 6 well plate and 3, 5 and 7 μ M of HK18 were added to incubate for 24 hours. After treatment, cells were collected and loaded with Annexin V-FITC and PI for staining and followed by flow cytometric analysis. 20mg / ml digitonin was added to act as positive control. (a) Control. (b) 0.014 % DMSO. (c) 20 mg/ml digitonin. (d) 3 μ M HK18. (e) 5 μ M HK18. (f) 7 μ M HK18. Data are from a representative of four separate experiments.

5.1.2 Induction of DNA Fragmentation by HK18 on R-HepG2 Cells

Moreover, the DNA of HK18 treated R-HepG2 cells were extracted and subjected to gel electrophoresis to check the occurrence of DNA fragmentation. R-HepG2 cells were incubated with various concentrations of HK18 as 1, 3, 5, 7 and 10 μM for 24 hours. Samples without HK18 and with 0.02 % DMSO were used as medium control and solvent control respectively. After 24 hours incubation, DNA ladder developed in the cells treated with 3, 5, 7 and 10 μM of HK18 but not in the control cells, solvent control cells and cells treated with 1 μM of HK18 (Fig 5.2). This indicated that HK18 could induce DNA fragmentation at the concentrations above 3 μM after 24 hours incubation.

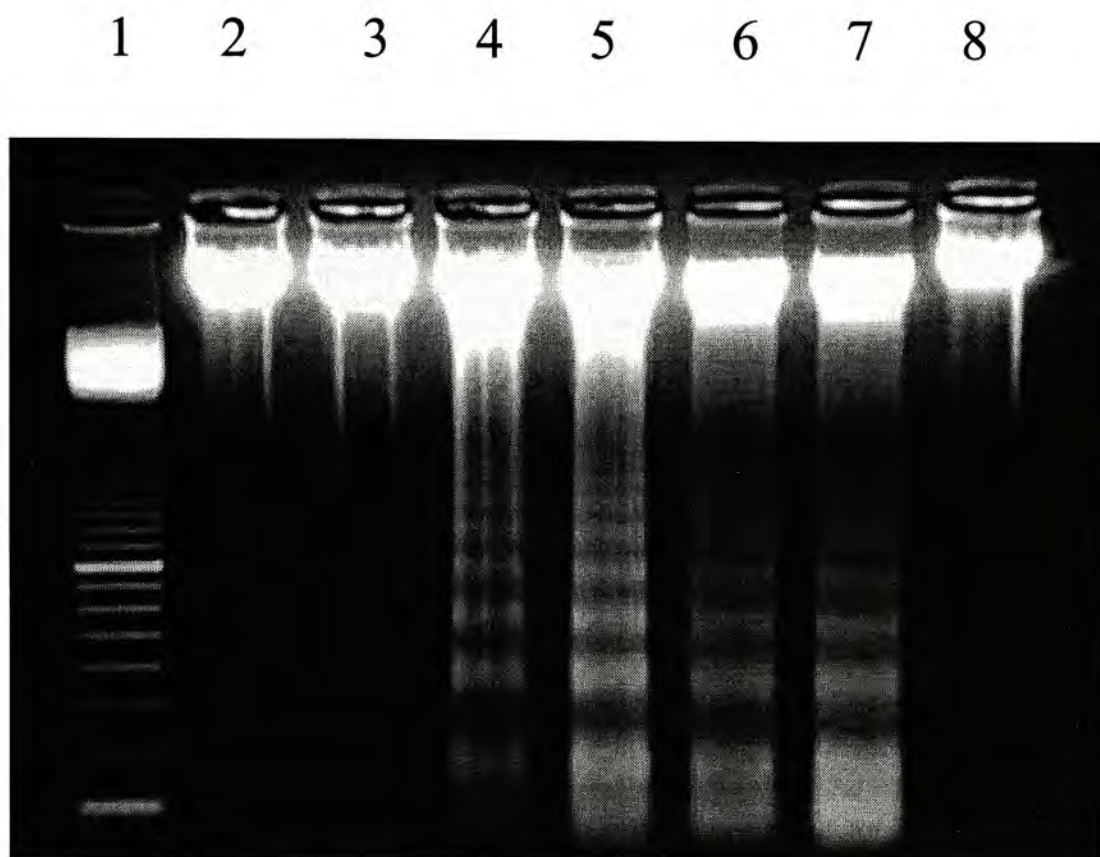


Fig 5.2 Induction of DNA fragmentation in HK18 treated R-HepG2 cells. 2×10^5 cells / ml of R-HepG2 cells were seeded into a 6 well plate and various concentrations of HK18 were added for 24 hours incubation. After treatments, cells were collected and DNA was extracted and subjected to gel electrophoresis. Lane 1: 100 base pairs marker. Lane 2: Medium control. Lanes 3 – 7: 1, 3, 5, 7 and 10 μ M of HK18. Lane 8: 0.02 % DMSO solvent control. Data are from a representative of five separate experiments.

5.2 Study of the Underlying Mechanisms of HK18 Induced Apoptosis in R-HepG2 Cells

As HK18 could induce PS externalization as well as DNA fragmentation, it seems that HK18 could induce R-HepG2 cells to undergo apoptosis. Therefore, the mechanisms of how HK18 induce R-HepG2 cells to undergo apoptosis were studied in the following sections.

5.2.1 The Role of Mitochondria in HK18 Induced Apoptosis of R-HepG2 Cells

5.2.1.1 HK18 Induced Mitochondrial Membrane Depolarization in R-HepG2 Cells

First of all, the effect of HK18 on the mitochondrial membrane potential (Ψ_m) of R-HepG2 cells was studied. In this experiment, R-HepG2 cells were treated with 3, 5 and 7 μM of HK18 for 12 and 24 hours. After treatment, the cells were collected and loaded with JC-1 dye for flow cytometric analysis. The results were shown in Fig 5.3. The density plot was divided into two regions. Cells which fell in the region R2 were those with collapsed Ψ_m . The percentage of cells in R1 increased from 14.3 % of control to 26.3 %, 30.8 % and 35.8 % of 3, 5 and 7 μM for 12 hours incubation of HK18 respectively. There were around 1.8 folds, 2.2 folds and 2.5 folds of the control. The percentage of cells in R2 further increased to 31.9 %, 32.1 % and 57.4 % of 3, 5 and 7 μM for 24 hours incubation of HK18 respectively, which were about 2.2 folds, 2.2 folds and 4 folds of the control. Thus, HK18 could induce mitochondrial membrane depolarization in a concentration and time

dependent manner.

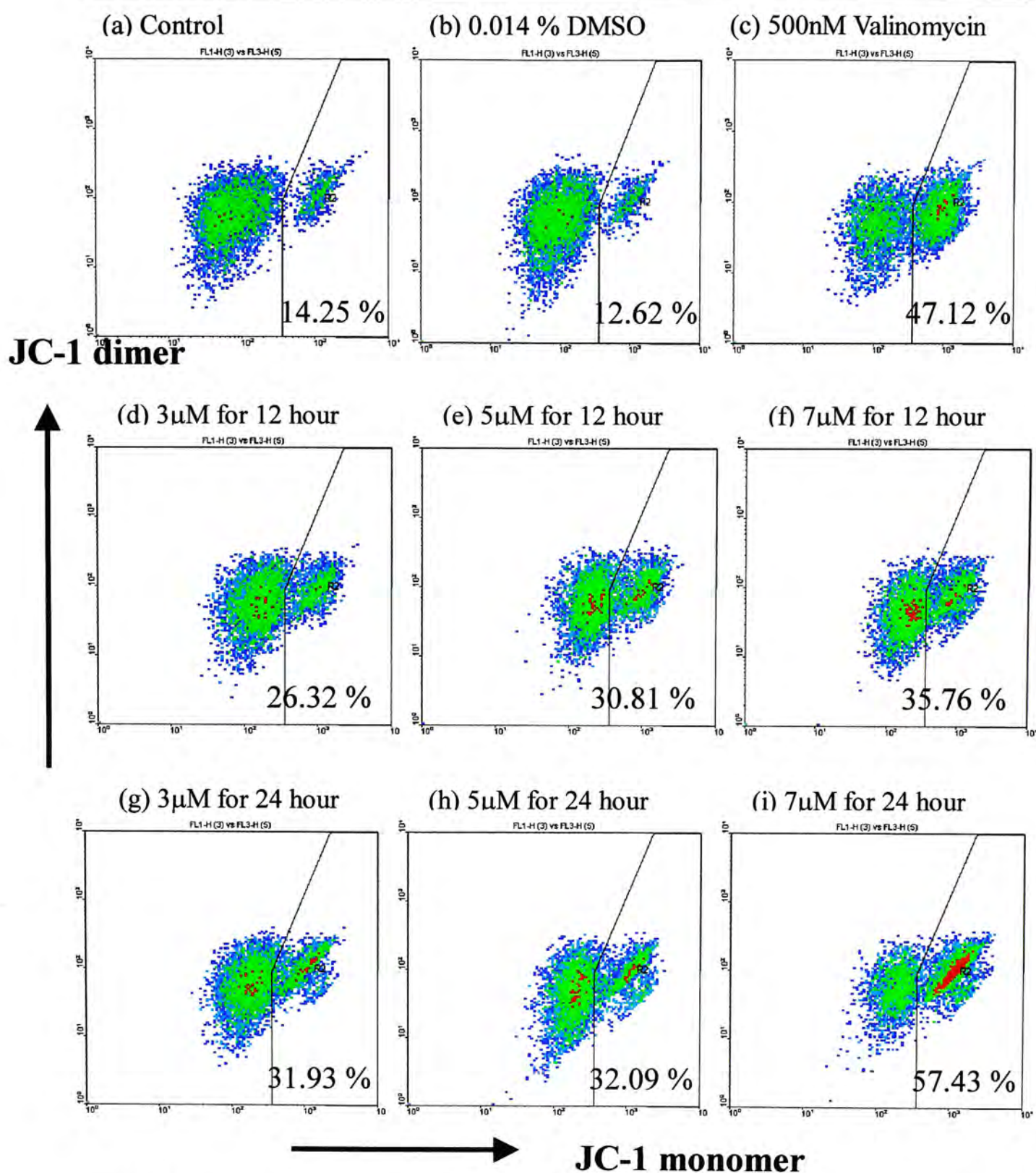


Fig 5.3 Induction of mitochondrial membrane potential depolarization in HK18 treated R-HepG2 cells. 2×10^5 cells / ml were seeded into a 6 well plate and various concentrations of HK18 were added for 24 and 48 hours incubation. After treatments, cells were loaded with JC-1 and fluorescence intensity was recorded by flow cytometry. (a) and (b) control and 0.014 % DMSO solvent control. (c) 500 nM valinomycin as positive control. (d)-(f) 3, 5 and 7 μ M HK 18 for 24 hr incubation. (g)-(i) 3, 5 and 7 μ M of HK18 for 48 hr incubation. Data are from a representative of four separate experiments.

5.2.1.2 Addition of Bongkreikic Acid Reduced HK18 Cytotoxicity on R-HepG2 Cells

To see whether MPT involve in HK18 induced R-HepG2 cells death, Bongkreikic acid (BA) was added to treat R-HepG2 cells with HK18. In this experiment, R-HepG2 cells were incubated with 5 μ M HK18 with or without 25 μ M BA for 24 hours. Then MTT assay was performed to obtain the percentage survival. As shown in Fig 5.4, HK18 induced about 85 % cell death in R-HepG2 cells. However, in the presence of 25 μ M BA, the percentage of survival aroused to around 50 % of the control and it was significantly higher ($p < 0.001$) than that under 5 μ M HK18 treatment.

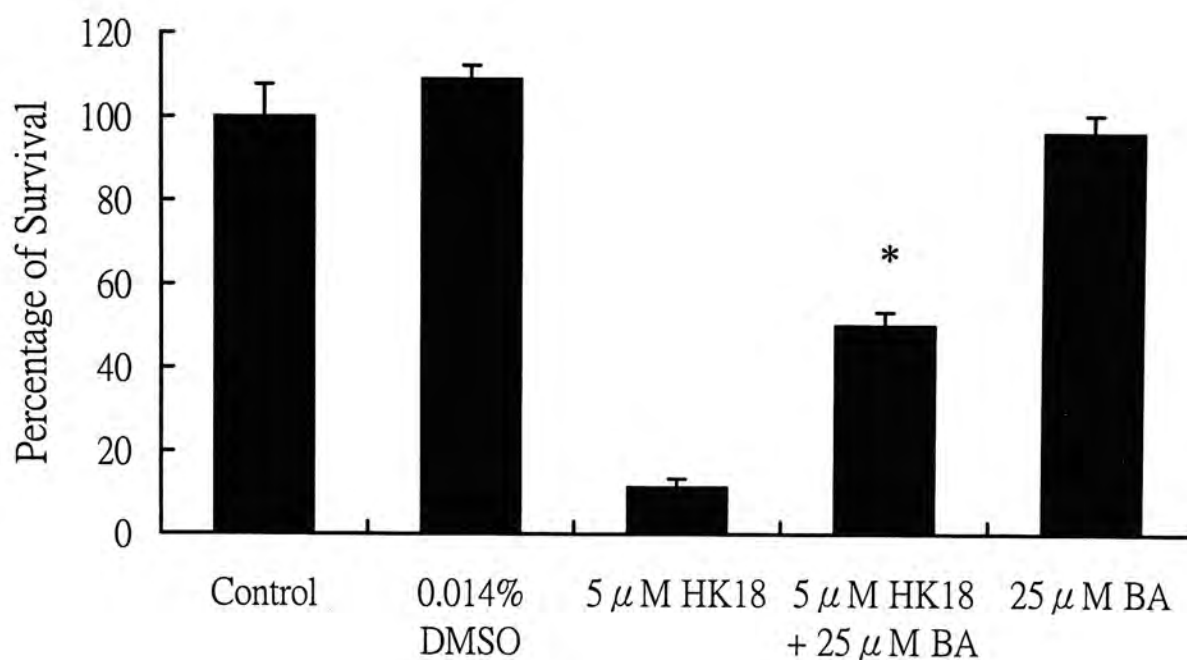


Fig 5.4 Addition of Bongkreikic acid (BA) reduced HK18 cytotoxicity on R-HepG2 cells. 2×10^5 cells / ml of R-HepG2 cells were seeded to a 96 well plate. 5 μM of HK18 was added in the presence or absence of 25 μM BA. After 24 hours, MTT assay was performed to obtain the percentage of survival. Percentage of survival was calculated as relative to the control that is expressed as 100 %. The mean marked with (*) indicated the value is significantly higher (* $p < 0.001$) than the value in cells under 5 μM HK18.

5.2.1.3 Elevation of Intracellular Hydrogen Peroxide Level in HK18 Treated R-HepG2 Cells

The intracellular hydrogen peroxide (H_2O_2) level of HK18-treated R-HepG2 cells was then studied. R-HepG2 cells were treated with 5 μ M HK18 for 12 and 24 hours and were then loaded with DCF which detects the intracellular H_2O_2 level. Flow cytometric analysis was then performed and the change of DCF fluorescence intensity (the fluorescence peak shift to right hand side implied cells having higher intracellular H_2O_2 level and vice versa) was recorded and plotted as histogram. The results were shown in Fig 5.5, and the marker M1 showed the cells with higher fluorescence intensity. After 12 and 24 hours, R-HepG2 cells included in M1 region increased from the basal level of control 8 % to 43.8 % and 34.3 % respectively which is around 5.5 folds and 4.3 folds of the control. The fluorescence intensity of the 0.01 % DMSO solvent control coincided with the control.

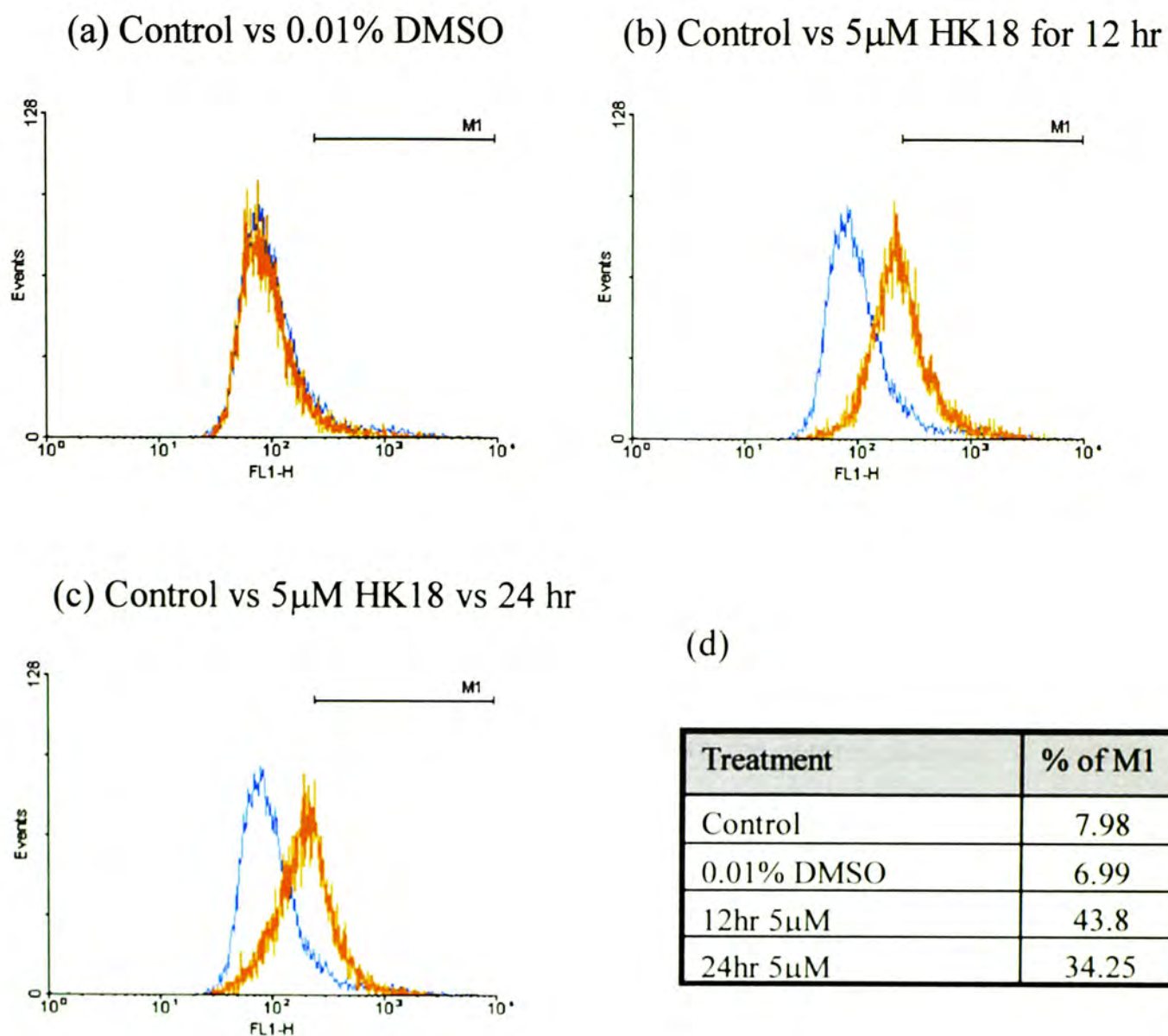


Fig 5.5 Intracellular H₂O₂ level of R-HepG2 cells was enhanced by HK18. 2 x 10⁵ cells / ml of R-HepG2 cells were seeded into a 6 well plate with 5 μ M of HK18 for 12 or 24 hours incubation. After treatments, cells were collected and loaded with DCF. The marker M1 showed the percentage of cells with higher DCF intensity, which reflected cells with higher intracellular H₂O₂ level. (a) Histogram plotting control against 0.01% DMSO solvent control. (b) Histogram plotting control against 5 μ M of HK18 for 12 hours. (c) Histogram plotting control against 5 μ M of HK18 for 24 hours. (d) The table summarizes the percentage of cells in M1 region. Data are from a representative of three separate experiments.

5.2.1.4 Elevation of Intracellular Ca^{2+} Level in HK18 Treated R-HepG2 Cells

Moreover, the change of intracellular Ca^{2+} level of R-HepG2 cells upon HK18 was studied. R-HepG2 cells were treated with 5 μM of HK18 for 12 and 24 hours and were then loaded with Fluo-3. Flow cytometric analysis was carried out and the alternation of fluorescence intensity was recorded. Cells with higher fluorescence intensity indicated higher intracellular Ca^{2+} level and were appeared as a shift of the fluorescence peak into right hand side of the histogram. As observed in Fig 5.6, cells having higher fluorescent intensity (as indicated by M1 region) increased from 8.5 % of control to 31.5 % and 23.1 % of 12 and 24 hours treatments, which were around 3.7 folds and 2.7 folds of the control. The fluorescence peak of the 0.01 % DMSO solvent control coincided with the control. Besides, a positive control with 40 $\mu\text{g}/\text{ml}$ ionomycin was performed and most of the cells fell in M1 region.

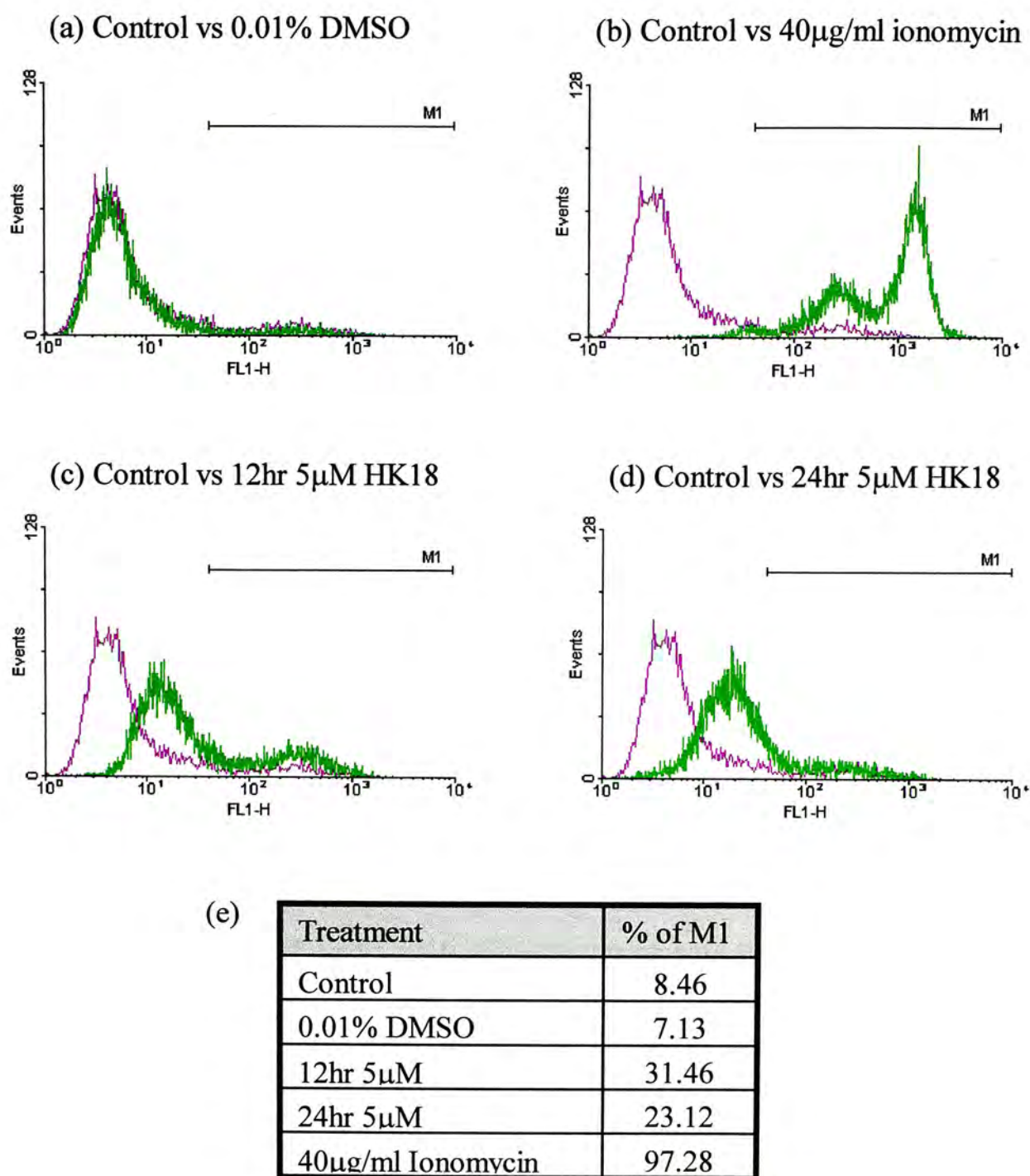


Fig 5.6 Intracellular Ca^{2+} level of R-HepG2 cells was enhanced by HK18. 2×10^5 cells / ml of R-HepG2 cells were seeded into a 6 well plate and 5 μ M of HK18 was added for 12 and 24 hours incubation. After treatment, cells were collected and loaded with Fluo-3. The marker M1 showed the percentage of cells with higher Fluo-3 intensity, which reflected cells with higher intracellular Ca^{2+} level. (a) Histogram plotting control against 0.01% DMSO solvent control. (b) Histogram plotting control against the positive control (40 μ g / ml Ionomycin). (c) Histogram plotting control against 5 μ M of HK18 for 12 hours. (d) Histogram plotting control against 5 μ M of HK18 for 24 hours. (e) The table summarizes the percentage of cells within M1 region. Data are from a representative of four separate experiments.

5.3 Downstream Biochemical Changes Induced by HK18 on R-HepG2 Cells

5.3.1 Activation of Caspase 3 of R-HepG2 Cells by HK18 as Demonstrated by Western Blot

The activity of HK18 on the activation of caspase 3 of R-HepG2 cells was analyzed by Western blot. R-HepG2 cells were treated with 3, 5 and 7 μM of HK18 for 24 hours. As shown in Fig 5.7 a, HK18 activated caspase 3 in a dose dependent manner as the pro-caspase 3 level (35 kDa) decreased when the concentrations of HK18 increased.

Furthermore, the protein level of PARP was also elucidated. Fig 5.7 b indicated that HK18 induced the cleavage of PARP in a dose dependent manner. The protein level of intact PARP (116 kDa) decreased with the cleaved PARP fragment (85 kDa) increased when the concentration of HK18 increased.

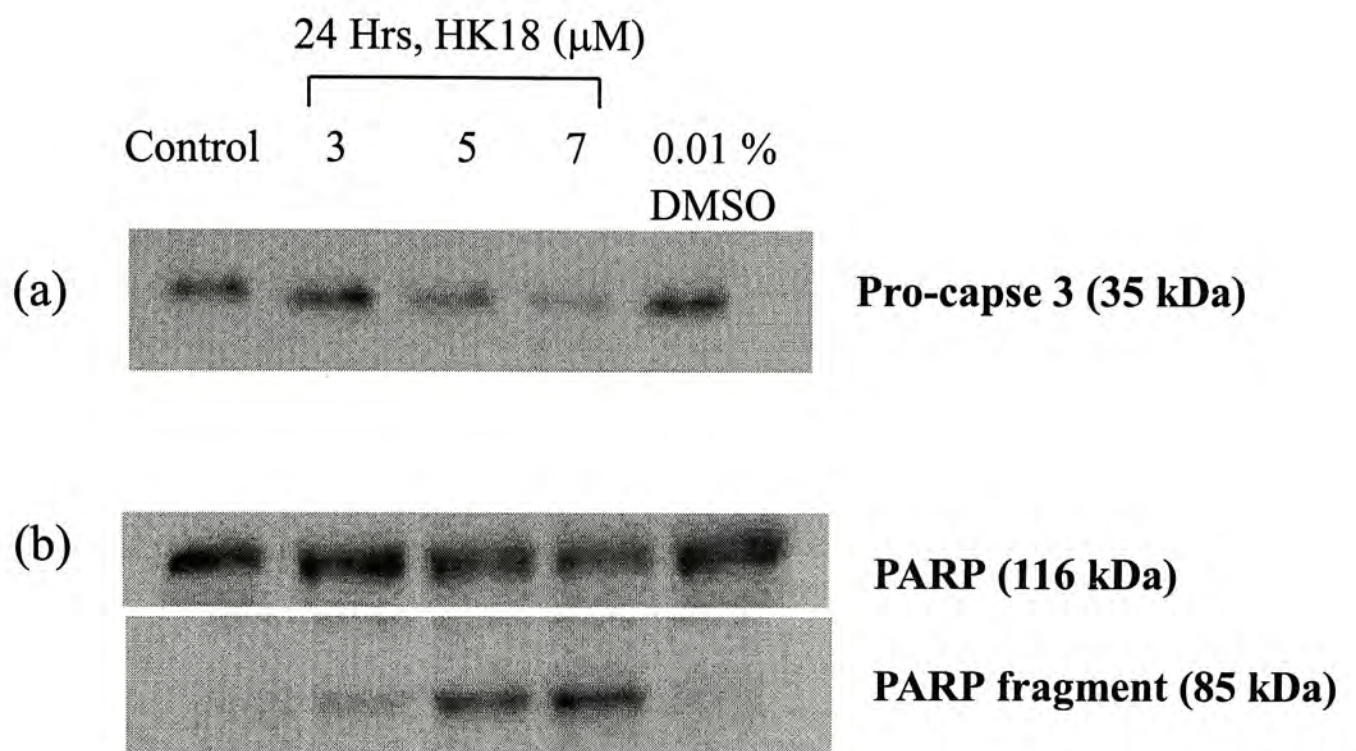


Fig 5.7 Activation of caspase 3 and induction of PARP cleavage by HK18 on R-HepG2 cells. R-HepG2 cells were treated with various concentrations of HK18 for 24 hours and were then subjected to Western analysis. (a) Probed with anti-pro-caspase 3 (35 kDa) antibodies. (b) Probed with anti-PARP (116 kDa for intact PARP and 85 kDa for cleaved PARP) antibodies. Data are from a representative of three separate experiments.

5.3.2 Induction of Caspases Activation of R-HepG2 Cells by HK18 as Demonstrated by Enzymatic Activity Assays

Caspases enzymatic activities were then analyzed in HK18 treated R-HepG2 cells. R-HepG2 cells were treated with 5 μ M HK18 for 12 and 24 hours, then total protein was extracted. After that the protein samples were incubated with caspase 3 specific substrate that had been conjugated with fluorescent AMC. Cleavage of the substrate Ac-DEVD-AMC will release the fluorescent AMC which can be measured by fluorescence spectrometer. Amount of AMC being released is directly proportional to the activity of caspase 3 present in the protein extract.

It was found that caspase 3 activity has been enhanced by HK18 as shown in Fig 5.8. The caspase activities of medium control and 0.01 % DMSO solvent control were similar. However, in the presence of HK18, the caspase activity was 8.6 folds and 3.6 folds of the solvent control for 12 and 24 hours incubation. To check whether the increment was due to the enhanced caspase activity, caspase 3 specific inhibitor z-DEVD-fmk was added. In the presence of z-DEVD-fmk, the amount of AMC released was prohibited.

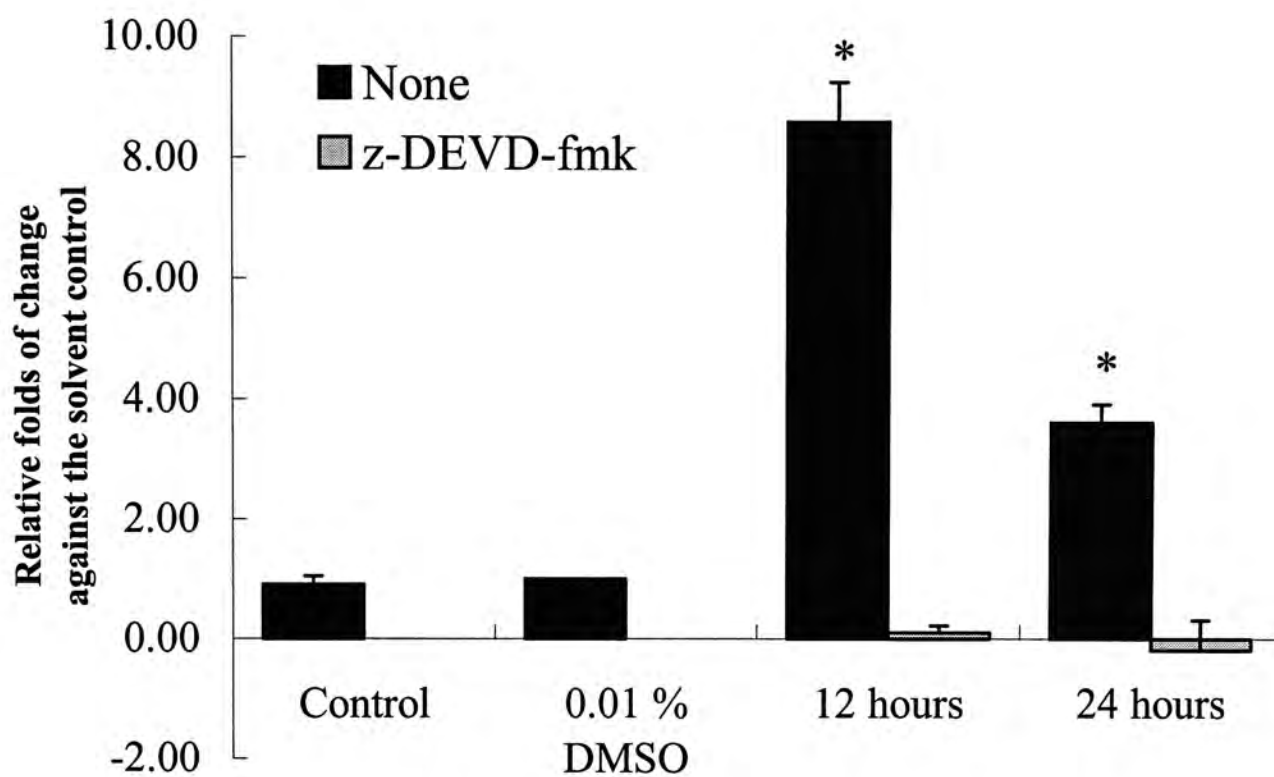


Fig 5.8 Caspase 3 enzymatic activity of R-HepG2 cells was enhanced by HK18. 2×10^5 cells / ml of R-HepG2 cells were seeded into 75 cm^2 flasks and medium, 0.01 % DMSO control or $5 \mu\text{M}$ of HK18 was added for 12 or 24 hours incubation. After treatment, cells were collected and lysed. The protein extract were incubated with caspase-3 specific substrate Ac-DEVD-AMC in the presence or absence of caspase-3 specific inhibitor z-DEVD-fmk. The fluorescence intensity of AMC released was measured and the amount was calculated according to the standard curve. Data are means of three separate experiments. The folds of change of treatments were calculated as relative to the solvent control that is expressed as 1 fold. Mean marked with (*) is significantly (* $p < 0.05$) higher than the solvent control.

Besides, the enzymatic activities of caspase 8 and 9 were also examined. To measure caspase 8 activity, caspase 8 specific substrate conjugated with fluorescent AMC Ac-IETD-AMC was used. The amount of AMC being released is directly proportional to the activity of caspase 8. And the caspase 8 specific inhibitor z-IETD-fmk was used for verification. As shown in Fig 5.9 a, there were no significant different between the control, 0.01 % DMSO solvent control and 5 μ M of HK18 for 12 hours incubation. However, the caspase 8 activity was reduced in cells under 5 μ M HK18 for 24 hours incubation.

On the other hand, for measuring the enzymatic activity of caspase 9, caspase 9 specific substrate conjugated with fluorescent AFC Ac-LEHD-AFC was used. The amount of fluorescent AFC being released was directly proportional to the activity of caspase 9. Caspase 9 specific inhibitor z-LEHD-fmk was used for verification. As illustrated in Fig 5.9 b, the caspase 9 activity was enhanced which was around 2.05 folds of the solvent control for 12 hours treatment. However, the activity after 24 hours treatment was lower than the solvent control.

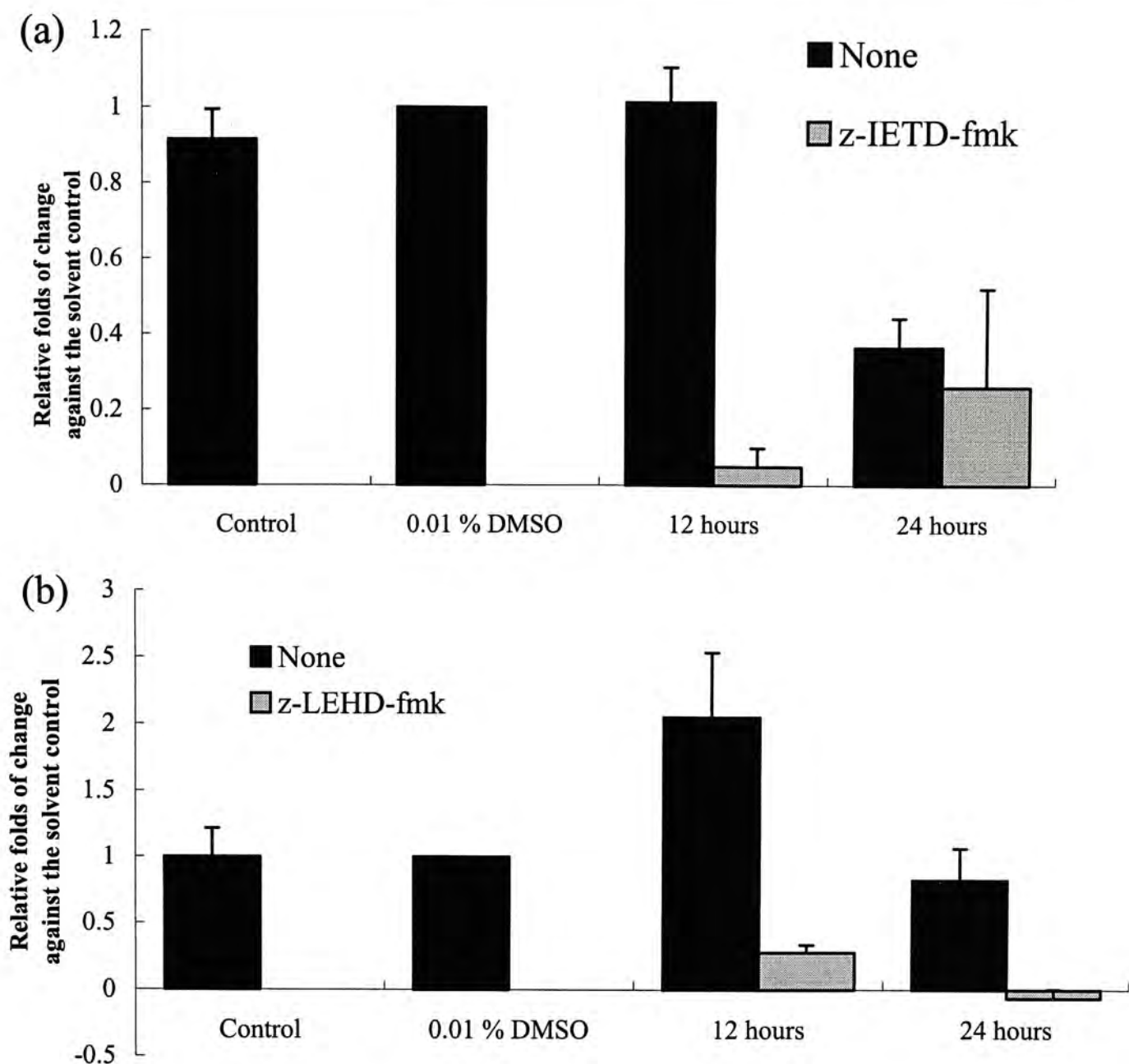


Fig 5.9 Caspase 9 enzymatic activity of R-HepG2 cells was enhanced by HK18 but not caspase 8. 2×10^5 cells / ml of R-HepG2 cells were seeded into 75 cm² flasks and medium, 0.01 % DMSO control or 5 μ M of HK18 was added for 12 or 24 hours incubation. After treatment, cells were collected and lysed. (a) The protein extract were incubated with caspase 8 specific substrate Ac-IETD-AMC in the presence or absence of caspase 8 specific inhibitor z-IETD-fmk. (b) The protein extract were incubated with caspase 9 specific substrate Ac-LEHD-AFC in the presence or absence of caspase 9 specific inhibitor z-LEHD-fmk. The fluorescence intensity of AMC or AFC released was measured and the amount was calculated according to the standard curve. Data are means of three separate experiments. The folds of change of treatments were calculated as relative to the solvent control that is expressed as 1 fold.

5.4 Down-regulation of the Anti-apoptotic Bcl-2 Protein of R-HepG2 Cells by HK18

The effect of HK18 on the Bcl-2 protein expression of R-HepG2 cells was studied. R-HepG2 cells were treated with 3, 5 and 7 μM of HK18 for 12 and 24 hours. The Bcl-2 level decreased as concentrations of HK18 increased. Thus HK18 could lower the Bcl-2 level in a concentration and time dependent manner as illustrated in Fig 5.10.

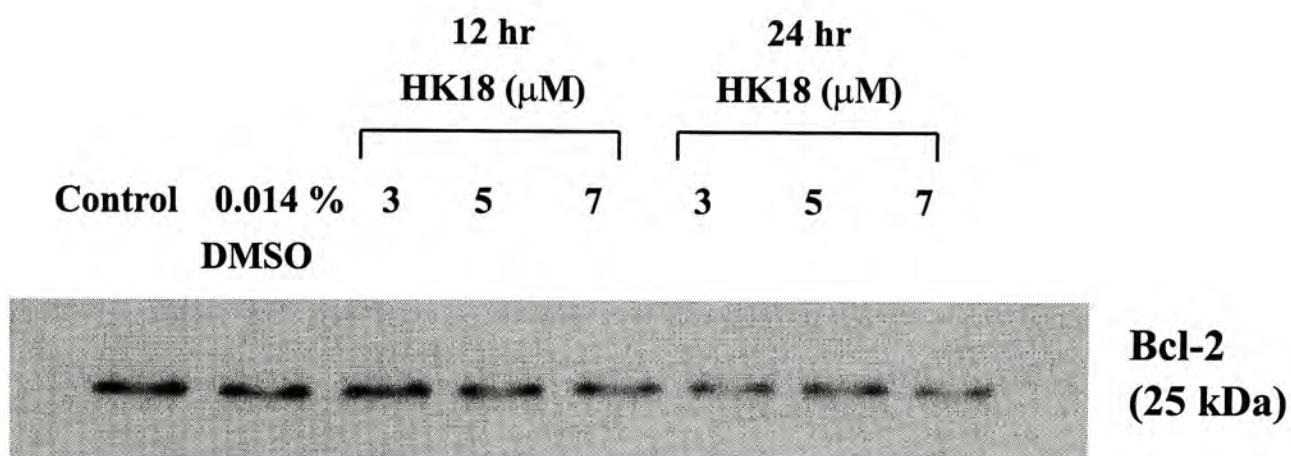


Fig 5.10 Down-regulation of Bcl-2 expression of R-HepG2 by HK18. R-HepG2 cells were treated with 3, 5 and 7 μM HK18 for 12 and 24 hours. The protein extracted was subjected to Western blot and probe with anti-Bcl-2 antibodies. Bcl-2 is a 25 kDa protein. Data are from a representative of two separate experiments.

5.5 HK18 Was Not a Substrate of P-glycoprotein

R-HepG2 cells were derived from HepG2 cells with the addition of DOX as mentioned in the chapter of Materials and Methods. Overexpression of p-glycoprotein (P-gp) and its encoding gene MDR-1 were proven by Western Blot and Northern Blot. In order to sustain the expression of P-gp, the presence of its substrates such as DOX, vincristine and other multidrug resistant substances is required. For the R-HepG2 cells, 1.2 μM of DOX is added to culture the cells to maintain the expression of P-gp (Chan *et al.*, 2000). Since HK18 was cytotoxic to R-HepG2 with a dosage much lower than DOX (2.5 μM of HK18 vs 68 μM of DOX), it seems that HK18 is not a substrate of P-gp.

In view of this, HK18 was used to treat R-HepG2 cells for a month and the expression of P-gp was examined in a time course manner. Along with HK18, R-HepG2 cells were treated with DOX or vincristine or without DOX. The results were shown in Fig 5.11, it showed that the P-gp level was substantially high within the period of treatment in the presence of DOX or vincristine as compared to the level of HepG2 cells. On the other hand, the P-gp level decreased gradually for treating with HK18 or withdrawal of DOX.

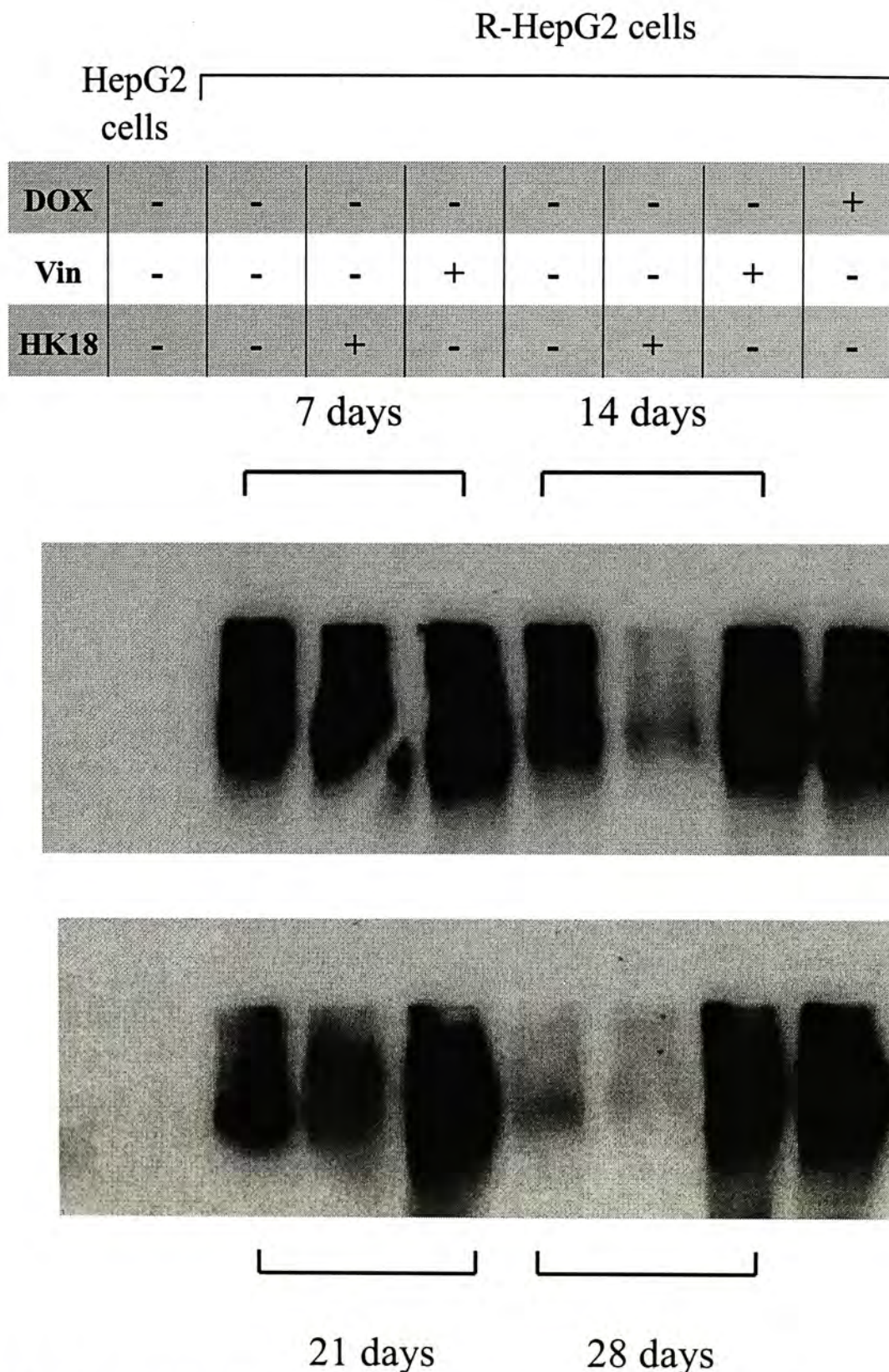
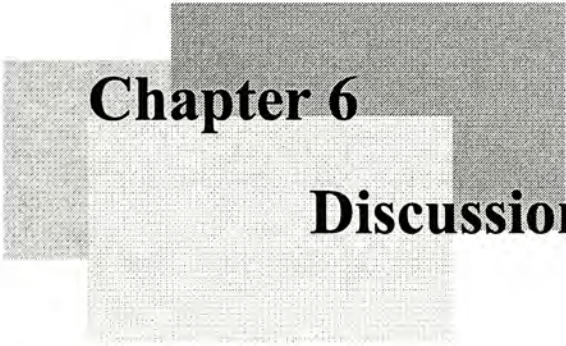


Fig 5.11 HK18 was not a substrate of P-glycoprotein. RHepG2 cells were cultured in the absence of DOX or in the presence of 1.2 μ M of HK18 or vincristine for 28 days. Protein was extracted every 7 days to check the expression of P-glycoprotein. Proteins of HepG2 and R-HepG2 cells, which were being maintained in 1.2 μ M DOX, were extracted for comparison.



Chapter 6
Discussion

6. Discussion

6.1 Cytotoxicity of HK18

6.1.1 HK18 was Cytotoxic to the Human Hepatocellular Carcinoma Cell Line HepG2 and Multidrug Resistant Human Hepatocellular Carcinoma Cell Line R-HepG2

First of all, the cytotoxicities of HK18 on the human hepatocellular carcinoma cell line HepG2 and its derivative, the multidrug resistant cell line R-HepG2 were studied. R-HepG2 cells were derived from HepG2 cells by prolong culturing HepG2 cells in the presence of stepwise increased concentrations of Doxorubicin (DOX), one of the multidrug resistant compounds. After a period of time, the cells have gained to over-express P-gp, which actively pumps out a series of intracellular anti-tumor drugs and hence forbids the accumulation of the drugs. The overexpression of P-gp in R-HepG2 cells were assessed by Western Blot to examine the protein expression level and assessed by Northern Blot to examine the transcriptional level of the MDR-1 gene, which encoded the P-gp (Chan *et al.*, 2000). It is well known that multidrug resistance has posed a great barrier in anti-tumor treatments, thus it is of value to invest on the exploitation of new anti-tumor agents, which can kill multidrug resistance cancer cells.

By the aid of MTT assay and tryphan blue exclusion assay, HK18 have found to exhibit cytotoxic effect in both HepG2 (Fig. 3.1 and 3.2) and R-HepG2 cell lines (Fig. 3.3 and 3.4) in a concentration and time dependent manner. The IC_{50} of HK18 obtained from MTT assay on HepG2 cells and R-HepG2 cells were 3.5 μ M

and 2.5 μM for 24 and 48 hours treatment respectively. And it was found that HK18 has a comparable IC_{50} with DOX on HepG2 cells (4.5 μM and 1 μM for 24 and 48 hours treatments) (Fig 3.1) and far more potent on R-HepG2 cells (IC_{50} of DOX : > 250 μM and 68 μM for 24 and 48 hours treatments) (Fig 3.3).

6.1.2 Study of the Toxicity of HK18

Apart from HepG2 and R-HepG2 cells, the cytotoxicity of HK18 was examined on the primary cell macrophages ($\text{M}\Phi$) in order to study the toxic effect of HK18 on normal cells. 2.5 μM and 5 μM of HK18 was used to treat $\text{M}\Phi$ for 48 hours. It have been found that 2.5 μM of HK18 induce around 10 % cell death on $\text{M}\Phi$ while around 50 % cell death on HepG2 and R-HepG2 cells (Fig 3.5). On the other hand, 5 μM of HK18 induce around 30 % cell death on $\text{M}\Phi$ and around 80 % on HepG2 as well as R-HepG2 cells. Thus, HK18 exerted more potent cytotoxic effects on the two tumor cell lines than on the normal cell, at least $\text{M}\Phi$. Pilot studies in our laboratory also demonstrated that HK18 is non-toxic to the lung fibroblast cell line, WI-38 (data not shown).

Since induction of hemolysis is a common feature of saponins, the hemolytic ability of HK18 was checked. It has been found that HK18 could induce hemolysis in high concentrations. The percentage of hemolysis for 3.5 μM and 10 μM was only around 3 % and 7 % respectively (Fig 3.6).

The toxic effect of HK18 on normal tissues was further studied by *in vivo*

study. 342 $\mu\text{g}/\text{kg}$ (equivalent to 5 μM final concentration) of HK18 was administered to mouse via intravenous injection for every alternative days for 2 weeks. The liver and heart tissue enzymatic levels (AST and ALT for liver and CK and LDH for heart) were then monitored. And it has shown that there was no elevation of neither one of the enzymes (Fig 3.7 and 3.8).

6.2 Mechanistic Studies of the Cytotoxic Effects of HK18 on HepG2 Cells

6.2.1 Apoptotic Cell Death Induction of HK18 on HepG2 Cells

As shown by MTT and trypan blue exclusion assays, HK18 has found to induce cell death of HepG2 cells. The death mode of HepG2 cells was then examined by phosphatidylserine (PS) externalization assay and DNA fragmentation assays, which are the frequently used biochemical assays for detection of apoptosis.

Phospholipids distributed across the plasma membrane asymmetrically, with phosphatidylcholine and sphingomyelin localized primarily in the extracellular surface while PS and phosphatidylethanolamine restricted almost exclusively to the intracellular surface under physiological conditions (Stryer, 1995). Upon apoptosis, the PS will flip from inner membrane into outer membrane, which is an important biochemical change for the removal of the dying cells by macrophages to prevent inflammation. PI is a DNA intercalating dye. It cannot get access to DNA in intact cells. However, it can stain the DNA of necrotic and late apoptotic cells since their plasma membrane was disrupted. Therefore, in the combination of PS flipping and

plasma membrane disruption, one can distinguish between viable, early apoptotic and necrotic / late apoptotic cells (Spactor *et al.*, 1998).

DNA fragmentation is another prevalent apoptotic biochemical changes (although not found in all apoptotic cells). During apoptosis, the activated caspases will activate endonuclease, which cleave DNA in the linker region between nucleosomes to produce oligonucleosomal DNA fragments. The DNA fragments can be detected as multiples of 180 – 200 bp and can be demonstrated as a ladder appearance upon gel electrophoresis. Results shown that HK18 induced PS externalization in a dose dependent manner for 24 hours treatment (Fig 4.2) and DNA fragmentation in a time dependent manner for 24 and 48 hours treatments (Fig 4.3).

6.2.2 Studies of the Underlying Mechanisms of HK18 Induced Apoptosis of HepG2 Cells

There were two main apoptotic pathways. One of them involved the death receptor and ligand binding. Binding of ligand molecules to the death receptors will induce cluster of the death domains of receptors. An adaptor protein FADD (Fas-associated death domain) then binds to the clustered receptor death domain via the death domain of the FADD. FADD also contain a death effector domain (DED), which then interact with the DED of pro-caspase 8. More than one molecules of pro-caspase 8 are being recruited to the death receptors. Such induced proximity of the pro-caspase will lead to auto-activation of pro-caspase 8 into catalytically active caspase 8 which then participate in apoptosis and activate pro-caspase 3 (Ashkenazi

and Dixit, 1998; Hengartner, 2000).

Mitochondria are involved in another apoptotic pathways. It is well known that mitochondria are responsible to produce energy for maintaining life of cells for a long history. However, recent discoveries have found that mitochondria also play an active role in apoptosis. In the mitochondrial dependent apoptotic pathway, a variety of apoptotic triggers such as oxidants and Ca^{2+} converge to mitochondria. This will lead to mitochondrial permeability transition (MPT) due to the opening of the MPT pore complex. The precise structure and components of the MPT pore complex is still under investigation. However, several components are believed to be involved. They are voltage dependent anion channel (VDAC) (i.e. porin) located in the outer mitochondrial membrane; adenine nucleotide translocator (ANT) located in the inner mitochondrial membrane; peripheral benzodiazepin receptor located in the outer mitochondrial membrane; creatine kinase located in intermembrane space; cyclophilin D located in the matrix and attached to ANT; hexokinase located in the cytosolic face of outer mitochondrial membrane and attached to VDAC as well as the Bcl-2 family members including Bcl-2 and Bax (Fig 4.4) (Arceci, 2000; Kroemer and Reed, 2000). Opening of the MPT pores will allow small solutes (<1.5 kDa) diffuse out from mitochondria into cytosol non-specifically. Mitochondrial membrane potential (Ψ_m) depolarization usually accompanied with MPT (Arceci, 2000; Kroemer and Reed, 2000; Crompton, 1999; Lemasters *et al.*, 1998).

The opening of MPT pores can be measured directly by confocal fluorescence microscopy (Halestrap, 1999). Calcein, a neutral green fluorophore will retain in cytosol when loaded to a normal viable cell. While tetramethylrhodamine

methylester (TMRM), a cationic red fluorophore will accumulate in negatively charged mitochondria. As a result, the viable cell will appear as red fluorescence dots (mitochondria) against green fluorescence background (cytosol). During MPT, MPT pore opening allow the entry of calcein into mitochondria and leakage of red fluorescence from the potential difference dissipated mitochondria and hence red dots disappear (Halestrap, 1999).

There are several well known conditions, which are able to induce MPT. They are oxidative stress, high intracellular calcium concentration, low ATP, high ADP, high pH and mitochondrial membrane potential depolarization (Lemasters *et al.*, 1998; Crompton, 1999). On the other hand, onset of MPT can be inhibited by MPT inhibitor. The widely used MPT inhibitors are cyclosporin A (CsA) and Bongrekrekic acid (BA). By the aid of these inhibitors, the role of MPT in apoptosis can be studied. CsA is a ligand of cyclophilin D, one of the components of MPT pore complex. Binding of CsA will induce conformational change of the cyclophilin D and inhibit its binding with the MPT pore complex and hence MPT is being inhibited. The inhibitory activity of BA is through another mechanism. BA is a ligand of the ANT, another component of MPT pore complex. Its binding will stabilize the ANT in a conformation that is unable to participate in MPT pore opening (Crompton, 1999; Zamzami *et al.*, 1996; Marchetti *et al.*, 1996).

Onset of MPT will lead to release of mitochondrial intermembrane apoptogenic proteins. However, how the release of these apoptogenic proteins takes place is controversial. One hypothesis is that opening of MPT pores allows water and

sucrose influx into matrix and hence causes matrix swelling. Since the inner mitochondrial membrane is highly folded so its surface area is greater than the outer membrane. Upon matrix swelling, inner mitochondrial membrane expanding will disrupt the outer membrane physically. Consequently, apoptogenic proteins will leak out from the boundary of outer membrane into cytosol and elicit apoptosis (Arceci, 2000; Kroemer and Reed, 2000; Crompton, 1999; Lemasters *et al.*, 1998).

Another hypothesis involves the participation of Bcl-2 family proteins. It has been found that the three dimensional structure of Bcl-X_L is similar to the pore forming bacterial toxin (Muchmore *et al.*, 1996). Thus it is thought that Bcl-2 family members may form pores in the mitochondrial outer membrane. The pro-apoptotic member Bax may oligomerize and insert into outer mitochondrial membrane to form ion-conducting channels or it may interact with VDAC to form large channels. Therefore, proteins can pass through the membrane freely (Gottlieb, 2000).

Up to now, several apoptogenic proteins have been found to release from mitochondria during mitochondria-dependent apoptosis. These include cytochrome c, apoptosis inducing factor (AIF), adenylate kinase-2 and Smac/DIABLO (Loeffler and Kroemer, 2000; Kohler *et al.*, 1999; Verhagen *et al.*, 2000; Du *et al.*, 2000; Scarlett and Murphy, 1997). Release of these proteins into cytosol will induce cellular catabolic destruction.

Smac (second mitochondria-derived activator of caspase) or also called as DIABLO (direct IAP binding protein with low pI) is a novel discovered apoptogenic

protein. They are released from mitochondria during apoptosis to promote caspase 9 activation by binding to the IAPs (inhibitor of apoptosis proteins) (Verhagen *et al.*, 2000; Du *et al.*, 2000). IAPs are inhibitors of caspase 3, 7 and 9 (Shi, 2002). Activated caspase 9 will expose its IAP-binding domain and hence IAP can bind and inhibit its enzymatic activities. The binding of IAP will further degrade the activated caspase 9 and hence apoptotic catabolic changes are inhibited. Therefore, IAPs must be removed for ensuring the caspase 9 activities (Wang, 2001). Smac / DIABLO is responsible for removing the IAPs by binding with them (Verhagen *et al.*, 2000; Du *et al.*, 2000; Zimmermann *et al.*, 2001; de Murcia *et al.*, 1997).

Cytochrome c is a 15 kDa protein which is involved in the electron transport chain for energy production. It is one of the apoptogenic proteins being released from mitochondria during apoptosis and they are important in the activation of procaspase 9 (Liu *et al.*, 1996; Yang and Cortopassi, 1998). Cytochrome c is bound to the inner membrane by anionic phospholipids, primarily cardiolipin. Actually, there are two pools of cytochrome c. The small pool (accounted for around 10 – 15 %) located at the mitochondrial intermembrane space via electrostatic interaction between the positively charged lysine residues of cytochrome c and negatively charged phosphate groups of cardiolipin (Bernardi *et al.*, 1999; Ott *et al.*, 2002; Shen *et al.*, 2001). The large pool is tightly bound to the inner membrane via hydrophobic interaction with the cardiolipin (Ott *et al.*, 2002). The loosely bound small pool will be released when ionic strength or pH change. For releasing the tightly bound pool, oxidation of the mitochondrial membrane especially the cardiolipin is needed (Shidoji *et al.*, 1999; Ott *et al.*, 2002).

AIF (apoptosis inducing factor) is a 57 kDa flavoprotein which being released from mitochondria during apoptosis. It can induce large scale DNA fragmentation, PS externalization and Ψ_m depolarization in a caspase independent manner (Susin *et al.*, 1996; Susin *et al.*, 1999; Loeffler *et al.*, 2001; Daugas *et al.*, 2000).

Studies have found that some saponins such as the saponins isolated from *Acacia victoriae* could induce apoptotic cell death via mitochondrial dependent pathway. Thus, the involvement of mitochondria in HK18 induced apoptosis of HepG2 cells was studied.

From the result, incubation of HK18 with HepG2 cells induced mitochondrial membrane depolarization in a dose and time dependent manner (Fig 4.5). MPT always induce Ψ_m depolarization, however not all Ψ_m depolarizations are caused by MPT (Lemasters *et al.*, 1998). Thus, the occurrence of MPT was further studied by the addition of MPT inhibitor BA. As shown in Fig 4.6, addition of BA could reduce the cytotoxicity of HK18 on HepG2 cells. Since BA is an inhibitor of MPT, it is obvious that MPT is pivotal to HK18 induced HepG2 cells apoptotic cell death.

As mentioned above, onset of MPT leads to apoptogenic proteins release from mitochondria although the releasing mechanism is still uncertain. The release of apoptogenic proteins were examined for HK18 treated HepG2 cells. It has been

found that HK18 could induce cytochrome c release (Fig 4.11). The amount of cytochrome c released at 12 hours treatment was smaller than 24 hours treatment. This might be due to the cytochrome c released at 12 hours treatment was from the loosely bound small pool cytochrome c. While at 24 hours treatment, the tightly bound large pool of cytochrome c also being released. In such mode of cytochrome c release, the ATP production via the electron transport chain might be allowed. Since it is well known that ATP is needed for the catabolic degradation during apoptosis, maintenance of ATP production is important. On the other hand, the release of AIF was also studied in HK18 treated HepG2 cells. As observed in Fig 4.11, AIF was induced to release for 24 hours treatment.

There are several MTP inducers so far identified such as mild oxidative stress, increase of intracellular Ca^{2+} level, reduced ATP level, and elevated pH (Crompton, 1999; Lemasters *et al.*, 1998). Among them, oxidative stress and elevated Ca^{2+} are most important and under intensive studies.

Although it has been found that apoptotic cell death can be carried out in anaerobic conditions, more studies provide evidences that ROS play an important role in the induction of apoptosis. It has been found that exposure of cells with oxidizing agents such as hydrogen peroxide and *tert*-Butylhydroperoxide would induce apoptotic cell death (Lemasters *et al.*, 1998). Moreover, it has been found that increase of intracellular ROS production was observed in apoptotic cell death induced by non-oxidative agents such as ionizing radiation and chemotherapeutic drugs (Chandra *et al.*, 2000; Hampton *et al.*, 1998). For example, addition of

selenium, an essential trace element with potent chemopreventive effect against cancer, to HepG2 cells would elicit intracellular ROS production followed by cytochrome c release, Ψ m depolarization, caspase 3 activation and DNA fragmentation (Shen *et al.*, 2001). Another example was etoposide induced apoptosis. Etoposide is a semisynthetic derivative of podophyllotoxin and is an anti-tumor agent used currently in treating a variety of hematopoietic and solid tumor. Etoposide has been found to induce apoptosis by interacting directly with macromolecular targets or by generating ROS. And its cytotoxicity has been reported to mediate by mitochondria including cytochrome c release, Ψ m depolarization, MPT and caspase 3 and 9 activation as well (Custodio *et al.*, 2002). Moreover, it has been found that the apoptotic inducing activities of these agents could be blocked by the addition of anti-oxidants *N*-acetylcysteine (NAC) (Shen *et al.*, 2001; Custodio *et al.*, 2002) and glutathione (Custodio *et al.*, 2002). Therefore, ROS seems to play an important role in apoptosis, though may not in all cases.

The mechanisms of how ROS induce apoptosis are still under investigation. But there were evidences that ROS induce apoptosis by acting on the MPT pore complex (Costantini *et al.*, 1996). It has been found that there was a cysteine residue in the ANT (one of the component of MPT pore complex), which is sensitive to oxidizing stress. Oxidation of this cysteine residue will lead to thiol cross-link between ANT molecules. The resulted ANT dimer would induce MPT pore opening (Costantini *et al.*, 2000a). Besides, ROS will cause elevation of intracellular Ca^{2+} level. The enhanced Ca^{2+} level can either come from extracellular space or internal stores. It has been found that ROS could act on the $\text{Na}^+ / \text{Ca}^{2+}$ exchanger which

normally exclude Ca^{2+} from cytosol into extracellular space or organelles. However, ROS could reverse the action of the exchanger to pump Ca^{2+} into cytosol instead (Suzuki *et al.*, 1997). Moreover, ROS would oxidize mitochondrial pyridine nucleotides NAD(P)H which would stimulate the release of Ca^{2+} from mitochondria (Suzuki *et al.*, 1997; Chakraborti *et al.*, 1999). The enhanced cytosolic Ca^{2+} level would then activate Ca^{2+} dependent catabolic enzymes such as proteases and endonucleases (Chakraborti *et al.*, 1999; McConkey and Orrenius, 1997). Besides, Ca^{2+} is also an inducer of MPT with unknown mechanism (Kroemer and Reed, 2000). Moreover, ROS may also activate nuclear transcriptional factors such as NF κ B, AP-1 and p53 which may up-regulate death proteins or produce inhibitors of survival proteins (Suzuki *et al.*, 1997; Chandra *et al.*, 2000).

On the other hand, besides serving as the inducer of MPT and apoptosis, ROS also has found to be the consequence of MPT. It is because during MPT, Ψ_m usually collapsed. Thus oxidative phosphorylation was uncoupled and the electron transport chain was disturbed. As a result, ROS production increases especially when cytochrome c was being released from mitochondria. Thus, they form a positive amplification feedback loop between ROS production and MPT (Costantini *et al.*, 2000b).

In view of the apoptosis and MPT inducing activities of ROS and Ca^{2+} , the participation of them were investigated in this research project. HepG2 cells were treated with HK18 for 12 and 24 hours and followed by flow cytometric analysis to measure the intracellular H_2O_2 and Ca^{2+} level. It has been found that HK18 enhanced

intracellular H_2O_2 in a time dependent manner (Fig 4.7). Since ROS level is related to the occurrence of MPT, the intracellular H_2O_2 level was further measured with Ψm simultaneously. As shown in Fig 4.8, HK18 could induce elevation of intracellular H_2O_2 level with collapsed Ψm simultaneously in a time dependent manner.

Apart from measuring intracellular H_2O_2 level, intracellular Ca^{2+} level was also examined. It has been found that HK18 could enhance intracellular Ca^{2+} level (Fig 4.9). However, the increment was not in a time dependent manner. It may be due to the optimal Ca^{2+} release was reached at 12 hours treatment; further longer treatment period did not affect the Ca^{2+} level anymore. Similarly, intracellular Ca^{2+} level was examined with Ψm simultaneously. As shown in Fig 4.10, HK18 enhanced intracellular Ca^{2+} level with decreased Ψm . And the increment at 12 and 24 hours were more or less the same.

It is well known that the Bcl-2 family proteins play an important role in apoptosis. Bcl-2 (homologue to CED-3 of *C. elegans*) was first identified from B cell lymphomas, where chromosomal translocations activate its expression at inappropriate high level (Reed, 1997). Bcl-2 family members can be divided into two groups as anti-apoptotic such as Bcl-2, Bcl- X_L , Bcl-w and Mcl-1 as well as the pro-apoptotic such as Bax, Bcl- X_S , Bak, Bid and Bad. The locations of the Bcl-2 family members vary from cytosol to intracellular compartments including nucleus, endoplasmic reticulum and mitochondria. In non-apoptotic normal cells, anti-apoptotic members including Bcl-2 and Bcl- X_L are localized at the

mitochondrial outer membrane while most of the pro-apoptotic members such as Bax and Bid are localized in cytosol. Upon apoptotic stimuli, they will redistribute in the cells. For example, the pro-apoptotic members including Bax and Bid will translocate to mitochondria to interact with the anti-apoptotic members or exert their effect on the mitochondria directly. There were evidences that Bax is able to form oligomer across the mitochondria membrane to form a non-specific pores, which has been proposed to be responsible for apoptogenic proteins release from mitochondria during apoptosis (Muchmore *et al.*, 1996; Gottlieb, 2000).

The Bcl-2 family members of HK18 treated HepG2 cells were studied. First of all, the protein expression level of the anti-apoptotic Bcl-2 was examined by Western blot analysis. It has been found that treating HepG2 cells with HK18 for 12 and 24 hours would suppress the Bcl-2 protein level in a dose and time dependent manner (Fig 4.15). The gene transcriptions of the bcl-2 family members were further investigated by RT-PCR. It has been found that treating HepG2 cells with HK18 for 12 and 24 hours would suppress the mRNA level of the anti-apoptotic bcl-2 and bcl-X_L. However, there was no change in the mRNA level of the pro-apoptotic bak. The suppression of HK18 on the mRNA of bcl-2 and bcl-X_L was not in a time dependent manner as to the protein expression did. This may be due to the effect of HK18 on transcription was optimal at 12 hours but not on the translation level.

Studies of development in the nematode *Caenorhabditis elegans* (*C. elegans*) have led to the discovery of genes whose function is critical for programmed cell death. There are three pivotal apoptotic genes: ced-3, ced-4 and ced-9, which encode

the proteins CED-3, CED-4 and CED-9. It was found that mutation of *ced-3* and *ced-4* would result in cell survival and differentiation even the cells should be removed normally (Ellis and Horvitz, 1986; Yuan and Horvitz, 1990). The *ced-3* gene was cloned and was found to be similar to the interleukin-1 β -converting enzyme of mammals. And it has been found that the CED protein acts as a cysteine protease to initiate programmed cell death in *C. elegans* (Yuan *et al.*, 1993). Later, It was found that CED-4 physically interacts with both CED-3 and CED-9 to form a multiple protein complex (Chinnaiyan *et al.*, 1997; Irmeler *et al.*, 1997). Upon binding with CED-4 in the presence of dATP / ATP, CED-3 will be activated and its activity is critical for cells to undergo apoptosis. On the other hand, binding of CED-9 to the complex would inhibit apoptosis (Seiffert *et al.*, 2002; Hengartner, 1999).

Since apoptosis is an evolutionarily conserved biochemical process, understanding of the apoptotic processes of *C. elegans* helps to learn and infer how the apoptotic processes work in mammalian cells. It has been found that mammals have counterparts of the three apoptotic related proteins of *C. elegans*. The mammalian interleukin-1 β -converting enzyme proteases or also known as caspases are homologous to the CED-3 protein (Yuan *et al.*, 1993). Besides the mammalian apoptotic protease activating factors -1 (Apaf-1) is homologous to the CED-4 (Hengartner, 1999) and the anti-apoptotic bcl-2 protein is homologous to the CED-9 (Chinnaiyan *et al.*, 1997; Spector *et al.*, 1997). Although human shares some of the apoptotic mechanisms with the *C. elegans*, the apoptotic mechanisms of human are much more complicated.

Up to now, 14 mammalian caspases have been identified and 7 of them have found to participate in apoptosis while the remaining are involved in inflammation (Shi, 2002). They share similarities in amino acid sequence, structure and substrate specificity (Earnshaw *et al.*, 1999). Actually apoptotic caspases can be divided into two categories, initiator caspases including caspase 2, 8, 9 and 10 as well as the effector caspases including caspase 3, 6 and 7. All caspases are synthesized as catalytically inactive precursor zymogens with three major domains: N-terminal prodomain, large subunit containing the active site and C-terminal small subunit. The prodomain varies in length and sequence, which is important in distinguish between initiator and effector caspases. Usually initiator caspases consist of a long prodomain and contain a sequence that promotes their interaction with activator molecules, either caspase recruitment domain (CARD) present in caspase 2 and 9 as well as the death effector domain (DED) present in caspase 8 and 10 (Zimmermann *et al.*, 2001; Shi, 2002; Earnshaw *et al.*, 1999).

For converting the zymogens into the active caspases, two proteolytic cleavages are required. The first cleavage divides the zymogen into large and small subunits while the second cleavage aimed to remove the prodomain. An active caspase is a tetramer of two large and two small subunits with two active sites (Earnshaw *et al.*, 1999). Activation of initiator caspases is mediated by several activator molecules, which subsequently lead to auto-activation of the initiator caspases via induced proximity. There are two major mechanisms for activating initiator caspases. One of them involves death receptor and another involves

mitochondria. As mentioned above, the activation of procaspase 8 requires the participation of death receptor, ligand of death receptor, FADD and several procaspase 8 molecules. (Ashkenazi and Dixit, 1998; Hengartner, 2000).

On the other hand, for the mitochondria dependent apoptosis, activation of procaspase 9 requires the formation of apoptosome. Apoptosome is formed by the interaction of apoptotic protease activating factors -1 (Apaf-1), cytochrome c and pro-caspase 9 in the presence dATP / ATP (Liu *et al.*, 1996). Apaf-1 is a 130 kDa protein which contains a CARD sequence (Li *et al.*, 1997). On binding with dATP / ATP (dATP is prefer over ATP for 1000 folds) (Li *et al.*, 1997), the Apaf-1 undergo conformational change which then allow cytochrome c binding. ATP hydrolysis is required since binding of non-hydrolysable ATP- γ would completely abolish the binding of cytochrome c (Li *et al.*, 1997; Hu *et al.*, 1999). Binding of cytochrome c induces further conformational change. This allows oligomerization of Apaf-1 molecules and causes the exposure of CARD of Apaf-1. As a result, procaspase-9 molecules are recruited to the complex via CARD-CARD interaction to form apoptosome. The induced proximity of the pro-caspase 9 molecules leads to its auto-activation into catalytically active caspase 9 (Hu *et al.*, 1999; Srinivasula *et al.*, 1998; Li *et al.*, 1997; Cai *et al.*, 1998). After that, pro-caspase 3 will be recruited to the apoptosome and is being activated by the activated caspase 9 (Hu *et al.*, 1999). Activated caspase 3 will then cause proteolytic cleavage of a series of substrates, which will then lead to the biochemical and morphological changes observed in apoptosis (Zimmermann *et al.*, 2001; Shi, 2002).

Actually, the apoptotic pathways mediated by death receptor and mitochondria can be cross-linked. It has been found that activated caspase 8 will cleave the cytosolic pro-apoptotic Bid. The truncated Bid will then translocate to mitochondria and induce cytochrome c release and subsequently apoptosome formation (Hengartner, 2000; Engels *et al.*, 2000; Gottlieb, 2000). By such mechanism, the apoptotic responses induced by caspase 8 will be amplified.

It is well known that caspases are the effector molecules. Their activities are critical for the occurrence of apoptotic biochemical alternations. It is particularly true for caspase 3. Caspase 3 is the most abundant caspase inside cells. No matter which apoptotic pathways is induced by the apoptosis inducing agent, the final destination usually directed to the activation of pro-caspase 3 (Zimmermann *et al.*, 2001). The activated caspase 3 will then act on a wide array of substrates which responsible for the catabolic degradation of cells. For example, murine caspase-activated DNase (CAD) (i.e. DNA fragmentation factor, DFF of human) is activated by caspase 3. CAD is synthesized in the complex with its inhibitor ICAD (inhibitor of CAD). Activated caspase 3 in apoptotic cells will act on the complex to release the ICAD and hence restore the endonuclease activity of CAD (Nagata, 2000).

There are numerous caspase substrates including structural components (such as actin and nuclear lamin), proteins involved in DNA metabolism and repair (such as DNA-depedent protein kinase and poly(ADP-ribose) polymerase) and inhibitors of deoxyribonuclease (such as caspase-activated DNase) etc. (Zimmermann *et al.*, 2001; Earnshaw *et al.*, 1999). Caspases are specific proteases,

which recognize at least four contiguous amino acids and cleave after the C-terminal of an Aspartic acid residue only. Each caspase recognize a specific amino acid sequence. Such substrate specific property can make use for study the caspase activity. By the aid of fluorescence or chromogen conjugated artificially constructed amino acids sequence, which consist the substrate recognition site, the activity of the caspase can be studied. The fluorescence or chromogen intensity is directly proportional to the caspase activity (Mack *et al.*, 2000).

The caspases activating activities of HK18 on HepG2 cells were studied. First of all, the protein expression level of caspase 3 was studied by Western blot analysis. As shown in Fig 4.12, incubation of HepG2 cells with HK18 reduced the protein level of pro-caspase 3 in a dose and time dependent manner. The reduced pro-caspase 3 was supposed to be converted into active caspase 3. It was then confirmed by examine the substrate of active caspase 3, PARP. It was found that the intact PARP decreased while the fragmented PARP increased when the concentration of HK18 increased (Fig 4.12).

The caspases activities were then examined by measuring their enzymatic activities. Caspase 3, caspase 8 and caspase 9 specific substrates were used. The substrates were conjugated with fluorescent materials. Upon cleavage by the caspase, the fluorescent material will be released which can be measured by fluorescent spectrometer. The fluorescence intensity is directly proportional to the caspase activity. It has been found that HK18 could induce the activities of caspase 3 of HepG2 cells in a time dependent manner (Fig 4.13). HK18 also induce the enzymatic

activity of caspase 9 of HepG2 under 12 hour and 24 hours treatments (Fig 4.14), however the activation was not time dependent. The activity of caspase 9 at 24 hours was slightly lower than 12 hours treatment. This may be due to the caspase 9 activity was optimal at 12 hours. As mentioned above, active caspase 9 will activate pro-caspase 3, which is pivotal for the apoptotic degradation. Once procaspase 3 have been activated, the cell will undergo apoptotic degradation. Thus, apoptosis might also occur even the activity of caspase 9 decreased in longer time treatment. Furthermore, the effect of HK18 on the activity of caspase 8 was also examined. It has been found that the activity of caspase 8 remained unchanged upon 12 hours HK18 treatment (Fig 4.14). Thus, activation of caspase 8 seems not involved in the apoptotic pathway of HK18 induced cell death. The caspase 8 activity decreased after 24 hours treatment. This may be because at that treatment period, large proportion of the cells died out and hence the intracellular enzymes lost their activities and even lower than the basal level. The enzymatic activities of caspase 3 and caspase 9 might also be affected.

Summarize of the above results, it can be concluded that HK18 could induce HepG2 cells to undergo apoptosis. MPT was induced by HK18, which may be due to the elevated intracellular ROS and Ca^{2+} levels. The anti-apoptotic protein Bcl-2 and Bcl-X_L were reduced by HK18. Apoptogenic proteins cytochrome c and AIF were released from mitochondria while the release of Smac remained to be elucidated. Cytochrome c released would then interact with Apaf-1 and pro-caspase 9 to form apoptosome. This led to pro-caspase 9 activation and subsequent pro-caspase 3 activation. The activated caspases would then activate an array of substrates, which

contributed to catabolic degradation of HepG2 cells. DNA fragmentation and PS externalization were resulted. Fig 6.1 summarizes the possible action mechanisms of HK18 exerting on HepG2 cells.

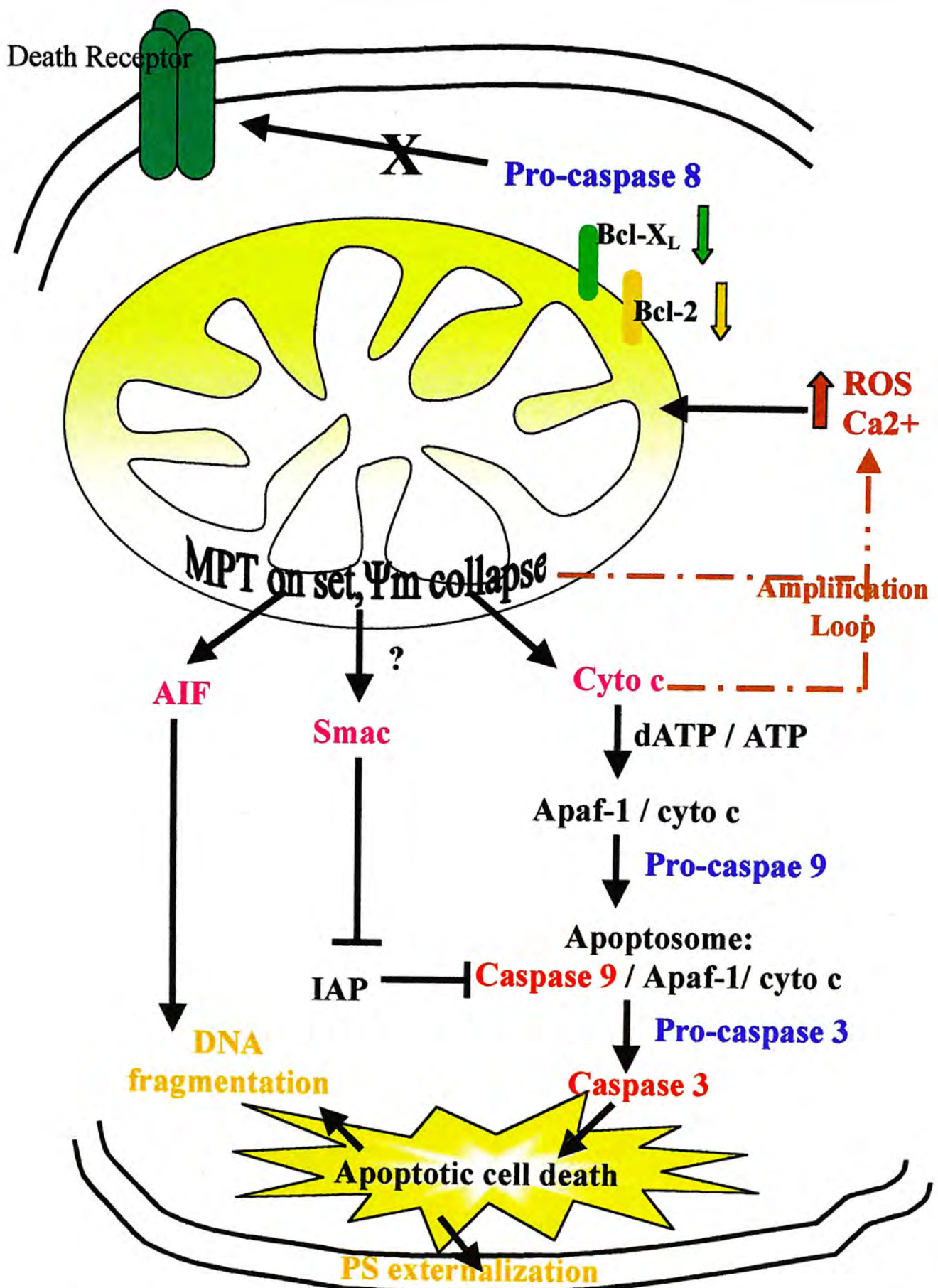


Fig 6.1 Summary of the possible action mechanisms of HK18 exerted on HepG2 cells.

6.3 Mechanistic Studies of the Cytotoxic Effects of HK18 on R-HepG2 Cells

6.3.1 Apoptotic Cell Death Induction of HK18 on R-HepG2 Cells

Similar to the study of HepG2 cells, the cell death mode of HK18 on R-HepG2 cells was examined by PS externalization and DNA fragmentation. It has been found that treating R-HepG2 cells with HK18 could induce PS externalization in a dose dependent manner (Fig 5.1). Besides, as shown in Fig 5.2, HK18 could induce DNA fragmentation on R-HepG2 cells after 24 hours treatment. By these two typical apoptotic cell death assays, HK18 has been proven to induce apoptosis in R-HepG2 cells.

6.3.2 Studies of the Underlying Mechanisms of HK18 Induced Apoptosis of R-HepG2 Cells

After proving the apoptotic inducing activities of HK18 on R-HepG2 cells, the underlying mechanisms of how HK18 induces apoptosis on R-HepG2 cells were investigated. First of all, the MPT-inducing activity of HK18 was examined. As mentioned before, MPT usually accompanied with mitochondrial membrane (Ψ_m) depolarization, hence the alternation of Ψ_m by HK18 on R-HepG2 cells was measured by flow cytometric analysis. The results were recorded in Fig 5.3. Treating R-HepG2 cells with HK18 for 12 and 24 hours would induce Ψ_m in a dose and time dependent manner. The occurrence of MPT in HK18 treated R-HepG2 cells were further examined by the addition of MPT inhibitor BA. It has been found that in the presence of BA, the cytotoxic effect of HK18 on R-HepG2 cells was diminished (Fig

5.4). Therefore, the apoptotic inducing activities of HK18 on R-HepG2 cells have been shown to be mediated by MPT.

Recently, there were numerous studies reported that elevated intracellular ROS and Ca^{2+} levels were two of the inducers of MPT onset. Thus, the intracellular H_2O_2 and Ca^{2+} levels of HK18 treated R-HepG2 cells were measured. It has been found that the intracellular H_2O_2 was elevated upon the treatment of HK18 (Fig 5.5). However, dissimilar to the case in HepG2 cells, the elevation of H_2O_2 in R-HepG2 cells was not in a dose dependent manner. The level of H_2O_2 at 12 hours treatment was higher than the 24 hours treatment. Similar results were observed in studying the intracellular Ca^{2+} level. It has been found that HK18 could enhance intracellular Ca^{2+} level (Fig 5.6). However, the enhancement at 12 hours treatment was greater than 24 hours treatment. The possible reason of this phenomenon may be due to the production or release of these two mediators to induce MPT was optimal at 12 hours already. And the intracellular levels of them leveled off and decreased afterwards.

As mentioned above, apoptosis and MPT were governed by the Bcl-2 family members. Thus, the involvement of Bcl-2 protein was examined in HK18 treated R-HepG2 cells by Western blot analysis. Bcl-2 is an anti-apoptotic protein, down-regulation of this protein will favor apoptotic cell death. It has been found that treating with HK18 for 12 and 24 hours, the protein level of Bcl-2 in R-HepG2 cells decreased in a concentration and time dependent manner (Fig 5.10).

As discussed in the previous paragraphs, pro-caspase 9 is being activated in

mitochondrial dependent apoptosis pathway. Activation of pro-caspase 9 requires the association of apoptosome, which comprised of Apaf-1, pro-caspase 9, cytochrome c and dATP. Formation of apoptosome will lead to the induced proximity of pro-caspase 9 molecules and hence auto-activation into enzymatic active caspase 9 is resulted. The activated caspase 9 will then bind and activate pro-caspase 3 into the enzymatic active form. The activated caspase 3 will then act on a variety of substrates and eventually leads to apoptotic biochemical alternations.

In view of this, the caspases activating activities of HK18 was studied. The activation of caspase 3 was first demonstrated by Western blot analysis. As observed from the film (Fig 5.7), treating R-HepG2 cells with HK18 for 24 hours would lower the protein level of pro-caspase 3. The diminished pro-caspase 3 should be converted into the active caspase 3. It was confirmed by analyzing with the protein level of PARP. It has been found that HK18 reduced the intact PARP level while enhanced the level of cleaved PARP fragment (Fig 5.7).

Besides of Western blot analysis, the enzymatic activity of caspase 3 was measured by its substrate cleaving activity. From Fig 5.8, it shows that treating R-HepG2 cells for 12 hours and 24 hours with HK18 would enhance its enzymatic activity. However, the activities at 12 hours was higher than at 24 hours. This might due to the optimal activity might have been reach at 12 hours. Another possible reason was that at 24 hours treatment, large proportion of the cells died out and hence their enzymes lost their activities. Similar results were obtained in measuring the enzymatic activity of caspase 9. The activity of caspase 9 increased upon 12 hours

HK18 treatment and returned to basal level (Fig 5.9 b).

Apart from caspase 3 and 9, the enzymatic activity of caspase 8 was also assessed. It has been found that treating R-HepG2 cells with HK18 for 12 hours did not change the enzymatic activity of caspase 8 hence, caspase 8 had not been activated by HK18 (Fig 5.9). Similarly, the activity of caspase 8 at 24 hours was lower than the basal level, which might due to dissipation of enzymatic activities in death cells.

R-HepG2 cells are multidrug resistant cells with the over-expression of P-glycoprotein (P-gp). P-gp is a 170 kDa trans- plasma membrane protein that is glycosylated at a single site at the extracellular face. It belongs to the ABC (ATP-binding cassette) transporters superfamily. Human P-gp (MDR-1) is a 1280 amino acids protein arranged into two homologous halves with each contains 6 transmembrane domains and an ATP-binding domain (Jones and George, 1998). It is encoded by the MDR-1 gene, which is located on chromosome 7 (Di Pietro *et al.*, 1999). They actively expel a variety of drugs differing in structures and action mechanisms in the expense of ATP. As a result, they prevent the accumulation of drugs inside the cell and hence the cell is free from the action of the drug. For instant, cells with overexpressed P-gp are resistant to doxorubicin, vincristine and methotrexate etc. that kill cells through different action mechanisms. P-gp transverses the plasma membrane to form pores. The diameter of the pore of hamster is around 5nm (Rosenberg *et al.*, 1997). The pore size of the P-gp in human is still under elucidation. But the recent findings reported that the pore diameter of human

P-gp is between 9 nm to 25 nm (Loo and Clarke, 2001).

For sustain the expression of P-gp on cell membrane, its substrates must be added for culturing. The substrate of P-gp varies in structure and action mechanisms, so it is difficult to generalize the characteristics of its substrates. However, recent studies found that there are several common properties among its substrate, they are hydrophobic, usually possess cationic charge (Szachowicz-Petelska *et al.*, 2001) (since the P-gp has a negatively charged hydrophobic cavity) and at least 2 planar rings. Fig 6.2 shows several well known substrates of P-gp. Therefore, according to the present knowledge, for an agent to be bound and then pumped out by P-gp, it should be (1) cationic charged (2) hydrophobic and (3) 3 dimensional structure smaller than the pore size of P-gp. As illustrated in Fig 6.2, the popular substrates of P-gp usually possess amine group(s). They usually become protonized in tumor cells, where glycolysis is preferred for energy production. As a result, these substrates (drugs) usually bear positive charge(s) in the cells and hence easily to be bound and pumped out by P-gp. In comparison of the structure of HK18 (Fig 1.5) with those well-known substrates, HK18 does not possess any amine group and hence should be neutral inside tumor cells. Although the 3 dimensional structure of HK18 was still unclear, we speculated that HK18 is not a substrate of P-gp since it is a neutral molecule.

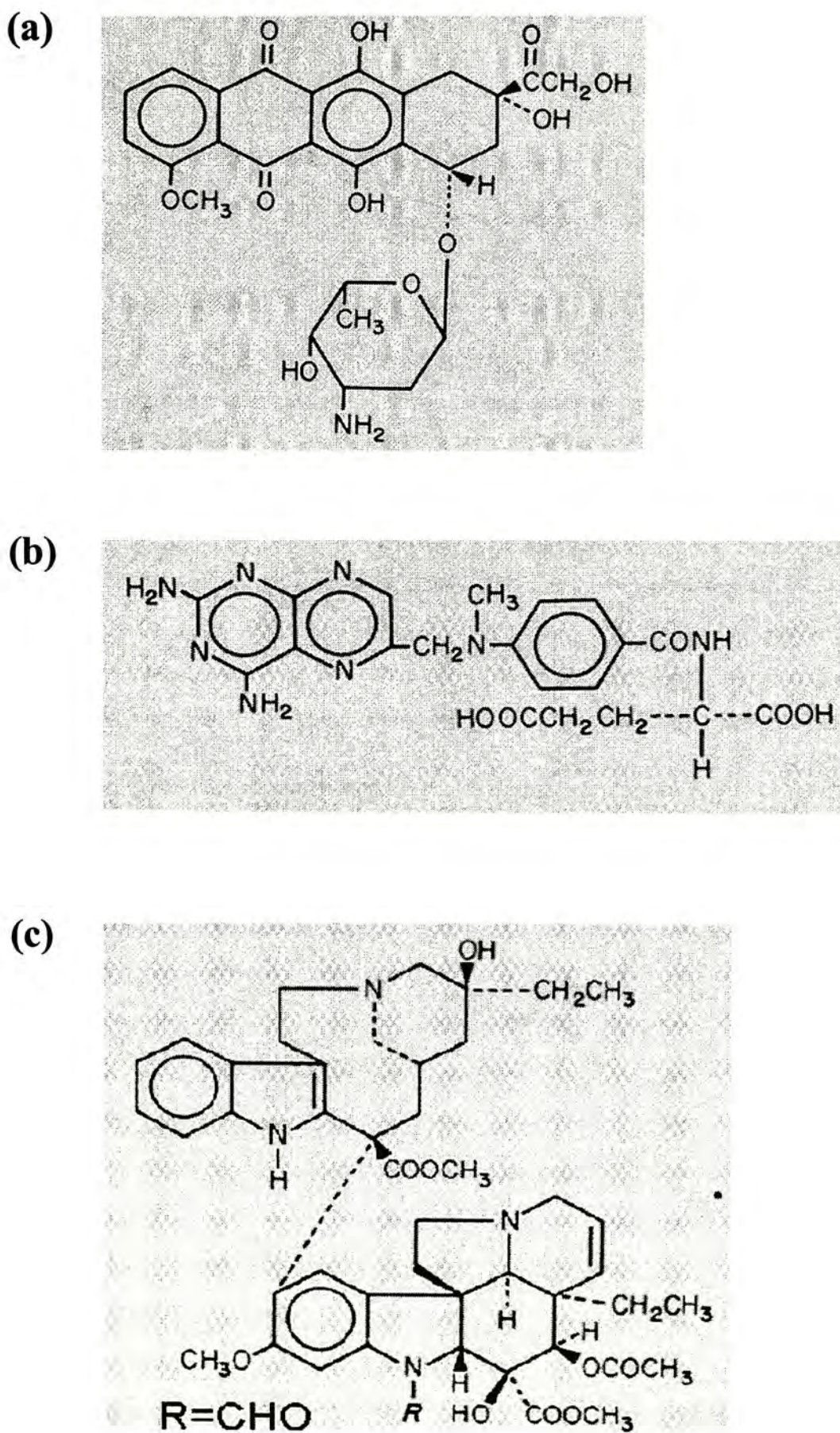


Fig 6.2 Structures of three substrates of P-gp. (a) Doxorubicin with M.W. 543.54. (b) Methotrexate with M.W. 454.46. (c) Vincristine with M.W. 824.94.

R-HepG2 cells used in our experiments have over-expressed P-gp, which have been proven by Western blot and Northern blot analysis (Chan *et al.*, 2000). Since they have over-expression of P-gp, the IC₅₀ of them toward DOX is much higher than their parental cells HepG2 (> 250 μM and 68 μM of R-HepG2 cells vs 4.5 μM and 1 μM of HepG2 cells for 24 and 48 hours respectively). However, HK18 have shown to have similar IC₅₀ towards both HepG2 and R-HepG2 cells. Furthermore, HK18 is a neutral molecule, thus we proposed that HK18 should not a substrate of P-gp as it could keep away from the pumping effect of P-gp. To examine this hypothesis, R-HepG2 cells were cultured in the presence of HK18 and then the protein expression level of P-gp was measured. R-HepG2 cultured in the presence of vincristine (one of the P-gp substrate) was used as a positive control. Besides, R-HepG2 cells were cultured with the withdrawal of DOX. In the absence of DOX, the P-gp level would decrease gradually. As shown in Fig 5.11, the P-gp expression level of vincristine-cultured R-HepG2 cells remained high throughout the study period. While the P-gp expression level of R-HepG2 cells in the presence of HK18 or absence of DOX decreased gradually. Therefore, HK18 is not a substrate of P-gp and hence could exert its effects on multidrug resistance cells.

As a summary, HK18 could induce R-HepG2 cells to undergo apoptosis. MPT was induced by HK18, which may be due to the elevated intracellular ROS and Ca²⁺ levels. It could reduce the expression of the anti-apoptotic Bcl-2 protein. However, the release of apoptogenic proteins such as cytochrome c, AIF and Smac remained to elucidate. It has been found that HK18 could induce caspase 9 activation, which might then lead to procaspase 3 activation. The activated caspases would then

activate an array of substrates, which contributed to catabolic degradation of HepG2 cells. DNA fragmentation and PS externalization were resulted. Furthermore, it has been found that HK18 was not a substrate of P-glycoprotein and thus it could induce apoptotic cell death in P-gp overexpressed R-HepG2 cells. Fig 6.3 summarized the possible action mechanisms of HK18 exerting on R-HepG2 cells.

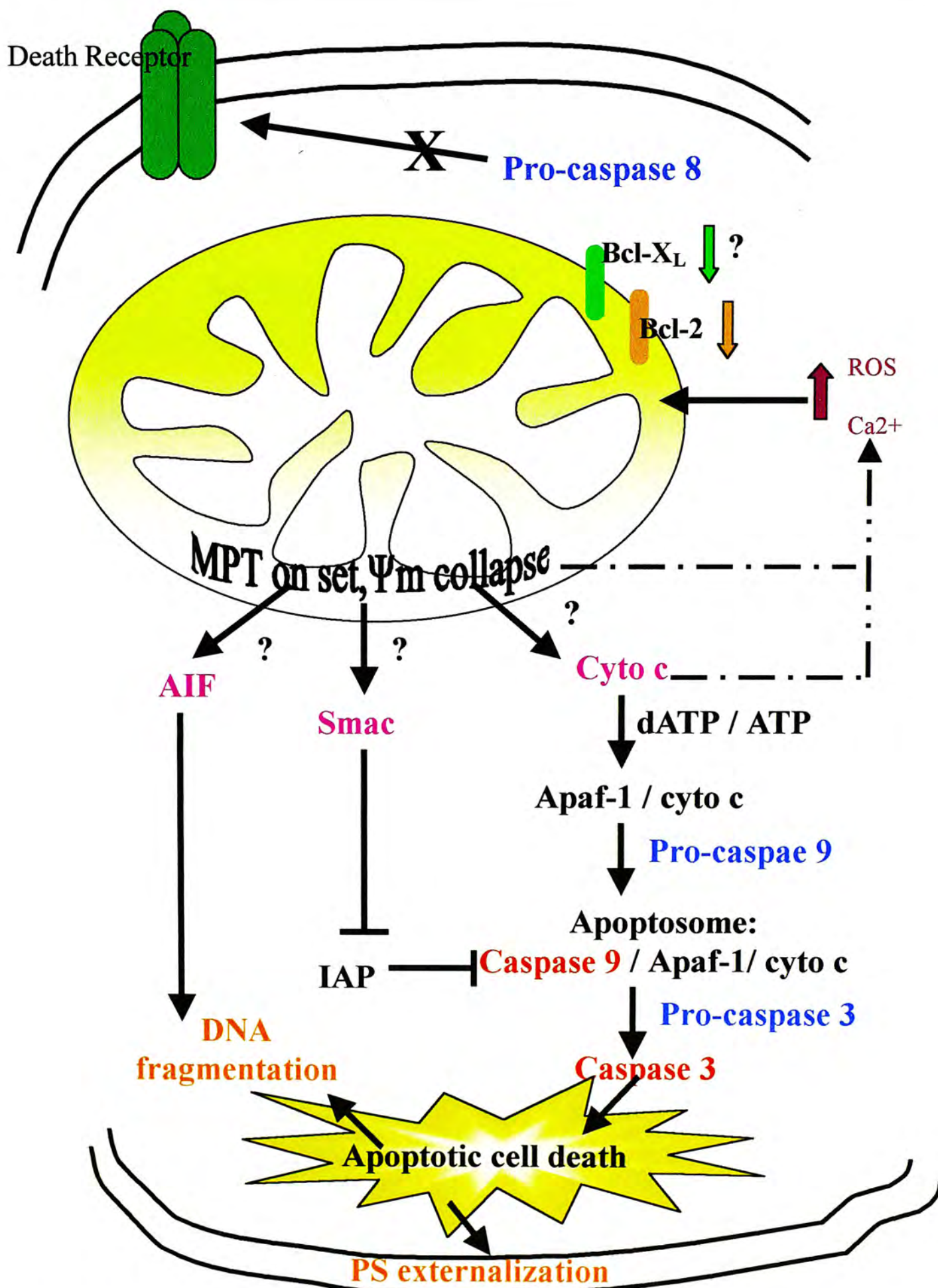


Fig 6.3 Summary of the possible action mechanisms of HK18 exerted of R-HepG2 cells.

Chapter 7

Future Perspectives

In the coming future, there are several directions that we can further study on HK18. First of all, the involvement of other anti-apoptotic and pro-apoptotic Bcl-2 family proteins in HK18 induced apoptotic cell death of HepG2 cells and R-HepG2 cells can be elucidated. Also, the release of other apoptogenic proteins such as Smac can be examined.

Moreover, as demonstrated in this research project, mitochondrial-dependent apoptotic pathway was involved in HK18 induced apoptosis in HepG2 cells and R-HepG2 cells. However, we do not know how HK18 exert its effect on the mitochondrion. It may either enter into the cells and act on mitochondria directly or trigger intracellular mediators which then converge to mitochondria. To elucidate these possibilities, cell-free systems can be used (Costantini *et al.*, 2000). Mitochondria can be isolated from HepG2 and R-HepG2 cells and then treated with HK18. After that, alternation of mitochondria can be monitored (e.g. measuring of mitochondrial membrane potential) to see does HK18 have direct effect on mitochondria. To further elucidate the release of apoptogenic proteins from mitochondria, the supernatant of the treated mitochondria can be mixed with nuclei purified from normal cells. The apoptogenic proteins will provoke apoptotic changes of nuclei such as chromatin condensation and DNA degradation. Alternatively, the supernatant of treated mitochondria can be mixed with cytosol from normal cells. The apoptogenic proteins present will induce pro-caspases activation, which can be measured by their enzymatic activities. On the other hand, if HK18 does not exert direct effect on mitochondria, it seems that it may first trigger mediators and then act on mitochondria. This route can be studied by first treating

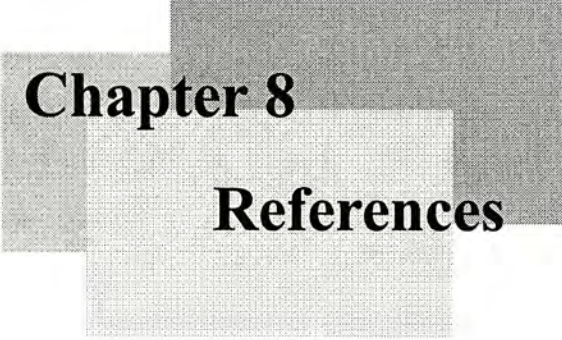
cells with HK18 and the cytosol was collected. The cytosol, which contains apoptosis mediators, can then add to mitochondria isolated from normal cells. The alternation of mitochondria can be monitored.

Besides the usage of cell-free systems, we would like to conjugate HK18 with fluorescent label. By these labeled HK18, the route of how HK18 act on the cells can be traced.

Furthermore, the structure of HK18 can be modified in order to enhance its solubility (it is insoluble in water) and promote its anti-tumor potencies.

Moreover, the dimensions of HK18 can be elucidated by X-ray crystallography. Thus we can see does HK18 can pass through the pore of P-glycoprotein. If its dimensions is greater then the pore size which has been proposed to be 9 – 25 nm (Szachowicz-Petelska *et al.*, 2001), then HK18 will not be a substrate of P-glycoprotien as it cannot pass through the pore.

Apart from these, the anti-tumor activities of HK18 on HepG2 and R-HepG2 cells with *in vivo* model can be carried out. The pilot study of the anti-tumor activity of HK18 on HepG2 tumor bearing nude mice showed that administration of 860 μg of HK18 per kg of mice via intravenously injection every alternate day (equivalent to 12.5 μM concentration) could cause a 70 % reduction of tumor weight after 3 weeks treatment (data not shown). If sufficient HK18 can be organic synthesized, we will repeat the *in vivo* experiments in future.



Chapter 8
References

- Arceci, R. J. (2000). Can multidrug resistance mechanisms be modified? *Br J Haematol* **110**:285-291.
- Ashkenazi, A. and Dixit, V. M. (1998). Death receptors: signaling and modulation. *Science* **281**:1305-1308.
- Bernardi, P., Scorrano, L., Colonna, R., Petronilli, V., and Di Lisa, F. (1999). Mitochondria and cell death. Mechanistic aspects and methodological issues. *Eur J Biochem* **264**:687-701.
- Bok, J. W., Lerner, L., Chilton, J., Klingeman, H. G., and Towers, G. H. (1999). Antitumor sterols from the mycelia of *Cordyceps sinensis*. *Phytochemistry* **51**:891-898.
- Borrelli, F. and Izzo, A. A. (2000). The plant kingdom as a source of anti-ulcer remedies. *Phytother Res* **14**:581-591.
- Cai, J., Yang, J., and Jones, D. P. (1998). Mitochondrial control of apoptosis: the role of cytochrome c. *Biochim Biophys Acta* **1366**:139-149.
- Calis, I., Yuruker, A., Tasdemir, D., Wright, A. D., Sticher, O., Luo, Y. D., and Pezzuto, J. M. (1997). Cycloartane triterpene glycosides from the roots of *Astragalus melanophrurius*. *Planta Med* **63**:183-186.
- Cathcart, R., Schwiers, E., and Ames, B. N. (1983). Detection of picomole levels of hydroperoxides using a fluorescent dichlorofluorescein assay. *Anal Biochem* **134**:111-116.
- Chakraborti, T., Das, S., Mondal, M., Roychoudhury, S., and Chakraborti, S. (1999). Oxidant, mitochondria and calcium: an overview. *Cell Signal* **11**:77-85.
- Chan, J. Y., Chu, A. C., and Fung, K. P. (2000). Inhibition of P-glycoprotein expression and reversal of drug resistance of human hepatoma HepG2 cells by multidrug resistance gene (mdr1) antisense RNA. *Life Sci* **67**:2117-2124.
- Chandra, J., Samali, A., and Orrenius, S. (2000). Triggering and modulation of apoptosis by oxidative stress. *Free Radic Biol Med* **29**:323-333.

- Chavali, S. R., Francis, T., and Campbell, J. B. (1987). An in vitro study of immunomodulatory effects of some saponins. *Int J Immunopharmacol* **9**:675-683.
- Chavali, S. R. and Campbell, J. B. (1987). Immunomodulatory effects of orally-administered saponins and nonspecific resistance against rabies infection. *Int Arch Allergy Appl Immunol* **84**:129-134.
- Chavali, S. R., Barton, L. D., and Campbell, J. B. (1988). Immunopotentiality by orally-administered Quillaja saponins: effects in mice vaccinated intraperitoneally against rabies. *Clin Exp Immunol* **74**:339-343.
- Chinnaiyan, A. M., O'Rourke, K., Lane, B. R., and Dixit, V. M. (1997). Interaction of CED-4 with CED-3 and CED-9: a molecular framework for cell death. *Science* **275**:1122-1126.
- Cossarizza, A., Baccarani-Contri, M., Kalashnikova, G., and Franceschi, C. (1993). A new method for the cytofluorimetric analysis of mitochondrial membrane potential using the J-aggregate forming lipophilic cation 5,5',6,6'-tetrachloro-1,1',3,3'-tetraethylbenzimidazolcarbocyanine iodide (JC-1). *Biochem Biophys Res Commun* **197**:40-45.
- Costantini, P., Chernyak, B. V., Petronilli, V., and Bernardi, P. (1996). Modulation of the mitochondrial permeability transition pore by pyridine nucleotides and dithiol oxidation at two separate sites. *J Biol Chem* **271**:6746-6751.
- Costantini, P., Belzacq, A. S., Vieira, H. L., Larochette, N., de Pablo, M. A., Zamzami, N., Susin, S. A., Brenner, C., and Kroemer, G. (2000). Oxidation of a critical thiol residue of the adenine nucleotide translocator enforces Bcl-2-independent permeability transition pore opening and apoptosis. *Oncogene* **19**:307-314.
- Costantini, P., Jacotot, E., Decaudin, D., and Kroemer, G. (2000). Mitochondrion as a novel target of anticancer chemotherapy. *J Natl Cancer Inst* **92**:1042-1053.
- Craig, W. J. (1999). Health-promoting properties of common herbs. *Am J Clin Nutr* **70**:491S-499S.
- Crompton, M. (1999). The mitochondrial permeability transition pore and its role in cell death. *Biochem J* **341** (Pt 2):233-249.
-
-

- Custodio, J. B., Cardoso, C. M., and Almeida, L. M. (2002). Thiol protecting agents and antioxidants inhibit the mitochondrial permeability transition promoted by etoposide: implications in the prevention of etoposide-induced apoptosis. *Chem Biol Interact* **140**:169-184.
- de Murcia, J. M., Niedergang, C., Trucco, C., Ricoul, M., Dutrillaux, B., Mark, M., Oliver, F. J., Masson, M., Dierich, A., LeMeur, M., Walztinger, C., Chambon, P., and de Murcia, G. (1997). Requirement of poly(ADP-ribose) polymerase in recovery from DNA damage in mice and in cells. *Proc Natl Acad Sci U S A* **94**:7303-7307.
- Daugas, E., Nochy, D., Ravagnan, L., Loeffler, M., Susin, S. A., Zamzami, N., and Kroemer, G. (2000). Apoptosis-inducing factor (AIF): a ubiquitous mitochondrial oxidoreductase involved in apoptosis. *FEBS Lett* **476**:118-123.
- Daugas, E., Susin, S. A., Zamzami, N., Ferri, K. F., Irinopoulou, T., Larochette, N., Prevost, M. C., Leber, B., Andrews, D., Penninger, J., and Kroemer, G. (2000). Mitochondrio-nuclear translocation of AIF in apoptosis and necrosis. *FASEB J* **14**:729-739.
- Deng, S., Yu, B., Hui, Y., Yu, H., and Han, X. (1999). Synthesis of three diosgenyl saponins: dioscin, polyphyllin D, and balanitin 7. *Carbohydr Res* **317**:53-62.
- Dhar, J. D., Bajpai, V. K., Setty, B. S., and Kamboj, V. P. (1989). Morphological changes in human spermatozoa as examined under scanning electron microscope after in vitro exposure to saponins isolated from *Sapindus mukorossi*. *Contraception* **39**:563-568.
- Di Pietro, A., Dayan, G., Conseil, G., Steinfels, E., Krell, T., Trompier, D., Baubichon-Cortay, H., and Jault, J. (1999). P-glycoprotein-mediated resistance to chemotherapy in cancer cells: using recombinant cytosolic domains to establish structure-function relationships. *Braz J Med Biol Res* **32**:925-939.
- Du, C., Fang, M., Li, Y., Li, L., and Wang, X. (2000). Smac, a mitochondrial protein that promotes cytochrome c-dependent caspase activation by eliminating IAP inhibition. *Cell* **102**:33-42.
- Earnshaw, W. C., Martins, L. M., and Kaufmann, S. H. (1999). Mammalian caspases: structure, activation, substrates, and functions during apoptosis. *Annu Rev Biochem* **68**:383-424.

- Ellis, H. M. and Horvitz, H. R. (1986). Genetic control of programmed cell death in the nematode *C. elegans*. *Cell* **44**:817-829.
- Engels, I. H., Stepczynska, A., Stroh, C., Lauber, K., Berg, C., Schwenzler, R., Wajant, H., Janicke, R. U., Porter, A. G., Belka, C., Gregor, M., Schulze-Osthoff, K., and Wesselborg, S. (2000). Caspase-8/FLICE functions as an executioner caspase in anticancer drug- induced apoptosis. *Oncogene* **19**:4563-4573.
- Evans, M. J. and Scarpulla, R. C. (1988). The human somatic cytochrome c gene: two classes of processed pseudogenes demarcate a period of rapid molecular evolution. *Proc Natl Acad Sci U S A* **85**:9625-9629.
- Frankel, E. N., Kanner, J., German, J. B., Parks, E., and Kinsella, J. E. (1993). Inhibition of oxidation of human low-density lipoprotein by phenolic substances in red wine. *Lancet* **341**:454-457.
- Furlong, I. J., Lopez, M. C., Ascaso, R., Lopez, R. A., and Collins, M. K. (1998). Induction of apoptosis by valinomycin: mitochondrial permeability transition causes intracellular acidification. *Cell Death Differ* **5**:214-221.
- Garg, S., Doncel, G., Chabra, S., Upadhyay, S. N., and Talwar, G. P. (1994). Synergistic spermicidal activity of neem seed extract, reetha saponins and quinine hydrochloride. *Contraception* **50**:185-190.
- Gerber, M., Boutron-Ruault, M. C., Hercberg, S., Riboli, E., Scalbert, A., and Siess, M. H. (2002). [Food and cancer: state of the art about the protective effect of fruits and vegetables]. *Bull Cancer* **89**:293-312.
- Gottlieb, R. A. (2000). Mitochondria: execution central. *FEBS Lett* **482**:6-12.
- Green, D. R. and Reed, J. C. (1998). Mitochondria and apoptosis. *Science* **281**:1309-1312.
- Gruiz, K. (1996). Fungitoxic activity of saponins: practical use and fundamental principles. In "Saponins used in traditional and modern medicine" (G. R. Waller and K. Yamasaki, Eds.), pp. 527-534, Plenum Press, New York.
- Halestrap, A. P. (1999). Mitochondria make for a pore death. *Biologist* **46**:82-85.
- Hampton, M. B., Fadeel, B., and Orrenius, S. (1998). Redox regulation of the caspases during apoptosis. *Ann N Y Acad Sci* **854**:328-335.

- Hanausek, M., Ganesh, P., Walaszek, Z., Arntzen, C. J., Slaga, T. J., and Gutterman, J. U. (2001). Avicins, a family of triterpenoid saponins from *Acacia victoriae* (Benth), suppress H-ras mutations and aneuploidy in a murine skin carcinogenesis model. *Proc Natl Acad Sci U S A* **98**:11551-11556.
- Haridas, V., Higuchi, M., Jayatilake, G. S., Bailey, D., Mujoo, K., Blake, M. E., Arntzen, C. J., and Gutterman, J. U. (2001). Avicins: triterpenoid saponins from *Acacia victoriae* (Benth) induce apoptosis by mitochondrial perturbation. *Proc Natl Acad Sci U S A* **98**:5821-5826.
- Hasegawa, H., Matsumiya, S., Uchiyama, M., Kurokawa, T., Inouye, Y., Kasai, R., Ishibashi, S., and Yamasaki, K. (1994). Inhibitory effect of some triterpenoid saponins on glucose transport in tumor cells and its application to in vitro cytotoxic and antiviral activities. *Planta Med* **60**:240-243.
- Hengartner, M. O. (1999). Programmed cell death in the nematode *C. elegans*. *Recent Prog Horm Res* **54**:213-222.
- Hengartner, M. O. (2000). The biochemistry of apoptosis. *Nature* **407**:770-776.
- Hirano, T., Oka, K., Mimaki, Y., Kuroda, M., and Sashida, Y. (1996). Potent growth inhibitory activity of a novel *Ornithogalum* cholestane glycoside on human cells: induction of apoptosis in promyelocytic leukemia HL-60 cells. *Life Sci* **58**:789-798.
- Hostettmann, K and Marston, A. (1995). Introduction. pp. 1-17, Cambridge University Press, New York.
- Hostettmann, K and Marston, A. (1995). Occurrence and distribution. pp. 18-121, Cambridge University Press, New York.
- Hostettmann, K and Marston, A. (1995). Triterpene saponins - pharmacological and biological properties. In "Saponins" pp. 232-286, Cambridge University Press, New York.
- Hostettmann, K and Marston, A. (1995). Steroid saponins and steroid alkaloid saponins: pharmacological and biological properties. In "Saponins" pp. 287-306, Cambridge University Press, New York.
- Hostettmann, K., Marston, A., Maillard, M., and Wolfender, J. L. (2002). Search for molluscicidal and antifungal saponins from tropical plants. In "Saponins used in

traditional and modern medicine" (G. R. Waller and K. Yamasaki, Eds.), pp. 117-128, Plenum Press, New York.

Hu, K., Dong, A., Yao, X., Kobayashi, H., and Iwasaki, S. (1999). Antineoplastic steroidal saponins from rhizomes of *Dioscorea collettii* var. *hypoglauca*. In "Advances in plant glycosides, chemistry and biology" (C. Yang and O. Tanaka, Eds.), pp. 220-229, Elsevier Science B.V., Amsterdam.

Hu, Y., Benedict, M. A., Ding, L., and Nunez, G. (1999). Role of cytochrome c and dATP/ATP hydrolysis in Apaf-1-mediated caspase-9 activation and apoptosis. *EMBO J* **18**:3586-3595.

Irmeler, M., Hofmann, K., Vaux, D., and Tschopp, J. (1997). Direct physical interaction between the *Caenorhabditis elegans* 'death proteins' CED-3 and CED-4. *FEBS Lett* **406**:189-190.

Jang, M., Cai, L., Udeani, G. O., Slowing, K. V., Thomas, C. F., Beecher, C. W., Fong, H. H., Farnsworth, N. R., Kinghorn, A. D., Mehta, R. G., Moon, R. C., and Pezzuto, J. M. (1997). Cancer chemopreventive activity of resveratrol, a natural product derived from grapes. *Science* **275**:218-220.

Jones, P. M. and George, A. M. (1998). A new structural model for P-glycoprotein. *J Membr Biol* **166**:133-147.

Kenarova, B., Neychev, H., Hadjiivanova, C., and Petkov, V. D. (1990). Immunomodulating activity of ginsenoside Rg1 from *Panax ginseng*. *Jpn J Pharmacol* **54**:447-454.

Kim, H. E., Oh, J. H., Lee, S. K., and Oh, Y. J. (1999). Ginsenoside RH-2 induces apoptotic cell death in rat C6 glioma via a reactive oxygen- and caspase-dependent but Bcl-X(L)-independent pathway. *Life Sci* **65**:L33-L40.

Kim, S. E., Lee, Y. H., Park, J. H., and Lee, S. K. (1999). Ginsenoside-Rs4, a new type of ginseng saponin concurrently induces apoptosis and selectively elevates protein levels of p53 and p21WAF1 in human hepatoma SK-HEP-1 cells. *Eur J Cancer* **35**:507-511.

Kohler, C., Gahm, A., Noma, T., Nakazawa, A., Orrenius, S., and Zhivotovsky, B. (1999). Release of adenylate kinase 2 from the mitochondrial intermembrane space during apoptosis. *FEBS Lett* **447**:10-12.

- Konoshima, T., Takasaki, M., Ichiishi, E., Murakami, T., Tokuda, H., Nishino, H., Duc, N. M., Kasai, R., and Yamasaki, K. (1999). Cancer chemopreventive activity of majonoside-R2 from Vietnamese ginseng, *Panax vietnamensis*. *Cancer Lett* **147**:11-16.
- Kris-Etherton, P. M. and Keen, C. L. (2002). Evidence that the antioxidant flavonoids in tea and cocoa are beneficial for cardiovascular health. *Curr Opin Lipidol* **13**:41-49.
- Kroemer, G. and Reed, J. C. (2000). Mitochondrial control of cell death. *Nat Med* **6**:513-519.
- Kucuk, O. (2002). New opportunities in chemoprevention research. *Cancer Invest* **20**:237-245.
- Lacaille-Dubois, M. A., Hanquet, B., Rustaiyan, A., and Wagner, H. (1993). Squarroside A, a biologically active triterpene saponin from *Acanthophyllum squarrosum*. *Phytochemistry* **34**:489-495.
- Lacaille-Dubois, M. A. (1998). Saponins as immunoadjuvants and immunostimulants. In "Immunomodulatory agents from plants" (H. Wagner, Ed.), pp. 243-276, Birkhauser Verlag, Boston.
- Lee, B. H., Lee, S. J., Hur, J. H., Lee, S., Sung, J. H., Huh, J. D., Moon, C. K., and Hui, J. H. (1998). In vitro antigenotoxic activity of novel ginseng saponin metabolites formed by intestinal bacteria. *Planta Med* **64**:500-503.
- Lee, H. and Lin, J. Y. (1988). Antimutagenic activity of extracts from anticancer drugs in Chinese medicine. *Mutat Res* **204**:229-234.
- Lee, S. J., Sung, J. H., Lee, S. J., Moon, C. K., and Lee, B. H. (1999). Antitumor activity of a novel ginseng saponin metabolite in human pulmonary adenocarcinoma cells resistant to cisplatin. *Cancer Lett* **144**:39-43.
- Lee, S. J., Ko, W. G., Kim, J. H., Sung, J. H., Moon, C. K., and Lee, B. H. (2000). Induction of apoptosis by a novel intestinal metabolite of ginseng saponin via cytochrome c-mediated activation of caspase-3 protease. *Biochem Pharmacol* **60**:677-685.

- Lemasters, J. J., Nieminen, A. L., Qian, T., Trost, L. C., Elmore, S. P., Nishimura, Y., Crowe, R. A., Cascio, W. E., Bradham, C. A., Brenner, D. A., and Herman, B. (1998). The mitochondrial permeability transition in cell death: a common mechanism in necrosis, apoptosis and autophagy. *Biochim Biophys Acta* **1366**:177-196.
- Li, B., Yu, B., Hui, Y., Li, M., Han, X., and Fung, K. P. (2001). An improved synthesis of the saponin, polyphyllin D. *Carbohydr Res* **331**:1-7.
- Li, P., Nijhawan, D., Budihardjo, I., Srinivasula, S. M., Ahmad, M., Alnemri, E. S., and Wang, X. (1997). Cytochrome c and dATP-dependent formation of Apaf-1/caspase-9 complex initiates an apoptotic protease cascade. *Cell* **91**:479-489.
- Lijmbach, G. W. M., Cox, H. C., and Berends, W. (1970). elucidation of the chemical structure of bongkreic acid - I. *Tetrahedron* **26**:5993-5999.
- Liu, W. K., Xu, S. X., and Che, C. T. (2000). Anti-proliferative effect of ginseng saponins on human prostate cancer cell line. *Life Sci* **67**:1297-1306.
- Liu, X., Kim, C. N., Yang, J., Jemmerson, R., and Wang, X. (1996). Induction of apoptotic program in cell-free extracts: requirement for dATP and cytochrome c. *Cell* **86**:147-157.
- Loeffler, M. and Kroemer, G. (2000). The mitochondrion in cell death control: certainties and incognita. *Exp Cell Res* **256**:19-26.
- Loeffler, M., Daugas, E., Susin, S. A., Zamzami, N., Metivier, D., Nieminen, A. L., Brothers, G., Penninger, J. M., and Kroemer, G. (2001). Dominant cell death induction by extramitochondrially targeted apoptosis-inducing factor. *FASEB J* **15**:758-767.
- Loo, T. W. and Clarke, D. M. (2001). Determining the dimensions of the drug-binding domain of human P-glycoprotein using thiol cross-linking compounds as molecular rulers. *J Biol Chem* **276**:36877-36880.
- Mack, A., Furmann, C., and Hacker, G. (2000). Detection of caspase-activation in intact lymphoid cells using standard caspase substrates and inhibitors. *J Immunol Methods* **241**:19-31.

- Manthey, J. A., Grohmann, K., and Guthrie, N. (2001). Biological properties of citrus flavonoids pertaining to cancer and inflammation. *Curr Med Chem* **8**:135-153.
- Marchetti, P., Castedo, M., Susin, S. A., Zamzami, N., Hirsch, T., Macho, A., Haeffner, A., Hirsch, F., Geuskens, M., and Kroemer, G. (1996). Mitochondrial permeability transition is a central coordinating event of apoptosis. *J Exp Med* **184**:1155-1160.
- Matsuura, H. (2001). Saponins in garlic as modifiers of the risk of cardiovascular disease. *J Nutr* **131**:1000S-1005S.
- Mayer, A., Neupert, W., and Lill, R. (1995). Translocation of apocytochrome c across the outer membrane of mitochondria. *J Biol Chem* **270**:12390-12397.
- McConkey, D. J. and Orrenius, S. (1997). The role of calcium in the regulation of apoptosis. *Biochem Biophys Res Commun* **239**:357-366.
- Mickley, L. and Fojo, A. T. (1998). The MDR genes. In "Drug resistance in the treatment of cancer" (H. M. Pinedo and G. Giaccone, Eds.), pp. 100-131, Cambridge University Press, New York.
- Miyazaki, M. and Namba, M. (1994). Hepatocellular carcinomas. In "Atlas of human tumor cell lines" (A. Gazdar, Ed.), pp. 185-212, Academic Press, San Diego.
- Mochizuki, M., Yoo, Y. C., Matsuzawa, K., Sato, K., Saiki, I., Tono-oka, S., Samukawa, K., and Azuma, I. (1995). Inhibitory effect of tumor metastasis in mice by saponins, ginsenoside- Rb2, 20(R)- and 20(S)-ginsenoside-Rg3, of red ginseng. *Biol Pharm Bull* **18** :1197-1202.
- Muchmore, S. W., Sattler, M., Liang, H., Meadows, R. P., Harlan, J. E., Yoon, H. S., Nettesheim, D., Chang, B. S., Thompson, C. B., Wong, S. L., Ng, S. L., and Fesik, S. W. (1996). X-ray and NMR structure of human Bcl-xL, an inhibitor of programmed cell death. *Nature* **381**:335-341.
- Nagata, S. (2000). Apoptotic DNA fragmentation. *Exp Cell Res* **256**:12-18.
- Nakamura, O., Mimaki, Y., Nishino, H., and Sashida, Y. (1994). Steroidal saponins from the bulbs of *Lilium speciosum* x *L. nobilissimum* 'Star Gazer' and their antitumour-promoter activity. *Phytochemistry* **36**:463-467.

- Oakenfull, D. (2001). Soy protein, saponins and plasma cholesterol. *J Nutr* **131**:2971-2972.
- Oleszek, W. A. (2000). Saponins. In "Natural food antimicrobial systems" (A. S. Naidu, Ed.), pp. 295-324, CRC Oress.
- Osbourn, A. E., Bowyer, P, and Daniels, M. J. (1996). Saponin detoxification by plant pathogenic fungi. In "Saponins used in traditional and modern medicine" (G. R. Waller and K. Yamasaki, Eds.), pp. 547-555, Plenum Press, New York.
- Ott, M., Robertson, J. D., Gogvadze, V., Zhivotovsky, B., and Orrenius, S. (2002). Cytochrome c release from mitochondria proceeds by a two-step process. *Proc Natl Acad Sci U S A* **99**:1259-1263.
- Pakrashi, A., Ray, H., Pal, B. C., and Mahato, S. B. (1991). Sperm immobilizing effect of triterpene saponins from *Acacia auriculiformis*. *Contraception* **43**:475-483.
- Park, J. A., Lee, K. Y., Oh, Y. J., Kim, K. W., and Lee, S. K. (1997). Activation of caspase-3 protease via a Bcl-2-insensitive pathway during the process of ginsenoside Rh2-induced apoptosis. *Cancer Lett* **121**:73-81.
- Pervaiz, S. and Clement, M. V. (2002). A permissive apoptotic environment: function of a decrease in intracellular superoxide anion and cytosolic acidification. *Biochem Biophys Res Commun* **290**:1145-1150.
- Plohmann, B., Bader, G., Hiller, K., and Franz, G. (1997). Immunomodulatory and antitumoral effects of triterpenoid saponins. *Pharmazie* **52**:953-957.
- Qian, Z., Dai, X., and Ma, X. (1999). Review of studies on biological activities of soyasaponins. In "Advances in plant glycosides, chemistry and biology" (C. Yang and O. Tanaka, Eds.), pp. 193-195, Elsevier Science B. V., Amsterdam.
- Rajasekaran, M., Nair, A. G., Hellstrom, W. J., and Sikka, S. C. (1993). Spermicidal activity of an antifungal saponin obtained from the tropical herb *Mollugo pentaphylla*. *Contraception* **47**:401-412.
- Rao, A. V. and Sung, M. K. (1995). Saponins as anticarcinogens. *J Nutr* **125**:717S-724S.
- Ravikumar, P. R., Hammesfahr, P., and Sih, C. J. (1979). Cytotoxic saponins from the Chinese herbal drug Yunnan Bai Yao. *J Pharm Sci* **68**:900-903.

- Reed, J. C. (1997). Bcl-2 family proteins: strategies for overcoming chemoresistance in cancer. *In* "Apoptosis Pharmacological implications and therapeutics opportunities" (S. H. Kaufmann, Ed.), pp. 501-531, Academic Press, California.
- Reers, M., Smiley, S. T., Mottola-Hartshorn, C., Chen, A., Lin, M., and Chen, L. B. (1995). Mitochondrial membrane potential monitored by JC-1 dye. *Methods Enzymol* **260**:406-417.
- Riemersma, R. A., Rice-Evans, C. A., Tyrrell, R. M., Clifford, M. N., and Lean, M. E. (2001). Tea flavonoids and cardiovascular health. *QJM* **94**:277-282.
- Romussi, G., Cafaggi, S., and Bignardi, G. (1980). Hemolytic action and surface activity of triterpene saponins from *Anchusa officinalis* L. Part 21: On the constituents of Boraginaceae. *Pharmazie* **35**:498-499.
- Rosenberg, M. F., Callaghan, R., Ford, R. C., and Higgins, C. F. (1997). Structure of the multidrug resistance P-glycoprotein to 2.5 nm resolution determined by electron microscopy and image analysis. *J Biol Chem* **272**:10685-10694.
- Sasaki, S., Sumino, K., Hamajima, K., Fukushima, J., Ishii, N., Kawamoto, S., Mohri, H., Kensil, C. R., and Okuda, K. (1998). Induction of systemic and mucosal immune responses to human immunodeficiency virus type 1 by a DNA vaccine formulated with QS-21 saponin adjuvant via intramuscular and intranasal routes. *J Virol* **72**:4931-4939.
- Scarlett, J. L. and Murphy, M. P. (1997). Release of apoptogenic proteins from the mitochondrial intermembrane space during the mitochondrial permeability transition. *FEBS Lett* **418**:282-286.
- Seiffert, B. M., Vier, J., and Hacker, G. (2002). Subcellular localization, oligomerization, and ATP-binding of *Caenorhabditis elegans* CED-4. *Biochem Biophys Res Commun* **290**:359-365.
- Shen, H. M., Yang, C. F., Ding, W. X., Liu, J., and Ong, C. N. (2001). Superoxide radical-initiated apoptotic signalling pathway in selenite- treated HepG(2) cells: mitochondria serve as the main target. *Free Radic Biol Med* **30**:9-21.
- Shi, Y. (2002). Mechanisms of caspase activation and inhibition during apoptosis. *Mol Cell* **9**:459-470.

- Shidoji, Y., Hayashi, K., Komura, S., Ohishi, N., and Yagi, K. (1999). Loss of molecular interaction between cytochrome c and cardiolipin due to lipid peroxidation. *Biochem Biophys Res Commun* **264**:343-347.
- Shinkai, K., Akedo, H., Mukai, M., Imamura, F., Isoai, A., Kobayashi, M., and Kitagawa, I. (1996). Inhibition of in vitro tumor cell invasion by ginsenoside Rg3. *Jpn J Cancer Res* **87**:357-362.
- Single, B., Leist, M., and Nicotera, P. (1998). Simultaneous release of adenylate kinase and cytochrome c in cell death. *Cell Death Differ* **5**:1001-1003.
- Smaili, S. S., Hsu, Y. T., Youle, R. J., and Russell, J. T. (2000). Mitochondria in Ca²⁺ signaling and apoptosis. *J Bioenerg Biomembr* **32**:35-46.
- Smith, R. E., Donachie, A. M., Grdic, D., Lycke, N., and Mowat, A. M. (1999). Immune-stimulating complexes induce an IL-12-dependent cascade of innate immune responses. *J Immunol* **162**:5536-5546.
- Soldani, C. and Scovassi, A. I. (2002). Poly(ADP-ribose) polymerase-1 cleavage during apoptosis: An update. *Apoptosis* **7**:321-328.
- Spector, D. L., Goldman, B. D., and Leinwand, L. A. (1998). Apoptosis Assays. In "Cells A laboratory manual" Cold Spring Harbor Laboratory Press, New York.
- Spector, M. S., Desnoyers, S., Hoepfner, D. J., and Hengartner, M. O. (1997). Interaction between the *C. elegans* cell-death regulators CED-9 and CED-4. *Nature* **385**:653-656.
- Srinivasula, S. M., Ahmad, M., Fernandes-Alnemri, T., and Alnemri, E. S. (1998). Autoactivation of procaspase-9 by Apaf-1-mediated oligomerization. *Mol Cell* **1**:949-957.
- Stavrovskaya, A. A. (2000). Cellular mechanisms of multidrug resistance of tumor cells. *Biochemistry (Mosc)* **65**:95-106.
- Stryer, L. (1995). Oxidative Phosphorylation. In "Biochemistry" pp. 529-558, W. H. Freeman and Company, New York.
- Stryer, L. (1995). Membrane channels and pumps. In "Biochemistry" pp. 291-324, W. H. Freeman and Company, New York.

- Stryer, L. (1995). Membrane structure and dynamics. *In* "Biochemistry" pp. 267-290, W. H. Freeman and Company, New York.
- Surh, Y. J., Hurh, Y. J., Kang, J. Y., Lee, E., Kong, G., and Lee, S. J. (1999). Resveratrol, an antioxidant present in red wine, induces apoptosis in human promyelocytic leukemia (HL-60) cells. *Cancer Lett* **140**:1-10.
- Susin, S. A., Zamzami, N., Castedo, M., Hirsch, T., Marchetti, P., Macho, A., Daugas, E., Geuskens, M., and Kroemer, G. (1996). Bcl-2 inhibits the mitochondrial release of an apoptogenic protease. *J Exp Med* **184**:1331-1341.
- Susin, S. A., Lorenzo, H. K., Zamzami, N., Marzo, I., Snow, B. E., Brothers, G. M., Mangion, J., Jacotot, E., Costantini, P., Loeffler, M., Larochette, N., Goodlett, D. R., Aebersold, R., Siderovski, D. P., Penninger, J. M., and Kroemer, G. (1999). Molecular characterization of mitochondrial apoptosis-inducing factor. *Nature* **397**:441-446.
- Suzuki, Y. J., Forman, H. J., and Sevanian, A. (1997). Oxidants as stimulators of signal transduction. *Free Radic Biol Med* **22**:269-285.
- Szachowicz-Petelska, B., Figaszewski, Z., and Lewandowski, W. (2001). Mechanisms of transport across cell membranes of complexes contained in antitumour drugs. *Int J Pharm* **222**:169-182.
- Tava, A and Odoardi, M. (2002). Saponins from *Medicago* spp.: chemical characterization and biological activity against insects. *In* "Saponins used in food and agriculture" (G. R. Waller and K. Yamasaki, Eds.), pp. 97-109, Plenum Press, New York.
- Thiilborg, S. T., Cornett, C., and Lemmich, E. (2002). Investigations of molluscicidal saponins from the endod plant *Phytolacca dodecandra*. *In* "Saponins used in traditional and modern medicine" (G. R. Waller and K. Yamasaki, Eds.), pp. 151-164, Plenum Press, New York.
- Timberkova, A. E., Isaec, M. I., and Abubakirov, N. K. (1996). Chemistry and biological activity of triterpenoid glycosides from *Medicago sativa*. *In* "Saponins used in food and agriculture" (G. R. Waller, Ed.), pp. 171-182, Plenum Press, New York.

- Verhagen, A. M., Ekert, P. G., Pakusch, M., Silke, J., Connolly, L. M., Reid, G. E., Moritz, R. L., Simpson, R. J., and Vaux, D. L. (2000). Identification of DIABLO, a mammalian protein that promotes apoptosis by binding to and antagonizing IAP proteins. *Cell* **102**:43-53.
- Wang, X. (2001). The expanding role of mitochondria in apoptosis. *Genes Dev* **15**:2922-2933.
- Wargovich, M. J. (1999). Nutrition and cancer: the herbal revolution. *Curr Opin Clin Nutr Metab Care* **2**:421-424.
- Webb, S. J., Harrison, D. J., and Wyllie, A. H. (1997). Apoptosis: An overview of the process and its relevance in disease. In "Apoptosis Pharmacological implications and therapeutic opportunities" (S. H. Kaufmann, Ed.), pp. 1-33, Academic Press, California.
- Xu, J. P., Xu, R. S., and Li, X. Y. (1992). Four new cycloartane saponins from *Curculigo orchioides*. *Planta Med* **58**:208-210.
- Yang, J. C. and Cortopassi, G. A. (1998). Induction of the mitochondrial permeability transition causes release of the apoptogenic factor cytochrome c. *Free Radic Biol Med* **24**:624-631.
- Yu, B and Hui, Y (20021). Chemical synthesis of bioactive steroidal saponins. In "Glycochemistry: Principles, synthesis and applications" (P. G. Wang and W. C. Bertozzi, Eds.), pp. 163-176, Marcel Dekker, New York.
- Yuan, J., Shaham, S., Ledoux, S., Ellis, H. M., and Horvitz, H. R. (1993). The *C. elegans* cell death gene *ced-3* encodes a protein similar to mammalian interleukin-1 beta-converting enzyme. *Cell* **75**:641-652.
- Yuan, J. Y. and Horvitz, H. R. (1990). The *Caenorhabditis elegans* genes *ced-3* and *ced-4* act cell autonomously to cause programmed cell death. *Dev Biol* **138**:33-41.
- Zablotowicz, R. M., Hoagland, R. E., and Wagner, S. C. (1996). Effect of saponins on the growth and activity of rhizosphere bacteria. In "Saponins used in food and agriculture" (G. R. Waller, Ed.), pp. 83-95, Plenum Press, New York.

Zamzami, N., Susin, S. A., Marchetti, P., Hirsch, T., Gomez-Monterrey, I., Castedo, M., and Kroemer, G. (1996). Mitochondrial control of nuclear apoptosis. *J Exp Med* **183**:1533-1544.

Zehavi, U. and Polacheck, I. (1996). Saponins as antimycotic agents: glycosides of medicagenic acid. In "Saponins used in traditional and modern medicine" (G. R. Waller and K. Yamasaki, Eds.), pp. 535-546, Plenum Press, New York.

Zhang, C., Yang, X., and Xu, L. (1990). [Immunomodulatory action of the total saponin of *Gynostemma pentaphylla*]. *Zhong Xi Yi Jie He Za Zhi* **10**:96-70.

Zimmermann, K. C., Bonzon, C., and Green, D. R. (2001). The machinery of programmed cell death. *Pharmacol Ther* **92**:57-70.

On-Line References

<http://www.healthphone.com>

<http://www.brave-souls.com/resources/cancer13.html>

<http://www.ha.org.hk/hesd/nsapi>

<http://www.cancerbacup.org.uk/info/liver.htm>

http://health.yahoo.com/health/cancer_center/acs_crc/liver_cancer/index.html

CUHK Libraries



003955804